Information for Authors

AIM AND SCOPE

*Journal of Advances in Environmental Health Research (JAEHR)*is a quarterly peer-reviewed scientific journal published by Kurdistan University of Medical Sciences. The manuscripts on the topic of environmental science and engineering will be published in this journal. This contains all aspects of solid waste management, air pollution, water and wastewater, environmental monitoring and modeling, innovative technologies and studies related to the environmental science.

Instruction to Authors

MANUSCRIPTS

Manuscripts containing original material are accepted for consideration if neither the article nor any part of its essential substance, tables, or figures has been or will be published or submitted elsewhere before appearing in the *Journal of Advances in Environmental Health Research*. This restriction does not apply to abstracts or press reports published in connection with scientific meetings. Copies of any closely related manuscripts must be submitted along with the manuscript that is to be considered by the *Journal of Advances in Environmental Health Research*. Authors of all types of articles should follow the general instructions given below.

HUMAN AND ANIMAL RIGHTS

The research involves human beings or animals must adhere to the principles of the Declaration of Helsinki (http://www.wma.net/e/ethicsunit/helsinki.htm).

Types of Articles

- *Original article* which reports the results of an original scientific research should be less than 4000 words.
- *Review article* which represents the researches and works on a particular topic.
- *Brief communication* is a short research article and should be limited to 1500 words. This article contains all sections of an original article.
- *Case report* is a detailed report of an individual patient that may represent a previously non-described condition and contains new information about different aspects of a disease. It should be less than 2000 words.
- *Letter to the Editor* must be less than 400 words in all cases.
- *Book Review* must be less than 1000 words on any book topics related to the scope of *Journal of Advances in Environmental Health Research*.

SUBMISSION

- Only online submission is acceptable. Please submit online at: http://www.jaehr.muk.ac.ir
- This manuscripts should be divided into the following sections: (1) Title page, (2) Abstract and Keywords, (3) Introduction, (4) Materials and Methods, (5) Results and Discussion, (6) Acknowledgements, (7) Author contribution, (8) References, (9) Figure legends, (10) Tables and (11) Figures (figures should be submitted in separate files if the file size exceeds 2 Mb).
- Please supply a word count in title page.
- Use normal page margins (2.5 cm), and double-space throughout the manuscript.
- Use Times New Roman (12) font throughout the manuscript.
- Prepare your manuscript text using a Word processing package (save in .doc or .rtf format). Submissions of text in the form of PDF files are not permitted.

COVER LETTER

A covering letter signed by all authors should identify the corresponding author (include the address, telephone number, fax number, and e-mail address). Please make clear that the final manuscript has been seen and approved by all authors, and that the authors accept full responsibility for the design and conduct of the study, had access to the data, and controlled the decision to publish.

Authors are also asked to provide the names and contact information for three potential reviewers in their cover letter. However, the journal is not obliged to use the suggested reviewers. Final selection of reviewers will be determined by the editors.

AUTHORSHIP

As stated in the Uniform Requirements for Manuscripts Submitted to Biomedical Journals (http://www.icmje.org/icmje-recommendations.pdf), credit for authorship requires substantial contributions to: 1. Substantial contributions to the conception or design of the work; or the acquisition, analysis, or interpretation of data for the work; AND 2. Drafting the work or revising it critically for important intellectual content; AND 3. Final approval of the version to be published; AND 4. Agreement to be accountable for all aspects of the work in ensuring that questions related to the accuracy or integrity of any part of the work are appropriately investigated and resolved. Each author must sign authorship form attesting that he or she fulfills the authorship criteria. There should be a statement in manuscript explaining contribution of each author to the work. Acknowledgments will be limited to one page of *Journal of Advances in Environmental Health Research*, and those acknowledged will be listed only once.

Any change in authorship after submission must be approved in writing by all authors.

ASSURANCES
In appropriate places in the manuscript please provide the following items:
- If applicable, a statement that the research protocol was approved by the relevant institutional review boards or ethics committees and that all human participants gave written informed consent
- The source of funding for the study
- The identity of those who analyzed the data
- Financial disclosure, or a statement that none is necessary

TITLE PAGE
With the manuscript, provide a page giving the title of the paper; titles should be concise and descriptive (not declarative). Title page should include an abbreviated running title of 40 characters, the names of the authors, including the complete first names, the name of the department and institution in which the work was done, the institutional affiliation of each author. The name, post address, telephone number, fax number, and e-mail address of the corresponding author should be separately addressed. Any grant support that requires acknowledgment should be mentioned on this page. Word count of abstract and main text as well as number of tables and figures and references should be mentioned on title page. If the work was derived from a project or dissertation, its code should also be stated.

Affiliation model: Department, Institute, City, Country.
Example: Department of Environmental Health Engineering, School of Health, Kurdistan University of Medical Sciences, Sanandaj, Iran.

ABSTRACT
Provide on a separate page an abstract of not more than 250 words. This abstract should consist of ONE paragraph (Non-structured Abstract). It should briefly describe the problem being addressed in the study, how the study was performed, the salient results, and what the authors conclude from the results respectively. Three to seven keywords may be included. Keywords are preferred to be in accordance with MeSH (http://www.ncbi.nlm.nih.gov/mesh) terms.

CONFLICT OF INTEREST
Authors of research articles should disclose at the time of submission any financial arrangement they may have with a company whose product is pertinent to the submitted manuscript or with a company making a competing product. Such information will be held in confidence while the paper is under review and will not influence the editorial decision, but if the article is accepted for publication, a disclosure will appear with the article.
Because the essence of reviews and editorials is selection and interpretation of the literature, the *Journal of Advances in Environmental Health Research* expects that authors of such articles will not have any significant financial interest in a company (or its competitor) that makes a product discussed in the article.

REVIEW AND ACTION

Submitted papers will be examined for the evidence of plagiarism using some automated plagiarism detection service. Manuscripts are examined by members of the editorial staff, and two thirds are sent to external reviewers. Communications about manuscripts will be sent after the review and editorial decision-making process is complete within **3-6 weeks** after receiving the manuscript. After acceptance, editorial system makes a final language and scientific edition. No substantial change is permitted by authors after acceptance. It is the responsibility of corresponding author to answer probable questions and approve final version.

COPYRIGHT
Journal of Advances in Environmental Health Research is the owner of all copyright to any original work published by the

JOURNAL STYLE

Tables

Double-space tables and provide a title for each.

Figures

Figures should be no larger than 125 (height) x 180 (width) mm (5 x 7 inches) and should be submitted in a separate file from that of the manuscript. The name of images or figures files should be the same as the order that was used in manuscript (fig1, fig2, etc.). Only JPEG, tif, gif and eps image formats are acceptable with CMYK model for colored image at a resolution of at least 300 dpi. Graphs must have the minimum quality: clear text, proportionate, not 3 dimensional and without disharmonic language. Electron photomicrographs should have internal scale markers.

If photographs of patients are used, either the subjects should not be identifiable or the photographs should be accompanied by written permission to use them. Permission forms are available from the Editorial Office.

Scientific illustrations will be created or recreated in-house. If an outside illustrator creates the figure, the *Journal of Advances in Environmental Health Research* reserves the right to modify or redraw it to meet our specifications for publication. The author must explicitly acquire all rights to the illustration from the artist in order for us to publish the illustration. Legends for figures should be an editable text as caption and should not appear on the figures.

References

The Vancouver style of referencing should be used. References must be double-spaced and numbered as **superscripts** consecutively as they are cited. References first cited in a table or figure legend should be numbered so that they will be in sequence with references cited in the text at the point where the table or figure is first mentioned. List all authors when there are six or fewer; when there are seven or more, list the first six, then "et al." The following are sample references:

1. Maleki A, Shahmoradi B, Daraei H, Kalantar E. Assessment of ultrasound irradiation on inactivation of gram negative and positive bacteria isolated from hospital in aqueous solution. J Adv Environ Health Res 2013; 1(1): 9-14.
2. Buckwalter JA, Marsh JL, Brown T, Amendola A, Martin JA. Articular cartilage injury. In: Robert L, Robert L, Joseph V, editors. Principles of Tissue Engineering. 3rd ed. Burlington, MA: Academic Press; 2007. p. 897-907.
3. Kuczmarski RJ, Ogden CL, Grammer-Strawn LM, Flegal KM, Guo SS, Wei R, et al. CDC growth charts: United States. Advance data from vital and health statistics. No. 314. Hyattsville, Md: National Center for Health Statistics, 2000. (DHHS publication no. (PHS) 2000-1250 0-0431)
4. World Health organization. Strategic directions for strengthening nursing and midwifery services [online]. Available from:
URL:http://www.wpro.who.int/themesfocuses/theme3/focus2/nursingmidwifery.pdf2002

Units of Measurement

Authors should express all measurements in conventional units, with Système International (SI) units given in parentheses throughout the text. Figures and tables should use conventional units, with conversion factors given in legends or footnotes. In accordance with the Uniform Requirements, however, manuscripts containing only SI units will not be returned for that reason.

Abbreviations

Except for units of measurement, abbreviations are discouraged. Consult Scientific Style and Format: The CBE Manual for Authors, Editors, and Publishers (Sixth edition. New York: Cambridge University Press, 1994) for lists of standard abbreviations. Except for units of measurement, the first time an abbreviation appears, it should be preceded by the words for which it stands.

Chemical Structure

Structures should be produced with a chemical drawing program, preferably ChemDraw 4.5 or higher, and submitted in TIFF format to allow use of electronic files in production. Structures should also be submitted in native file formats, e.g., RDX.

For any more detail about the writing style for your manuscripts refer to:
http://www.jaehr.muk.ac.ir

Authorship Form

Title of the manuscript:

....

....

We, the undersigned, certify that we take responsibility for the conduct of this study and for the analysis and interpretation of the data. We wrote this manuscript and are responsible for the decisions about it. Each of us meets the definition of an author as stated by the International Committee of Medical Journal Editors (see http://www.icmje.org/icmje-recommendations.pdf). We have seen and approved the final manuscript. Neither the article nor any essential part of it, including tables and figures, will be published or submitted elsewhere before appearing in the *Journal of Advances in Environmental Health Research* [All authors must sign this form or an equivalent letter.]

Name of Author	Contribution	Signature

Please scan this form and upload it as a supplementary file in "Step 4" of submitting articles.

Table of Contents

Spatial distribution of fluoride in groundwater resources in selected parts of Kurdistan Province, Iran, using the geographical information system

Pegah Bahmani[1], Afshin Maleki[1], Amir Hossein Mahvi[2], Hiua Daraei[1], Esmaeil Ghahremani[1], Dariush Naghipour-Khalkhaliani[3]

1 Environmental Health Research Center, Kurdistan University of Medical Sciences, Sanandaj, Iran
2 Center for Solid Waste Research, Institute for Environmental Research AND School of Public Health, Tehran University of Medical Sciences, Tehran, Iran
3 School of Health, Guilan University of Medical Sciences, Rasht, Iran

Original Article

Abstract

Fluoride in drinking water has a profound effect on teeth. Since drinking water is an important source of fluoride, the evaluation of the fluoride content of water resources is necessary. Temporal variations and spatial distribution of fluoride in drinking water of some selected parts of Kurdistan Province, Iran, have been studied using geographic information system (GIS) techniques. Thus, 40 villages were selected and 80 samples taken in two wet and dry seasons in 2013. Fluoride concentration was measured via ion chromatography (IC) method. Geospatial analysis of the data was performed using the ArcGIS software developed by Environmental Systems Research Institute (Esri). The results showed that the average fluoride concentration in drinking water ranged from 0.096 to 1.102 mg/l with the concentration being less than 0.50 mg F/l in 57 samples (71.25%), between 0.51 and 1.0 mg F/l in 21 samples (26.25 %), and greater than 1.0 mg F/l in 2 samples (2.5%). No difference was observed between the concentrations of fluoride in the two-stage sampling with the nonparametric Wilcoxon test (P > 0.01).

KEYWORDS: Fluoride, Spatial Distribution, Kurdistan, Iran

Citation: Bahmani P, Maleki A, Mahvi AH, Daraei H, Ghahremani E, Naghipour-Khalkhaliani D. **Spatial distribution of fluoride in groundwater resources in selected parts of Kurdistan Province, Iran, using the geographical information system.** J Adv Environ Health Res 2015; 3(2): 71-7.

Introduction

The chemical composition of groundwater is a function of various factors and the interaction of these factors results in different types of water that can affect water consumption purposes.[1-4] Among the various characteristics of water quality, fluoride has unique properties. Based on guidelines for drinking water quality, fluoride, arsenic, and nitrate are key chemicals which have large scale health effects through drinking water exposure.[5,6] Fluoride is one of the essential micronutrients for humans and animals. However, shortage or excess of fluoride can cause serious dental and health problems in humans.[7] Since drinking water is an important way of receiving fluoride,[8-11] the evaluation of the fluoride content of water resources is necessary.

The concentration of fluoride in groundwater is variable and depends on several factors such as the pH, temperature, and solubility of fluorine-bearing minerals and other cations in water.[1,9,12] Therefore, the amount of fluoride in water in different regions varies according to the

Corresponding Author:
Pegah Bahmani
Email: pegah_bahmani@yahoo.com

chemical composition of water and aquifer conditions.[13] Previous studies have shown different amounts of fluoride in drinking water resources of Kermanshah[14] (0.32 mg/l), Kerman[15] (0.17 mg/l), Ahvaz[16] (0.31-0.51 mg/l), Zanjan[17] (0.56 mg/l), Kashan[18] (0.25 mg/l), and Hamedan[19] (0.19 mg/l). These conditions expose consumers to different concentrations of fluoride, and thus, the health aspect of fluoride exposure in each region is different. Hence, it is necessary to determine the relationship between water quality parameters in order to analyze the dominant chemical compounds in water and their trends and aquifer conditions. Therefore, the present study was undertaken to investigate the concentration of F and its correlation with physicochemical parameters of rural drinking water resources in Kurdistan Province, Iran.

Materials and Methods

This cross-sectional study was performed to determine the quality of drinking water of 40 villages in Kurdistan Province. A total of 80 samples were collected in wet and dry seasons (June and September) and were analyzed according to standard methods.[20] The concentration of fluoride and other anions was measured using ion chromatography (IC) method (Metrohm Compact IC plus 882). Descriptive statistics were used to interpret the results. In order to compare the results of the two phases of the study and because the date distribution was not normal, a non-parametric test (Wilcoxon test) was applied using SPSS software for (version 20, SPSS Inc., Chicago, IL, USA). To determine the correlation between physical and chemical characteristics of water, the Pearson correlation coefficient was used. The temporal variations and spatial distribution of fluoride concentrations in rural drinking water resources were studied using geographical information system (ArcGIS) software.

Results and Discussion

Figure 1 illustrates the variation in fluoride concentration in the studied water supplies during wet and dry seasons. Based on figure 1 average fluoride concentration in groundwater samples varied from 0.1 mg/l in Shahrak to 0.97 mg/l in Bodla. According to drinking water quality standards set by the Institute of Standards and Industrial Research of Iran (ISIRI)[21] and World Health Organization (WHO),[5] in 70% of samples fluoride concentration was less than the permissible limit (0.5 mg/l). In addition, only in 30% of the samples, fluoride content was at a permissible level. These results are in agreement with that of the studies by Maleki et al.[7] and Carton,[22] which show the low fluoride content of drinking water in Sanandaj, Iran. Based on the results of water fluoride measurement, it is likely that the incidence of dental caries in the study area is high. Therefore, fluoride can be provided by other sources such as foodstuff, tea, and toothpastes. Water fluoridation is not recommended because it is not a preferred method in Iran. Moreover, Carton also opposed water fluoridation.[22] The Iranian Fluoride Scientific Association has stated that fluoride concentrations greater than 0.7 mg/l have more disadvantages in comparison to its scarcity.[11] Therefore, the continuous monitoring of the fluoride content of water and screening of dental caries, especially in children, are necessary.

The study of the relation between fluoride concentration and other water quality parameters is important in order to explain the changes of fluoride levels in the aquifer. Hence, correlational studies were performed and the results are shown in table 1. pH is an important parameter affecting the solubility of fluoride. Results showed that pH value varies from 7.1 to 8.7. This condition represents an alkaline condition and it is suitable for the solubility of fluorine-bearing minerals. Saxena and Ahmed stated that at alkaline pH, fluoride is released into the water; however, at acidic pH, it remains in the soil.[23] In addition, fluoride can be replaced with other anions; hence, Ca^{2+}, Na^+, and hydroxyl ion may alter the concentration of

fluoride in water resources.[24,25] Therefore, when the calcium concentration exceeds the solubility of fluorite, the dissolution of fluorite will be limited.[13] Raju et al. observed a strong inverse correlation between F and Ca^{2+} in groundwater with a Ca content higher than the solubility of fluoride minerals.[25] For this reason, the main water cations and anions were determined and the results are presented in tables 2 and 3.

According to these tables, the concentration of calcium and sodium in the studied samples vary from 34 to 194 mg/l and 10 to 160 mg/l, respectively. According to table 3, the average concentration of Ca^{2+} (74.95 mg/l) was higher than Na^+ (71 mg/l), which may be the reason for the low concentration of fluoride in groundwater. Evidently, low fluorine-bearing minerals in the soil should not be ignored.
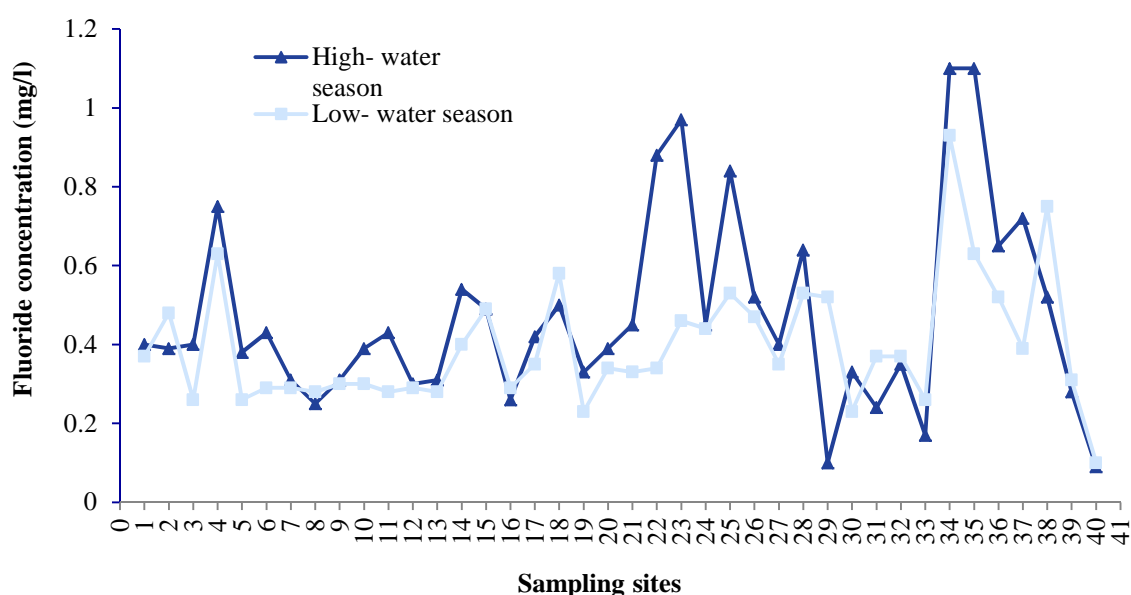
Figure 1. Fluoride concentration of different sampling sites in wet and dry seasons

Table 1. Correlation matrix of studied water quality parameters

	Ca	Mg	Na	K	F	HCO₃	Cl	SO₄	NO₃	TH	TDS	EC	pH
Ca	1												
Mg	0.71§	1											
Na	0.47§	0.58§	1										
K	0.27#	0.36*	0.19#	1									
F	0.29#	0.4*	0.15#	0.33*	1								
HCO₃	0.7§	0.51§	0.62§	0.27#	0.21	1							
Cl	0.62§	0.43§	0.64§	0.19#	0.12#	0.45§	1						
SO₄	0.57§	0.53§	0.80§	0.13#	0.002	0.33§	0.50§	1					
NO₃	0.06#	-0.12#	-0.12#	0.24#	016#	0.17#	-0.20#	0.04#	1				
TH	0.96§	0.87§	0.56§	0.37*	0.35*	0.88§	0.60§	0.61§	0.01#	1			
TDS	0.82§	0.84§	0.86§	0.34*	0.3#	0.9§	0.66§	0.77§	-0.02#	0.9§	1		
EC	0.82§	0.85§	0.86§	0.34*	0.31#	0.9§	0.65§	0.78§	0.02#	0.9§	0.99§	1	
pH	-0.27#	-0.25#	-0.24³#	-0.11#	-0.43§	-0.30#	-0.25³	-0.13#	0.14#	-0.27#	-0.27#	-0.28#	1

* Correlation is significant at the 0.05 level; § Correlation is significant at the 0.01 level; # Non-significant

TH: Total hardness; TDS: Total dissolved solid; EC: Electrical conductivity

Total dissolved solids (TDS) and electrical conductivity (EC) showed better correlation with fluoride than the other studied parameters. TDS amount in water samples ranged between 320 and 1270 mg/l. Calcium, magnesium, sodium, potassium, carbonate, bicarbonate, chloride, sulphate, and nitrates are the main ions that cause TDS.[26] Gillardet et al.[27] and Han et al.[28] announced that land use and environmental pollution caused by animal waste, agricultural fertilizers, and industrial and municipal wastewater may cause alteration in TDS. As seen in table 2, the mean concentration of total hardness of groundwater is higher than 270 mg/l CaCO₃.

Table 2. Average concentration of physicochemical parameters of groundwater in rural areas

| Village	Location Code	Ca	Mg	Na	K	SO$_4$	NO$_3$	CI	F	pH	TDS	EC	Alkalinity	TH
Amir Abad	1	80	11	37	9	17	20	10	0.39	7.5	490	715	260	240
Chomoghloo	2	46	9	64	5	16	16	7	0.44	7.7	430	650	232	148
Najafabad	3	65	19	56	1	34	8	6	0.33	7.6	520	795	282	240
Tazehabad	4	93	52	160	8	135	2	82	0.69	7.2	1270	1820	610	440
Bayeh	5	67	15	56	1	54	8	18	0.32	7.4	505	755	239	224
Zarinabad	6	57	24	51	2	26	17	14	0.36	7.3	510	770	266	240
Alahyari	7	64	2	49	2	25	17	13	0.30	7.3	400	595	195	160
Dirakloo	8	52	19	48	2	24	17	14	0.27	7.5	459	690	235	208
Muzafarabad	9	70	12	49	3	25	17	13	0.31	7.5	452	720	250	220
Zivieh	10	42	5	57	1	34	13	11	0.35	7.7	390	570	171	124
Saeedabad	11	67	9	31	1	7	23	8	0.36	7.3	395	590	210	200
Vinsar	12	98	15	123	2	166	37	31	0.30	7.5	815	1235	280	300
Ghandab Sufla	13	85	14	122	2	176	38	31	0.30	7.4	810	1240	230	260
Ghandab Olya	14	57	10	65	5	52	36	11	0.47	7.7	480	715	200	180
Dosar	15	82	20	102	6	77	32	45	0.49	7.2	725	1130	299	284
Babashaydolla	16	87	19	119	2	174	38	21	0.28	7.9	770	1200	245	288
Baharloo	17	82	13	118	2	158	36	29	0.39	7.9	809	1230	234	252
Jodaghyeh	18	103	28	84	7	70	23	30	0.54	7.6	815	1235	382	368
Miham Olya	19	49	14	19	1	11	12	4	0.28	7.5	320	470	178	172
Miham Sufla	20	65	16	35	1	14	19	12	0.37	7.4	450	660	234	224
Gharbelaghkhan	21	34	19	78	19	85	32	24	0.39	7.8	490	750	188	160
Qzblagh	22	116	33	55	9	59	8	30	0.61	8.0	800	1225	393	420
Kotan Sufla	23	148	33	55	18	59	206	81	0.71	8.3	925	1380	250	500
Maydanmofazar	24	101	25	29	9	16	20	11	0.44	7.9	665	938	365	352
Jafarabad	25	90	22	65	3	52	28	23	0.68	8.7	660	1010	310	311
Golblagh	26	67	19	43	1	19	38	8	0.50	8.6	490	715	246	240
Aqcheghonbad	27	194	6	124	4	163	6	167	0.38	8.0	1130	1660	375	500
Engiarkh	28	99	24	138	4	138	3	157	0.59	7.4	992	1460	360	342
Kharabechoaarkh	29	89	44	139	5	141	3	225	0.32	7.3	903	1500	166	398
Aghblagh Tghamin	30	77	15	17	1	9	17	9	0.28	7.9	425	630	227	248
Ochgol	31	58	2	29	1	6	32	4	0.31	8.0	330	477	160	150
Khosroabad	32	65	11	75	8	49	21	16	0.32	7.1	550	825	252	203
Aminabad	33	65	11	73	8	51	21	16	0.21	7.2	541	820	249	203
Bodla	34	49	11	72	1	15	38	5	0.97	8.0	465	700	237	164
Darvishkhaki	35	85	37	134	10	48	4	111	0.87	7.4	910	1460	400	360
Maghot	36	58	9	57	1	37	10	10	0.59	7.9	440	670	216	178
Babareshani	37	82	17	86	4	38	16	73	0.56	7.2	720	1020	264	270
Khandanqoli	38	69	25	88	2	53	37	27	0.64	7.5	650	1015	299	272
Dehragheh	39	65	12	37	1	10	46	5	0.30	7.7	420	630	210	208
Shahrak	40	59	11	10	1	12	1	10	0.10	7.4	330	473	190	190
Permissible maximum (mg/l) (ISIRI-1053)		250	50	200	-	400	50	400	1.50	-	1500	-	-	500
WHO guideline		-	-	200	-	500[**]	50	250[*]	1.5	6.5-8.5[*]	1500[*]	-	-	-

[*] Recommendation based on aesthetic consideration such as taste and color; [**] No health-based guideline value is set; however, values less than 500 mg/l are recommended due to gastrointestinal damage
TDS: Total dissolved solid; EC: Electrical conductivity; TH: Total hardness

Table 3. Descriptive statistics of elemental concentration for the studied parameters

Parameter	n (in each season)	Dry season				Wet season			
		Mean	SD	Min	Max	Mean	SD	Min	Max
EC	40	945.0	347.00	470.0	1820.0	816.0	312.00	110.0	1655.0
TDS	40	627.0	228.00	320.0	1270.0	564.0	188.00	290.0	1108.0
pH	40	7.6	0.35	7.0	8.7	7.5	0.22	6.8	8.0
Ca	40	78.5	27.30	34.0	194.0	71.4	21.30	32.0	166.0
Mg	40	17.9	10.90	2.0	52.0	13.6	6.80	3.0	41.0
Na	40	72.8	38.20	17.0	160.0	69.2	35.50	10.0	161.0
K	40	4.5	4.50	1.0	19.0	4.5	4.40	0.5	20.0
HCO$_3$	40	328	104.00	202.0	744.0	288.0	80.00	183.0	645.0
Cl	40	37.4	42.50	4.0	225.0	34.4	36.10	2.3	202.0
SO$_4$	40	59.1	53.20	6.0	176.0	61.0	48.50	6.0	168.0
F	40	0.4	0.14	0.1	0.9	0.5	0.09	1.1	0.7

EC: Electrical conductivity; TDS: Total dissolved solid; SD: Standard deviation
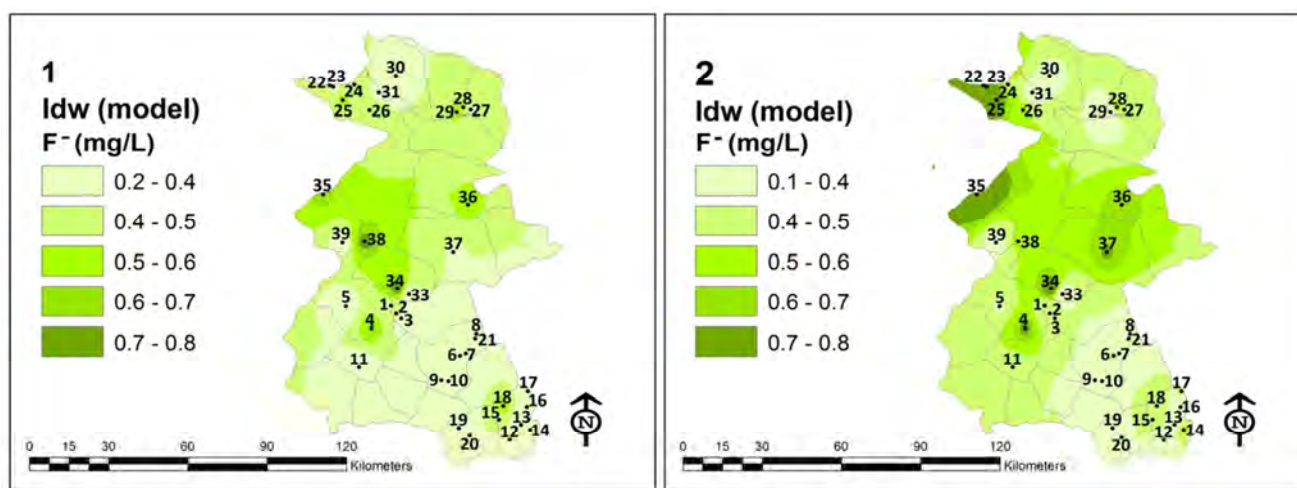
Figure 2. Spatial distribution of fluoride in groundwater in low and high water seasons

According to the finding of Govardhan Das, water with fluoride concentration of higher than 1.5 mg/l has a hardness of lower than 200 mg/l.[29] Thus, the relationship between water hardness and fluoride seems reasonable. A positive correlation was observed between fluoride and other anions and cations except pH. These results are similar to findings by other researchers.[4,9]

Except pH, EC (µS/cm), alkalinity (mg/l CaCO$_3$), and TH (mg/l CaCO$_3$), all other parameters are expressed in mg/l.

Figure 2 shows the spatial distribution of fluoride and reveals that high concentrations of fluoride can be seen in the northern part of the region. Statistical analysis (Wilcoxon test) demonstrated that there was no significant difference between the fluoride concentrations of samples collected in wet and dry seasons (P > 0.01).

Results also showed that the majority of anions and cations are within the standard ranges (except nitrate in one sample). The results showed that water hardness in all the villages is temporary hardness, which was categorized as completely hard, hard, and slightly hard. According to geochemical facies, calcium and bicarbonate are the dominant cation and anion, respectively, introducing calcic-bicarbonate as the water type. The high concentration of bicarbonate ions in the water is due to erosion and weathering of carbonate and silicate minerals. Correlation coefficients showed the highest correlation between bicarbonate and Ca^{2+} (Table 1).

Conclusion

The present study attempted to investigate the fluoride concentration of groundwater in rural areas of Northeastern Kurdistan Province, and its correlation with other physicochemical parameters of water quality. It was found that the groundwater is slightly alkaline and hard in nature. In 70% of samples, fluoride concentration was lower than the permissible limit set by ISIRI. Therefore, the continuous monitoring of the fluoride content of water and screening for dental caries especially in children are necessary.

Conflict of Interests

Authors have no conflict of interests.

Acknowledgements

References

1. Sharma P. Groundwater quality in some villages of rajasthan (India): focused on fluoride. Journal of Environmental Researh and Development 2007; 1(4): 383-91.
2. Andre L, Franceschi M, Pouchan P, Atteia O. Using geochemical data and modelling to enhance the understanding of groundwater flow in a regional deep aquifer, Aquitaine Basin, south-west of France. Journal of Hydrology 2005; 305(1–4): 40-62.
3. Ostovari Y, Zare Sh, Harchegani H, Asgari K. Effects of geological formation on groundwater quality in Lordegan Region, Chahar-mahal-va-Bakhtiyari, Iran. International Journal of Agriculture and Crop Sciences 2013; 5(17): 1983-92.
4. Maleki A, Teymouri P, Rahimi R, Rostami M, Amini H, Daraei H, et al. Assessment of chemical quality of drinking water in rural area of Qorveh city, Kurdistan province, Iran. J Adv Environ Health Res 2014; 2(1): 22-9.
5. World Health Organization. Guidelines for Drinking-Water Quality. Geneva, Switzerland: World Health Organization; 2011.
6. Mahvi AH, Zazoli MA, Younecian M, Nicpour B, Babapour A. Survey of Fluoride Concentration in Drinking Water Sources and Prevalence of DMFT in the 12 Years Old Students in Behshar City. Journal of Medical Sciences 2006; 6(4): 658-61.
7. Maleki A, Ghahremani E, Zandsalimi Y, Tymouri P, Daraei H, Rezaee R, et al. Temporal and spatial variation of drinking water quality in a number of Divandareh villages, Iran: with emphasis on fluoride distribution. J Adv Environ Health Res 2014; 2(3): 174-80.
8. Nouri J, Mahvi AH, Babaei AA. Regional pattern distribution of groundwater fluoride in the shush aquifer of Khuzestan County, Iran. Fluoride 2006; 39(4): 321-5.
9. Dobaradaran S, Mahvi AH, Dehdashti S, Dobaradaran S, Shoara R. Correlation of Fluoride with some inorganic constituents in groundwater of Dashtestan, Iran. Fluoride 2009; 42(1): 5-8.
10. Dobaradaran S, Mahvi AH, Dehdashti S. Drinking water fluoride and child dental caries in Dashtestan, Iran. Fluoride 2008; 41(3): 220-6.
11. Dobaradaran S, Mahvi AH., Dehdashti S. Fluoride content of bottled drinking water available in Iran. Fluoride 2008; 41(1): 93-4.
12. Jeong CH. Effect of land use and urbanization on hydrochemistry and contamination of groundwater from Taejon area, Korea. Journal of Hydrology 2001; 253(1–4): 194-210.
13. Raju NJ., Dey S, Das K. Fluoride contamination in groundwaters of Sonbhadra District, Uttar Pradesh, India. Current Science 2009; 96(7): 979-85.
14. Sharafi K, Karami A, Pirsaheb M, Moradi M. Physicochemical Quality of Drinking Water of Kermanshah Province. Zahedan J Res Med Sci 2013; 15(12): 44. [In Persian].
15. Pooreslami H, Khazaeli P, Masoodpoor H. Fluoride Content of Drinking Waters in Kerman/Iran. J Kerman Univ Med Sci 2008; 15(3): 5-9. [In Persian].
16. Basir L, Khanehmasdjedi M, Haghighi M, Ne'mati asl S. Evaluation and comparison of floozies and DMFT and their relation with the amount of fluoride in three flowing source of drinking water (Karoon, Maroon, Karkheh) in 12-15 years old students in Khozestan 2002. J Dent Sch Shahid Beheshti Univ Med Sci 2006; 24(1): 14-23. [In Persian].
17. Nasehi Nia HR, Naseri H. A survey of fluoride dosage in drinking water and DMF index in Damghan city. Journal of Water and Wastewater 2014; 15(8): 70-2. [In Persian].
18. Mostafaie G, Rabani D, Iranshahi L. Quality of drinking water in Kashan in 1999-2000. Feyz 2003; 7(1): 13-9. [In Persian].
19. Samarghandi MR, Sadri GH. The amount of fluoride in the drinking water distribution network from the cities of Hamadan and the Bahar of the year 1999-2000. Sci J Hamdan Univ Med Sci 2001; 8(3): 42-7. [In Persian].

20. Eaton AD, Franson MA. Standard Methods for the Examination of Water & Wastewater. Washington, DC: American Public Health Association; 2005.

21. Institute of Standards and Industrial Research of Iran. Drinking water-Physical and chemical specifications. ISIRI-1053 [Online]. [cited 1991]; Available from: URL: http:// www. isiri.org/portal/files/std/213.pdf

22. Carton RJ. Review of the 2006 united states national research council report: fluoride in drinking water. Fluoride 2006; 39(3): 163-72.

23. Saxena V, Ahmed S. Dissolution of fluoride in groundwater: a water-rock interaction study. Environmental Geology 2001; 40(9): 1084.

24. Wenzel W, Blum WE. Fluorine speciation and mobility in f-contaminated soils. Soil Science 1992; 153(5): 357-64.

25. Raju DV, Raju NJ, Kotaiah B. Complexation of Fluoride Ions with Alum-Flocs at Various pH Values during Coagulation and Flocculation. J Geol Soc India 1993; 42(1): 51-4.

26. United States.Environmental Protection Agency. Quality criteria for water. Washington, DC: U.S. Environmental Protection Agency; 1976.

27. Gillardet J, Dupre B, Louvat P, Allegre CJ. Global silicate weathering and CO2 consumption rates deduced from the chemistry of large rivers. Chemical Geology 1999; 159(1–4): 3-30.

28. Han G, Liu CQ. Water geochemistry controlled by carbonate dissolution: A study of the river waters draining karst-dominated terrain, Guizhou Province, China. Chemical Geology 2004; 204(1–2): 1-21.

29. Govardhan Das SV. The fluoride problem-options for community water supply in Andhra Pradesh (India), [Project]. Leicestershire, UK: Water, Engineering and Development Centre, Lough Borough University of Technology; 1994.

Macroinvertebrate diversity indices: A quantitative bioassessment of ecological health status of an oxbow lake in Eastern India

Dipankar Ghosh[1], Jayanta Kumar Biswas[1]

1 Department of Ecological Engineering and Environmental Management, University of Kalyani, Kalyani, India

Original Article

Abstract

Aquatic macroinvertebrates, which play a significant role in the food chain of an ecosystem, are used in fresh water quality assessment to identify the environmental stress resulting from a variety of anthropogenic disturbances. Seasonal surveys of macroinvertebrate communities were conducted from April 2013 to March 2014 in Chhariganga oxbow lake of Nadia District of West Bengal, an eastern state of India. In order to bioassess water quality and aquatic health analysis using diversity indices, viz. Shannon-Wiener and Simpson's diversity index, species richness and evenness, and total abundance with composition trends were carried out. Taxon richness values of 14, 14, and 18, evenness values of 0.80, 0.71, and 0.73, Shannon-Wiener Index values of 2.10, 1.88, and 2.12, and Simpson's index values of 0.15, 0.22, and 0.20 were determined for macroinvertebrates found during pre-monsoon, monsoon, and post-monsoon period, respectively. In the present study, low diversity indices, like the Shannon-Wiener Index, demonstrated clearly that the selected lake is polluted and has high anthropogenic activity which has rendered the lake bad to poor health status especially during monsoon season. Therefore, it is necessary to regulate and prevent the jute retting process, and its intensity and density during the monsoon to enhance biodiversity in order to ensure sustainable management and conservation of aquatic environment of the oxbow lake.

KEYWORDS: Oxbow Lake, Macroinvertebrate, Diversity Index, Aquatic Health, Bioassessment

Citation: Ghosh D, Biswas JK. **Macroinvertebrate diversity indices: A quantitative bioassessment of ecological health status of an oxbow lake in Eastern India.** J Adv Environ Health Res 2015; 3(2): 78-90.

Introduction

Macroinvertebrates include those "organisms large enough to be caught with a net or retained on a sieve with a mesh size of 250-1000μ".[1] These organisms can be benthic, inhabiting substrates like sediments, debris, or logs, or pelagic, swimming freely in the water column. They play an essential role in the aquatic habitat and food web. Apart from fishery resources and periphyton, ecological assessment of aquatic systems using macroinvertebrates has been one of the frequently used protocols for indication of water quality in standard water management. Macroinvertebrate abundance, community structure, and ecological function have long been used to characterize water quality in freshwater ecosystems. While many taxa contribute to biodiversity in stream ecosystems, macroinvertebrates play a central ecological role in many stream ecosystems and are among the most ubiquitous and diverse organisms in fresh waters.[2] Because of their cosmopolitan nature, inhabiting all freshwater habitats of the world, macroinvertebrates are not only useful as bioindicators, but helpful in ameliorating polluted water. As they have low mobility (i.e.,

---

Corresponding Author:
Jayanta Kumar Biswas
Email: biswajoy2000@yahoo.com

sedentary, sessile, or nearly sedentary) and life cycles of several weeks and or years, they reflect cumulative effects of the present and past conditions of an aquatic ecosystem. They can often be extremely productive and abundant and are good indicators of environmental conditions, toxic contamination for localized conditions and site specific impacts, and changing water qualities. They make a good study specimen, because they are abundant, readily surveyed, and taxonomically rich[3] and easy to collect and identify.[1,4] Macroinvertebrates usually consist of a heterogeneous collection of evolutionary diverse taxa. For that reason, different species will react to different changes in aquatic environment, natural as well as imposed, and physical as well as chemical.[1] The use of benthic macroinvertebrates to assess the overall health status of aquatic environments remains the most suitable, reliable, and widely acclaimed method globally. The qualitative and quantitative studies of their diversity are of great importance.

Benthic invertebrates were used as bioindicators for studies of the impact of environmental perturbations on the aquatic ecosystems.[5,6] Macroinvertebrates are attractive targets of biological monitoring efforts as they are a diverse group of long-lived, sedentary species that react strongly and often, predictably to human influence on aquatic ecosystems.[7] They are most frequently used in biomonitoring studies as their responses to organic and inorganic pollution have been extensively documented.[8,9] The use of benthic macroinvertebrates has been discussed in the assessment of freshwater bodies.[10] They have sensitive life stages that respond to stress and integrate effects of both short-term and long-term environmental stressors[11] and are important areas for maintaining biodiversity.[12,13] Macroinvertebrates and water quality are interrelated; thus, macroinvertebrates are a potential indicator of water quality.[14] They are more efficient bioindicators in understanding the ecological health of an aquatic ecosystem, compared to chemical and microbiological data, which at least illustrate short-term fluctuations.[15-17] Biomonitoring studies with the use of macroinvertebrates to rate the quality of both lotic and lentic water bodies have been widely reviewed.[18-21]

However, the use of aquatic macroinvertebrate in bioassessment of water quality and aquatic health in India has rather limited documentations.[22-30] Few studies have been carried out on its ecological aspects in oxbow lakes. Greater macroinvertebrate diversity was observed in the lentic system of the Hansadanga Beel oxbow lake, than other biotic communities. The Hansadanga Beel oxbow lake is situated at longitude 88° 33/E, latitude 23° 24/N, in Nadia district of West Bengal, an eastern province of India. Its anthropogenic activities were observed to be influencing the changing of sediment redox potential values for alteration of macroinvertebrate communities in the water body.[31] The diversity analysis of benthic macroinvertebrates of West Bengal oxbow lake ecosystems and their role in the assessment of water quality and aquatic health are not well known. Existing works on the macrobenthic fauna of the oxbow lakes in Nadia District, in particular, and West Bengal, in general, are quite scanty. Therefore, a survey of macroinvertebrate communities and an analysis of macroinvertebrates were performed using diversity indices and structure and composition trends with abundance in an oxbow lake ecosystem in Nadia District, India. They were conducted for the quantitative and biological assessment of aquatic health status of the oxbow lake ecosystem.

Materials and Methods

The Chhariganga oxbow lake, abandoned, fractioned, and derived from the river Ganga is located in Nakashipara development block of

Nadia District, West Bengal, an eastern Indian province. It is situated at 23.5800° N latitude, 88.3500° E longitude, about 90 Km from the Kalyani University Campus, Nadia, and nearly 40 Km from the line of Tropic of Cancer towards the north. It is a fresh water source and semi-open type oxbow lake, and receives water from the river Ganga during monsoon season through a narrow channel at the North East corner of a loop of the river. The oxbow lake is spread over an area of 145.69 acres with an annual average depth of 8.5 ft. It also stores rain water. The catchment area of the oxbow lake is nearly 600 hectares (Figure 1).

In the changed climate of this region, three distinct annual seasons are observed; the monsoon or rainy season generally from July to October, post-monsoon season or winter from November to February, and pre-monsoon or dry season from March to June. There was an occasional inundation of the surrounding banks during the monsoon. The oxbow lake is subjected to all forms of human activities including jute retting during monsoon season, agriculture, and fishing. It is the only source of irrigation water to the immediate agriculture communities.

The methods by which macroinvertebrates are collected in aquatic systems can be diverse, depending on the physical characteristics of the aquatic habitat. In shallow waters, samples can be collected using kick sampling technique with a hand net, whereas deeper waters require larger instruments like grab sampler. In this study, we collected benthic macroinvertebrates from the oxbow lake during the three seasons, viz. pre-monsoon, monsoon, and post-monsoon seasons, from April 2013 to March 2014. We collected the organisms using a D-frame net (0.5 mm mesh) and following hand picking method. We took the samples at 1 × 1 m locations from an area of nearly 100 m^2 in order to include all possible microhabitats. In some areas with the presence of large bushes, we first picked out the bushes and washed them into the net to remove pupae and other attached macro-invertebrates. For the bank-roots and macrophytes, we collected benthic invertebrates using a hand net made of mesh bolting silk of 100 µm. We collected the sediment in a plastic container of 15 l volume. Water was added and stirred vigorously while the floating fauna were sieved using 250 µm size sieve and the un-floated fauna were handpicked. Mud samples of 1 l were collected from the bottom of the lake using an Ekman grab. All the animals collected were immediately fixed in formaldehyde (4%) in the field, and then, transferred to 70% ethyl alcohol for preservation. In general, macroinvertebrates are taxonomically identified using key identification guides, and some samples may require examination under a dissection microscope.[1]

Figure 1. Map showing the study area

Identification can be carried out at two possible levels; family or genus/species. Genus/species level identification provides more accurate information on ecological condition and population sensitivity, but identification at family level awards more precision to the taxonomists, and thus, requires less expertise and time to complete.[4] In this study, macroinvertebrates were sorted and identified to the lowest possible taxon (species/genus or families) and counted under a stereomicroscope in the laboratory with the help of an identification manual and literatures.[32-38]

To understand a particular biotic community, it is very important to attain certain indices for the purpose of community analysis of the macroinvertebrates. Most assessment methods for macroinvertebrates are taxonomical, whereby analysis of a particular species, groups, or population is carried out.[1] The assessment of these groups can further be conducted in either of three approaches; saprobic, diversity, and biotic approaches. Saprobic approach indicates specific tolerance to pollution by a specific indicator species, whereas diversity approach utilizes the community structure as evaluation for ecosystem health. The biotic approach combines both saprobic and diversity approaches in the assessment of water quality. Examples of indices used in macroinvertebrate study are the Shannon-Wiener diversity index (H′), Family Biotic Index (FBI), and Biological Monitoring Work Party (BMWP). The biotic index and score systems are efficient in assessing organic pollution and eutrophication, but poor in assessing toxic and physical pollution. Low diversity indicates low quality and high diversity indicates good quality of water. Therefore, to obtain a fair overall assessment of the quality of a water body, both methods are essential and need to be combined with alternative methods of evaluating biota response.[39] Washington believes diversity measures are useful for describing community structure, but not the pollution level of water bodies.[40] The same author maintains that biotic indices must be limited to environments polluted with easily degradable organic matter (sewage) and not by other types of pollutants.[40] Benthic macroinvertebrate species are differentially sensitive to many biotic and abiotic factors in their environment. Consequently, macroinvertebrate community structure has commonly been used as an indicator of the condition of an aquatic system.[41] Diversity indices are efficient in indicating physical and toxic pollution which stress most species in a community without encouraging replacement species. However, although high diversity does indicate good quality water, low diversity may not necessarily indicate low quality. To evaluate the distribution and diversity between sampling sites, community indices such as abundance, richness, evenness, and the Simpson and Shannon-Wiener diversity indices were used. Statistical analysis of biological indices, such as taxa richness, evenness (E), and the Shannon-Wiener and Simpson's diversity indices was performed using diversity index formulas 1 and 2.

(1) Simpson's index (D)[42]: $D = \Sigma \, (p_i)^2$

where p_i is the proportion of important value of the ith taxon ($p_i = n_i/N$), n_i is the importance value index of ith taxon, and N is the importance value index of all the taxa).

Simpson's index gives relatively little weight to the rare taxa and more weight to the common taxa. It weighs towards the abundance of the most common taxon. It ranges in value from 0 (low diversity) to a maximum of 1-1/s, where s is the number of taxon.

(2) Shannon-Wiener Index (H′) [43]: $H' = - \Sigma \, p_i \log p_i$

where p_i is the proportion of importance value of the ith taxon ($p_i = n_i/N$, n_i is the

importance value of ith taxon and N is the importance value of all the taxa).

This diversity index helps in calculation of taxon relative abundance. A large H value indicates greater diversity, as influenced by a greater number and/or a more equitable distribution of taxon. The index values range between 0 and 5, where higher index values demonstrate higher diversity, while low index values are considered to indicate pollution. Diversity and anthropogenic disturbances are inversely related. The Shannon-Wiener index takes account of taxon richness as well as abundance. It is simply the information entropy of the distribution, treating genus as symbols and their relative population sizes as the probability. The advantage of this index is that it takes into account the number of taxon and the evenness of the taxon. The index is increased either by having additional unique taxon, or by having greater taxon evenness. The Evenness Index is the relative distribution of individuals among taxonomic groups within a community and is expressed as:

Evenness Index (E).[44]: E= H′/logS

where H′ is the Shannon–Wiener Diversity Index, and log S is the natural log of the total number of taxon (S defined as taxon richness) recorded. It is used for the degree to which the abundances are equal among the groups present in a sample or community.

Results and Discussion

Macroinvertebrates' seasonal occurrence, compositions, and diversity indices are illustrated in table 1. Phylum Arthropoda (Class Insecta) accounted for 64.34% (83 no/m²), 94.15% (338 no/m²), and 82.72% (158 no/m²) of total macroinvertebrates surveyed during pre-monsoon, monsoon, and post-monsoon periods, respectively. Water scorpion dominated this Class Insecta during all seasons from April 2013 to March 2014. Dragonfly larvae and water strider was found the least during pre-monsoon, dragonfly larvae and damselfly larvae during

monsoon, non-biting midge larvae/blood worm during post-monsoon in this class. Phylum Arthropoda (Class Crustacea) accounted for 0.78% (1 no/m²), 1.39% (5 no/m²), and 7.33% (14 no/m²) of total macroinvertebrates surveyed during pre-monsoon, monsoon, and post-monsoon periods, respectively. While prawn dominated the class during pre-monsoon and monsoon periods, freshwater crab dominated the class during post-monsoon period. Fresh water mite (Family: Limnocharidae) representing Phylum Arthropoda (Class Arachnida) was found to be the lone macro-invertebrate during post-monsoon period in 2013-2014 with 0.52% (1 no/m²) of total macroinvertebrates surveyed. Right handed freshwater gilled snail with 24.81% (32 no/m²) dominated Phylum Mollusca during pre-monsoon period, when left handed freshwater pouch snail occurred the least with 2.33% (3 no/m²). Left handed freshwater pouch snail was found (7 no/m²) to be the single Mollascan with 1.95% of the total macroinvertebrates during monsoon period. It was dominant with 3.14% during post-monsoon period, while freshwater mussel was found to be the least with 1.05% in the oxbow lake. Aquatic segmented earth worm in the Phylum Annelida was dominant during all the seasons. Leeches were present only during post-monsoon period in that phylum. Average abundance of macroinvertebrates was found to be 129, 359, and 191 numbers, while average biomass was weighed at 95.64, 286.65, and 178.56 gm/m² of the lake water, respectively, during pre-monsoon, monsoon, and post-monsoon periods. Macroinvertebrates' richness of 14, 14, and 18, taxon evenness values of 0.80, 0.71, and 0.73, Shannon-Wiener Index values of 2.10, 1.88, and 2.12, and Simpson Index values of 0.15, 0.22, and 0.20 were determined for macroinvertebrates found during the three seasons, respectively. Seasonal compositions and diversity indices of macroinvertebrate occurrence in phyla are presented in table 2.

Shannon-Wiener Index values of 0.73, 0.29, and 0.65, evenness values of 0.52, 0.21, and 0.40, and Simpson Index values of 0.53, 0.89, and 0.69 were observed, respectively, during the three seasons for macroinvertebrates when occurred in different phyla. Seasonal occurrence, compositions, and diversity indices of different groups found in each phylum are given in table 3. Shannon-Wiener Index values of 0.99, 0.90, and 1.27, evenness values of 0.71, 0.65, and 0.79, and Simpson Index values of 0.43, 0.51, and 0.33 were obtained during the three seasons for the macroinvertebrate groups when occurred in each phylum. Figure 2 depicts the seasonal variations in occurrence while figure 3 demonstrates seasonal variations in macroinvertebrates' diversity indices. Seasonal variations in phyla diversity indices are illustrated in figure 4. Figure 5 highlights the seasonal variations in group diversity indices while figure 6 accommodates variations in numbers in phyla in a year. Seasonal variations in occurrence of groups in each phylum are shown in figure 7.

Table 1. Seasonal distributions and diversity indices of macroinvertebrates

Macroinvertebrate (Common Name)	Taxa	PRM	PRM	MON	MON	POM	POM
		no	%	no	%	no	%
Phylum Arthropoda Class Insecta							
Riffle beetle/larvae and Beetle	Coleoptera (family Elmidae)	11.00	8.53	-	-	5.00	2.62
Dragonfly larvae	Odonata (family Gomphidae)	1.00	0.78	3.00	0.84	2.00	1.05
Non-biting midge larvae/blood worm	Chironomidae (family)	-	-	5.00	1.39	1.00	0.52
Biting midge larvae	Ceratopogonidae (family)	3.00	2.33	19.00	5.29	9.00	4.71
Damselfly larvae	Odonata (order)	-	-	3.00	0.84	-	-
Water boatmen	Corixidae (family)	6.00	4.65	17.00	4.74	15.00	7.85
Water scorpion	Nepidae (family)	32.00	24.81	126.00	35.10	76.00	39.79
Water measurer	Hydrometridae (family)	11.00	8.53	56.00	15.60	22.00	11.52
Water strider	Gerridae (family)	1.00	0.78	13.00	3.62	5.00	2.62
Water scavenger beetle adult/larvae	Hydrophilidae (family)	15.00	11.63	89.00	24.79	21.00	10.99
Mosquito larvae and pupae	Culicidae (family)	3.00	2.33	7.00	1.95	2.00	1.05
Phylum Arthropoda Class Crustacea							
Freshwater prawn	Decapoda (order)	1.00	0.78	3.00	0.84	2.00	1.05
Freshwater crab	Decapoda (order)	-	-	2.00	0.56	12.00	6.28
Phylum Arthropoda Class Arachnida							
Fresh Water mite	Acarina (family Limnocharidae)	-	-	-	-	1.00	0.52
Phylum Mollusca							
Freshwater mussel	Bivalvia (class)	9.00	6.98	-	-	2.00	1.05
Freshwater snail (Right handed gilled)	Gastropoda (class)	32.00	24.81	-	-	6.00	3.14
Freshwater snail (Left handed pouch)	Viviparidae (family)	3.00	2.33	7.00	1.95	6.00	3.14
Phylum Annelida							
Leeches	Hirudinea (class)	-	-	-	-	1.00	0.52
Segmented worm (aquatic earthworm)	Oligochaeta (class)	1.00	0.78	9.00	2.51	3.00	1.57
Average abundance [no/m^2]		129.00	100	359.00	100	191.00	100
Average Biomass (gm/m^2)		95.64		286.65		178.56	
Macroinvertebrate richness		14.00		14.00		18.00	
Shannon-Wiener Index		2.10		1.88		2.12	
Taxon evenness		0.80		0.71		0.73	
Simpson's Index		0.15		0.22		0.20	

PRM: Premonsoon; MON: Monsoon; POM: Postmonsoon

Table 2. Seasonal phyla compositions and diversity indices of macroinvertebrates

Occurrence in Phyla	PRM	PRM	MON	MON	POM	POM
	no	%	no	%	no	%
Phylum Arthropoda Class Insecta	83.00	64.34	338.00	94.15	158.00	82.72
Phylum Arthropoda Class Crustacea	1.00	0.78	5.00	1.39	14.00	7.33
Phylum Arthropoda Class Arachnida	0	0	0	0	1.00	0.52
Phylum Mollusca	44.00	34.11	7.00	1.95	14.00	7.33
Phylum Annelida	1.00	0.78	9.00	2.51	4.00	2.09
Total abundance (no/m^2)	129.00	100	359.00	100	191.00	100
Phyla richness	4.00		4.00		5.00	
Shannon-Wiener Index	0.73		0.29		0.65	
Phyla evenness	0.52		0.21		0.40	
Simpson's Index	0.53		0.89		0.69	

PRM: Premonsoon; MON: Monsoon; POM: Postmonsoon

Table 3. Taxon frequency distributions and diversity indices of macroinvertebrates

Occurrence of group in each phylum	PRM	PRM	MON	MON	POM	POM
	no	%	no	%	no	%
Phylum Arthropoda Class Insecta	9.00	64.29	10.00	71.43	10.00	55.56
Phylum Arthropoda Class Crustacea	1.00	7.14	2.00	14.29	2.00	11.11
Phylum Arthropoda Class Arachnida	0	0	0	0	1.00	5.56
Phylum Mollusca	3.00	21.43	1.00	7.14	3.00	16.67
Phylum Annelida	1.00	7.14	1.00	7.14	2.00	11.11
Group richness	14.00	100	14.00	100	18.00	100
Phyla richness	4.00		4.00		5.00	
Shannon-Wiener Index	0.99		0.90		1.27	
Group evenness	0.71		0.65		0.79	
Simpson's Index	0.43		0.51		0.33	

PRM: Premonsoon; MON: Monsoon; POM: Postmonsoon
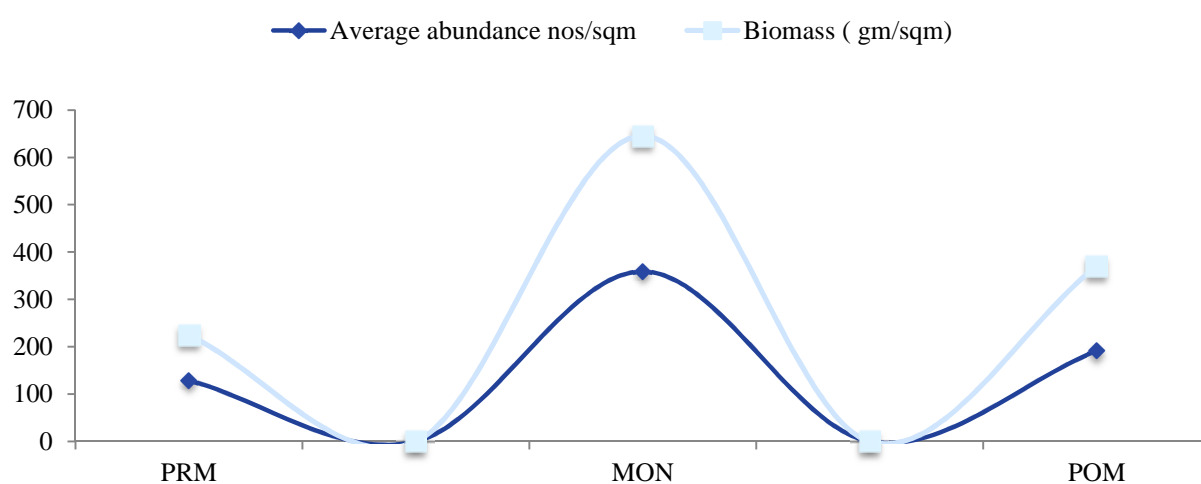
Figure 2. Seasonal variations in occurrence of macroinvertebrates
PRM: Premonsoon; MON: Monsoon; POM: Postmonsoon

http://jaehr.muk.ac.ir
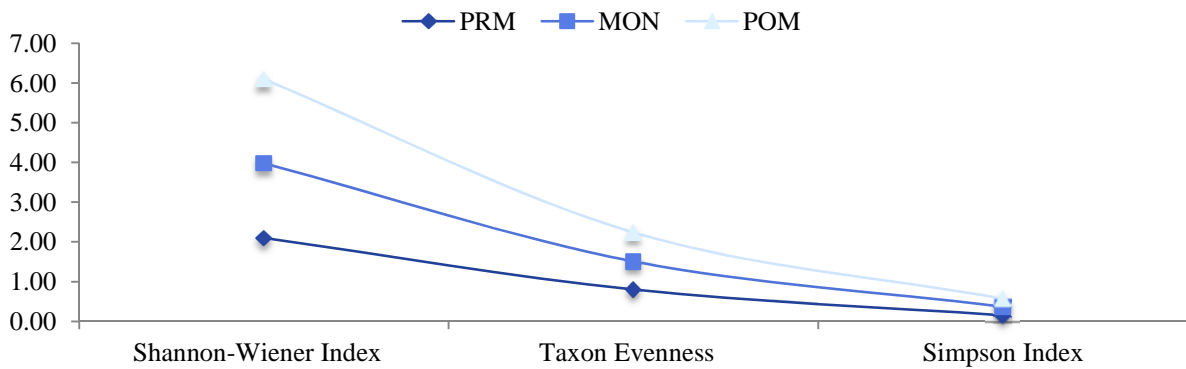
Figure 3. Seasonal variations in macroinvertebrate diversity indices
PRM: Premonsoon; MON: Monsoon; POM: Postmonsoon
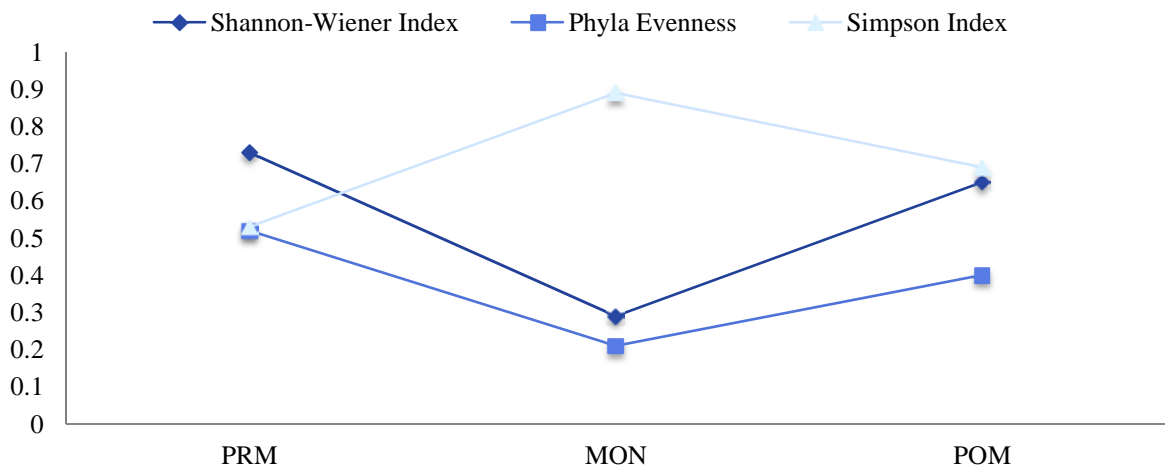
Figure 4. Seasonal variations in phyla diversity indices of macroinvertebrates
PRM: Premonsoon; MON: Monsoon; POM: Postmonsoon
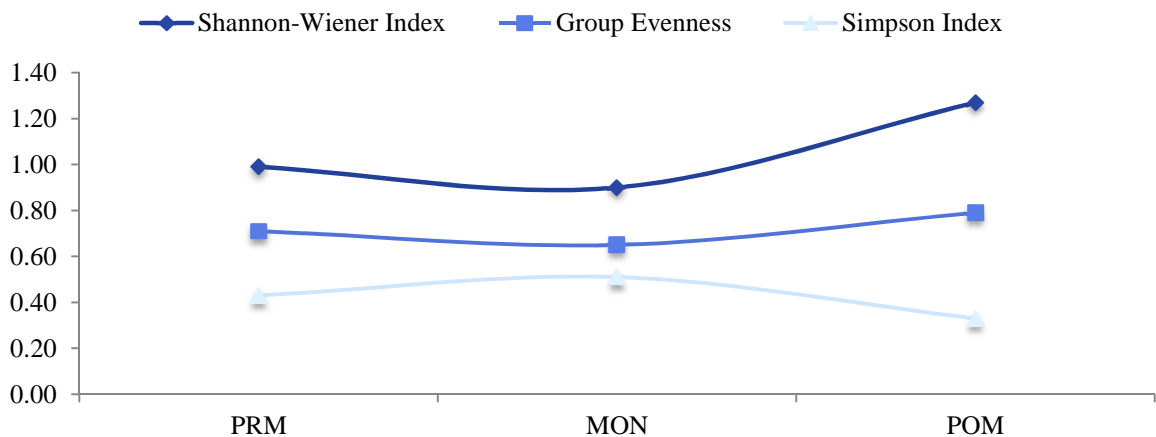
Figure 5. Variations in taxon frequency diversity indices of macroinvertebrates
PRM: Premonsoon; MON: Monsoon; POM: Postmonsoon
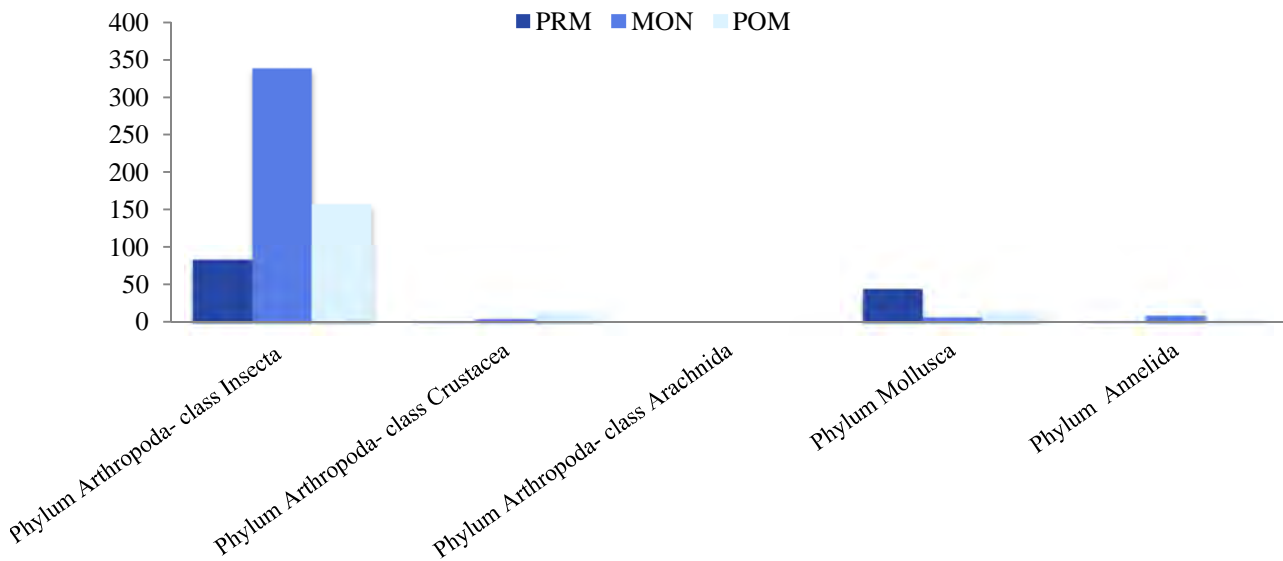
Figure 6. Variations in numbers of macroinvertebrates grouped in phyla in a year
PRM: Premonsoon; MON: Monsoon; POM: Postmonsoon
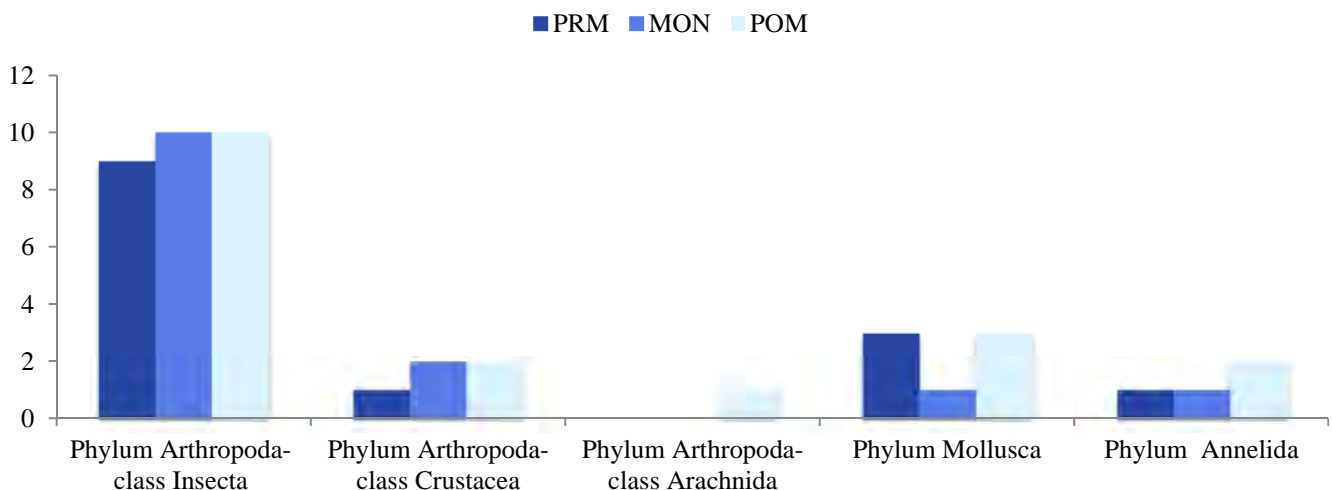
Figure 7. Seasonal variations in taxon frequency distributions
PRM: Premonsoon; MON: Monsoon; POM: Postmonsoon

Lower Shannon-Wiener diversity indices were observed during jute retting during monsoon period. The same decrease in diversity index was reported during October[45] and was attributed to emergence of several groups of aquatic insects prior to sampling or some movement into shallower parts of the lake during the hottest time of the year. Similarly, diversity index for the different species was generally low in the coconut husk retting zones (0.68 to 1.20) when compared to the non-retting zones (0.88 to 2.97) of Kerala backwaters in India.[22] Lower Shannon-Wiener diversity index values were found between 0.67 and 1.77 using macroinvertebrates in Bangalore lakes.[23] Shannon-Wiener diversity index of quite similar patterns were also reported[24] (1.28 to 2.31) with maximum and (0.27 to 1.53) minimum values which are much lower than the present findings. Seasonal

change was found; like lowest Shannon-Wiener diversity index during October and highest during July. The change was attributed to poor water exchange insufficient for self-purification. In that study,[24] insecta (Chironomidae and Culicidae) showed higher incidence in the coconut husk retting zones when compared to non-retting zones in lakes. Macroinvertebrate diversity index values from 0.49 to 1.40 and dominance index of between 0.30 and 0.72 are reported in tropical urban wetlands in Bangalore.[25] Shannon-Wiener index values of 1.8-3.07 with macroinvertebrates were found in a lake in Turkey[46], the lower value of which is in agreement with the findings of the present study. Lower Shannon-Wiener diversity values (0.35-1.81) and similar low Simpson's diversity index values (0.20-0.79) were observed in Bangalore inlets.[26] Evenness was found at quite similar range (0.56 to 0.97) in inlets in Bangalore. Much lower values of Shannon-Wiener Index (0.30-0.69) and quite similar evenness index values (0.53-0.97), using aquatic insects, were also reported for oxbow lake water in Assam.[27] Macroinvertebrate fauna species density values of 140–1113 no/m², which is quite similar or a little higher than that of the present study (129-359 no/m²) were observed in mangrove ecosystem in India.[28] Moreover, compared to the present study results, quite similar dominance values of 0.17-0.50, almost similar diversity values of 1.80-2.83, and quite similar evenness values of 0.45-0.72 were observed.[28] Almost similar Shannon-Weiner diversity index values of macroinvertebrates (2.00 to 2.38) were observed in oxbow lakes in Assam. [30] They concluded that there was a good diversity in oxbow lakes in Assam where evenness index values (0.45-0.56) were lower than that of this study.[30] Quite similar Shannon-Wiener diversity (H) values (1.967-2.625), lower evenness (E) values (0.357-0.600), and higher dominance index (C) values (0.776- 0.903) were

also observed in south Nigerian rivers.[47] Quite smaller Shannon-Wiener diversity index values of macroinvertebrate community were observed in Hansadanga Beel, an oxbow lake in Nadia District.[31] They were within the range of 0.943-1.551 (with average values of 1.231 in premonsoon, 1.473 in monsoon, and 1.113 in postmonsoon period) which indicates an intermediate scale of pollution.[31]

The Shannon-Wiener Index was found to be the most reliable in assessing river water quality using macrozoobenthos.[48] According to the Water Framework Directive, the relationship between the indices and ecological level is as follows: high status: higher than 4 bits/individual, good status: 4-3 bits/individual, moderate status: 3-2 bits/individual, poor status: 2-1 bits/individual, and bad status: 1-0 bits/individual.[49] Shannon-Wiener Index values of macro-invertebrates in all the cases from April 2013 to March 2014 in this study (showed lowest values during monsoon, unlike the Simpson Index values which were highest, especially during monsoon) ranged from 0.29 to 2.12. The lower index values thus efficiently and reliably suggested the bad to poor state of the aquatic health of this semi-closed oxbow lake ecosystem with an indication to pollution. These findings prove once again that diversity and anthropogenic disturbances are inversely related. This pollution status showed similarity to assessment results of diversity indices of rotifer,[50] zooplankton,[51] phytoplankton,[52] and macrophytes[53] on the same oxbow lake during the same time period as the study.

Conclusion

The purpose of the present investigation was to present a general account of benthic macroinvertebrates' composition and diversity to rate the aquatic health status using the aquatic benthic fauna. Low diversity values of Shannon-Wiener and Simpson indices in the present study clearly

show that the selected lake is polluted and has high anthropogenic activity. Hence, this lake is not suitable for growth of fish especially during monsoon season. Therefore, it is necessary to regulate and prevent jute retting processes, and their intensity and density in the lake during the monsoon to enhance biodiversity in order to ensure sustainable management and conservation of aquatic environment of this oxbow lake. It was also proven that biological data are useful for the detection of pollution. To understand the lake ecosystem and its health, understanding about the ecology (life cycle and secondary production) of macroinvertebrates is necessary. Thus, the study would hopefully be a reference archive for future studies on aquatic health of oxbow lake ecosystems in the region. The information obtained is crucial in serving as baseline data for various agencies, including governmental academic, and nongovernmental institutions, to take actions for more efficient sustainable management of this oxbow lake in particular and others in the country in general.

Conflict of Interests

Authors have no conflict of interests.

Acknowledgements

References

1. Ziglio G, Flaim G, Siligardi M. Biological Monitoring of Rivers.Volume 2 of Water Quality Measurements. New Jersey, NJ: Wiley; 2006.
2. Strayer DL. Challenges for freshwater invertebrate conservation. Journal of the North American Benthological Society 2006; 25(2): 271-87.
3. Dodson SI, Lillie RA. Zooplankton communities of restored depressional wetlands in wisconsin, USA. Wetlands 2001; 21(2): 292-300.
4. Barbour MT, Gerritsen J, Snyder BD. Rapid Bioassessment Protocols for Use in Streams and Wadeable Rivers: Periphyton, Benthic Macroinvertebrates, and Fish. Washington, DC: U.S. Environmental Protection Agency, Office of Water; 1999.
5. Lenat DR, Penrose DL, Eagleson KW. Variable effects of sediment addition on stream benthos. Hydrobiologia 1981; 79(2): 187-94.
6. Victor R, Ogbeibu AE. Macrobenthic invertebrates of a stream flowing through farmlands in Southern Nigeria. Environmental Pollution Series A, Ecological and Biological 1985; 39(4): 337-49.
7. Rosenberg DM, Resh VH. Freshwater Biomonitoring and Benthic Macroinvertebrates. Berlin, Germany: Springer; 1992. p. 1-194.
8. Thorne R, Williams P. The response of benthic macroinvertebrates to pollution in developing countries: a multimetric system of bioassessment. Freshwater Biology 1997; 37(3): 671-86.
9. Girgin S, Kazanci N, Dugel M. Ordination and classification of macroinvertebrates and environmental data of a stream in Turkey. Water Sci Technol 2003; 47(7-8): 133-9.
10. Odiete WO. Environment Physiology of Animal and Pollution. Lagos, Nigeria: Diversified Resources Ltd; 1999.
11. Environmental Protection Agency. Lake and Reservoir Bioassessment and Biocriteria: Technical Guidance Document. Washington, DC: EPA; 1998.
12. Meyer JL, Strayer DL, Wallace JB, Eggert SL, Helfman GS. The Contribution of Headwater Streams to Biodiversity in River Networks1. Journal of the American Water Resources Association 2007; 43(1): 86-103.
13. Richardson JS, Danehy RJ. A Synthesis of the Ecology of Headwater Streams and their Riparian Zones in Temperate Forests. Forest Science 2007; 53(2): 131-47.
14. Sharma RC, Rawat JS. Monitoring of aquatic macroinvertebrates as bioindicator for assessing the health of wetlands: A case study in the Central Himalayas, India. Ecological Indicators 2009; 9(1): 118-28.
15. Ravera O. Ecological monitoring for water body management. Proceedings of monitoring Tailormade III. Proceedings of the International Workshop on Information for Sustainable Water Management; 2000 Sep 25-28; Nunspeet, Netherlands; 2000. p. 157-67.
16. Ikomi RB, Arimoro FO, Odihirin OK. Composition, distribution and abundance of macro-invertebrates of

the upper reaches of River Ethiope, Delta State, Nigeria. The Zoologist 2005; 3: 68-81.

17. George AD, Abowei JF, Alfred-Ockiya JF. The Distribution, Abundance and Seasonality of Benthic Macro Invertebrate in Okpoka Creek Sediments, Niger Delta, Nigeria 2010. Research Journal of Applied Sciences Engineering and Technology 2009; 2(1): 11-8.

18. Ogbeibu AE, Oribhabor BJ. Ecological impact of river impoundment using benthic macro-invertebrates as indicators. Water Res 2002; 36(10): 2427-36.

19. Thadeus Imoobe TO, Ohiozebau E. Pollution status of a tropical forest river using aquatic insects as indicators. African Journal of Ecology 2010; 48(1): 232-8.

20. Omoigbe MO, Ogbeibu AE. Environmental Impacts of Oil Exploration and Production on the Macrobenthic Invertebrate Fauna of Osse River, Southern Nigeria. Research Journal of Environmental Sciences 2010; 4(2): 101-14.

21. Olomukoro JO, Dirisu A. Macroinvertebrate community of a post lindane treated stream flowing through derived savannah in southern Nigeria. Tropical Freshwater Biology 2012; 21(1): 67-82.

22. Nandana SB. Retting of coconut husk - a unique case of water pollution on the South West coast of India. International Journal of Environmental StudiesVolume 52, Issue 1-4, 1997 1997; 52(1-4): 335-55.

23. Chellapandian B, Ramachandra T. Aquatic macroinvertebrate diversity and water quality of bangalore lakes. Proceedings of the Lake 2010. Wetlands, Biodiversity and Climate Change; 2010 Dec 22-24; Bengaluru, India.

24. Latha C, Thanga VS. Macroinvertebrate diversity of Veli and Kadinamkulam lakes, South Kerala, India. J Environ Biol 2010; 31(4): 543-7.

25. Alakananda B, Mahesh MK, Supriya G, Boominathan M, Balachandran C, Ramachandra TV. Monitoring Tropical Urban Wetlands through Biotic indices. J Biodiversity 2011; 2(2): 91-106.

26. Balachandran C, Dinakaran S, Alkananda B, Boominathan M, Ramachandra TV. Monitoring aquatic macroinvertebrates as indicators for assessing the health of lakes in Bangalore, Karnataka. International Journal of Advanced Life Sciences 2012; 5(1): 19-33.

27. Gupta S, Narzary R. Aquatic insect community of lake, Phulbari anua in Cachar, Assam. J Environ Biol 2013; 34(3): 591-7.

28. Kumar PS, Khan AB. The distribution and diversity of benthic macroinvertebrate fauna in Pondicherry mangroves, India. Aquat Biosyst 2013; 9(1): 15.

29. Rashid R, Pandit AK. Macroinvertebrates (oligochaetes) as indicators of pollution: A review. J Ecol Nat Environ 2014; 6(4): 140-4.

30. Doley N, Kalita S. A study on macro-invertebrate population in relation to some water and soil quality parameters in the wetlands of lower subansiri basin, India. J Environ Res Develop 2014; 8(3A): 785-95.

31. Chakrabarty D, Das SK. Alteration of macroinvertebrate community in tropical aquatic systems in relation to sediment redox potential and overlaying water quality. International Journal of Environment Science and Technology 2006; 2(4): 327-44.

32. Pennak RW. Fresh-Water Invertebrates of the United States: Protozoa to Mollusca a Wiley-Interscience publication. Hoboken, NJ: Wiley; 1989.

33. Edmondson TE. Ward and Whipple, Freshwater Biology. Hoboken, NJ: Wiley; 1993.

34. Merritt RW, Cummins KW. An Introduction to the Aquatic Insects of North America. Dubuque, Iowa: Kendall/Hunt Publishing Company; 1996.

35. Jessup BK, Markowitz A, Stribling JB. Family-level Key to the Stream Invertebrates of Maryland and Surrounding Areas. Queenstown, MD: Maryland Department of Natural Resources; 1999.

36. Subramanian KA. Dragonflies and Damselflies of Peninsular India-A Field Guide. E-Book of Project Lifescape. Bangalore, India: Indian Academy of Sciences; 2005.

37. Subramanian KA, Sivaramakrishnan KG. Aquatic Insects of India-A fieldguide. Bangalore, India: Ashoka Trust for Research in Ecology and Environment (ATREE) Small Grants Programme; 2007.

38. Stroud Water Research Centre. Identification Guide to Freshwater Macroinvertebrate. [Online]. [cited 2015]; Available from: URL: http://www.stroudcenter.org/education/MacroKey_Co mplete.pdf

39. Hewitta G. River quality investigations. Part 1: Some diversity and biotic indices. Journal of Biological Education 1991; 25(1): 44-52.

40. Washington HG. Diversity, biotic and similarity indices: A review with special relevance to aquatic ecosystems. Water Research 1984; 18(6): 653-94.

41. Ortiz JD, Puig MA. Point source effects on density, biomass and diversity of benthic macroinvertebrates in a Mediterranean stream. River Research and Applications 2007; 23(2): 155-70.

42. Simpson EH. Measurement of Diversity. Nature 1949; 163: 688.

43. Shannon CE, Weaver W. The Mathematical Theory of Communication. Champaign, IL: University of Illinois Press; 1963. p. 117.

44. Pielou EC. An introduction to mathematical ecology. Hoboken, NJ: Wiley-Interscience; 1969.

45. Bass D, Potts C. Invertebrate Community Composition and Physicochemical Conditions of Boehler Lake, Atoka County, Oklahoma. Proc Okla Acad Sci 2001; 81: 21-9.

46. Duran M, Akyildiz GK. Evaluating Benthic Macroinvertebrate Fauna and Wate Quality of Suleymanli Lake (Buldan-Denizli) in Turkey. Acta zool bulg 2011; 63(2): 169-78.

47. Olomukoro JO, Dirisu AR. Macroinvertebrate Community and Pollution Tolerance Index in Edion and Omodo Rivers in Derived Savannah Wetlands in Southern Nigeria. Jordan Journal of Biological Sciences 2014; 7(1): 19-24.

48. Kalyoncu H, Zeybek M. An application of different biotic and diversity indicesfor assessing water quality: A case study in the RiversCukurca and Isparta (Turkey). African Journal of Agricultural Research 2011; 6(1): 19-27.

49. Plotka N, Ebrahmi M, Hui Z, Crisosto T, Pajak G, Spychala E. Ecological Status of the Lake Durowskie in Poznan Based on Benthic Macro-invertebrates [Online]. [cited 2009 Aug 1]; Available from: URL: http://www.restlake.amu.edu.pl/download/archive-2009/Report_Benthic_Macro-invertebrates.pdf

50. Ghosh D, Biswas JK. Rotifera diversity indices: assessment of aquatic health of an ox-bow lake ecosystem in west Bengal. International Journal of Current Research 2014; 6(12): 10554-7.

51. Ghosh D, Biswas JK. Zooplankton Diversity Indices: Assessment of an Ox-Bow Lake Ecosystem for Sustainable Management in West Bengal. International Journal of Advanced Biotechnology and Research 2015; 6(1): 37-43.

52. Ghosh D, Biswas JK. Impact of jute retting on phytoplankton diversity and aquatic health: Biomonitoring in a tropical oxbow lake. Journal of Ecological Engineering 2015; 16(5): 15-25.

53. Ghosh D, Biswas JK. Biomonitoring macrophytes and abundance for rating aquatic health of an oxbow lake ecosystem in Ganga River basin. American Journal of Phytomedicine and Clinical Therapeutics. 2015; 3(10): 602-21.

Experimental design and response surface modeling for optimization of humic substances removal by activated carbon: A kinetic and isotherm study

Ahmad Reza Yazdanbakhsh[1], Yalda Hashempour[2]

1 Department of Environmental Health Engineering, School of Public Health, Shahid Beheshti University of Medical Sciences, Tehran, Iran
2 Students Research Committee, Department of Environmental Health Engineering, School of Public Health, Shahid Beheshti University of Medical Sciences, Tehran, Iran

Original Article

Abstract

The presence of humic acid (HA) in water treatment processes is very harmful and the cause of undesirable color, taste, and smell. Drinking water containing high concentrations of humic substances can be the cause of many health problems. Therefore, the removal of these compounds from water resources is a very important topic. In this research, response surface methodology (RSM) has been used to optimize the effect of main operational variables responsible for higher HA removal by activated carbon (AC). A three-level Box–Behnken factorial design (BBD) was used to optimize initial concentration of HA, time, pH, and AC dose for humic substances removal. The characterization of AC was carried out using scanning electron microscopy (SEM), energy-dispersive X-ray spectroscopy (EDS), and X-ray diffraction (XRD) analysis. A coefficient of determination (R^2) value of 0.98, model F-value of 82.32 and its low P (F < 0.0001), and low value of coefficient of variation (9.94%) indicated the fitness of the response surface quadratic model during the present study. At initial optimum concentration (5.25 mg HA/l), pH (5.85), contact time (36.01 minutes), and dose (1.38 g AC/L), the model predicted 1.90 mg HA/l. Equilibrium adsorption of HA onto AC had best fitness with the Freundlich isotherm and pseudo-second-order kinetic model.

KEYWORDS: Humic Substances, Kinetics, Drinking Water, Adsorption

Introduction

Humic substances are a group of non-biodegradable organic material which must be removed from drinking water sources. An essential part of humic substances in water is humic acids (HAs).[1] HAs are natural polyelectrolytes which are formed due to the decomposition of plants, animals, and other organisms in the form of biological activity in soil and natural waters.[2] Hydrophilic compounds are amorphous and have varied molecular weight. Their physical and chemical properties make them special.[3] Functional groups of humic substances are carboxylic, phenolic, carbonyl, and hydroxyl acids, acetaldehyde, and methoxy. The presence of phenolic and carboxyl groups creates a stable negative charge in aqueous environments.[4,5] Humic substances make up about 40 to 90% of dissolved organic matter in water. The physical

Corresponding Author:
Yalda Hashempour
Email: yalda.hashempour@yahoo.com

and chemical properties of these organic materials in water depend on their source.[5] Sources of humic substances in water include leakage through the soil, sediment, aquatic animals, plants, and effluents from sewage treatment plants.[1] The concentration of humic substances in natural waters is usually in the range of 0.1 to 10 mg/l.[5,6] The presence of humic substances in water treatment processes is very harmful and the cause of undesirable color, taste, and smell. On the other hand, as a result of chlorination of these waters, dangerous and carcinogenic byproducts such as trihalomethanes (THMs) are produced.[7] Humic substances in water interfere with the removal of heavy metals by forming complexes with metal. In addition, humic substances can form complexes with heavy metals, pesticides, and herbicides that lead to a migration of these compounds in aqueous solutions and an increase in their concentration. This is an important issue in water.[7] The high concentrations of humic substances in water disrupt the performance of ion exchange resins and membranes in water treatment.[8] In addition to the above problems, some sources have reported that drinking water containing high concentrations of HA can be a cause of black foot disease.[5,6] Thus, the removal of these compounds from drinking water and other water resources is of significant importance.

Conventional treatment methods (coagulation, flocculation, sedimentation, and disinfection) cannot completely remove humic substances from water and are only able to remove 20 to 50% of them.[4,9] On the other hand, other methods of removing organic materials, including ion exchange, evaporation, reverse osmosis, and chemical precipitation, often have high costs and disposal of their sludge is difficult.[10,11] Therefore, the use of a low-cost adsorbent that is able to remove high amounts of organic matter and improve the quality of drinking water is a necessity. Several absorbents such as clay, zeolite, chitosan, and metal oxides

are used to adsorb humic substances.[10,12,13] Activated carbon (AC) is extensively used in the removal of organic compounds from water, because the absorbent has a high active surface and has shown an efficient performance.[10] The purpose of this study was to investigate the use of AC as a model adsorbent for the removal of HA from water. The experimental work includes the assessment of factors influencing the adsorption of HA on AC by means of Box–Behnken factorial design (BBD) in response surface methodology (RSM). The adsorption kinetics of HA on AC under various conditions were also studied.

Materials and Methods

Commercial AC used in this study was a Merck (Merck KGaA, Darmstadt, Germany) product. The stock solution of HA was made according to the standard method[14] and was stored in a refrigerator at 4 ± 0.1 °C before use. All solutions used in each run were prepared by diluting the stock solution. The commercial AC was dipped in 5% hydrochloric acid for 24 hours, followed by washing with deionized water until the water pH was stable (pH = 6.52–6.70). After drying for 24 hours at 105 °C, AC was used as an absorbent. The morphological properties of AC were observed using a scanning electron microscope (SEM-EDS, TESCAN Vega Model, Brno, Czech Republic). The crystal structure and crystallinity of the composites were examined using X-ray diffraction (XRD) analysis with a Rigaku D/MAXYA diffractometer with Ni-filtered Cu Ka radiation as X-ray source (Theta-Theta model, STOE, Germany).

The BBD consisted of three levels (low, medium, and high coded as -1, 0, and +1). The complete design consisted of 29 runs which were performed in duplicate to optimize the levels of selected variables (initial concentration of HA, pH, contact time, and AC dose). The lowest and highest levels of HA initial concentration were 5 and 50 mg/l, pH 3 and 9,

time 1 and 60 minutes, and AC dose 0.5 and 1.5 g/l. The HA removal efficiency was multiplying regressed the different parameters by the least square methods as follows:

$$Y = \beta_0 + \sum \beta_i X_i + \sum \beta_{ij} X_i^2 + \sum \beta_{ij} X_i X_{ij} \qquad [2]$$

where Y is the predicted response variable, β_0, β_i, β_{ii}, and β_{ij} are constant regression coefficients, and X_i and X_j (i = 1, 3; j = 1, 3, i ≠ j) represent the independent variable.[15]

The accuracy and fitness of the above model was evaluated by R^2 and F values. Table 1 shows the BBD matrix along with experimental and predicted values for HA removal. The predicted values for HA removal were obtained by applying the quadratic model (Design Expert software, version 7, Stat-Ease, Inc., Minneapolis, Mn, USA). The optimum values of the variables for HA removal were obtained by solving the regression equation, and analyzing the response surface contour plots and constraints for the variables using the same software. The goal determined for HA removal was maximum HA removal.

All experiments were performed at room temperature and in batch mode in 250 ml beakers by mixing 100 ml of the desired HA solution. The mixture was shaken at 200 rpm for the desired duration of time. The mixture was then filtered through 0.45 μ filter and the final concentration of HA in the supernatant solution was determined by measuring the absorbance at the maximum wavelength of 254 nm using a UV-visible spectrophotometer (DR5000). The amount of HA adsorbed (mg/g) was calculated based on the following equation:

$$q_e = \frac{(C_0 - C_e)}{M} V \qquad [3]$$

where q_e is the amount (mg) of absorbed HA on per g of AC, C_0 and C_t are HA concentration (mg) before adsorption and after adsorption in time t, respectively. V is initial volume of solution (l), and m the weight of absorbent (g).

The pH of zero charge point (pH_{zpc}) of AC

was determined according to the pH drift procedure.[4,5]

Among the various isotherm equations that are used for analysis of absorption data in aqueous environments, the Langmuir and Freundlich isotherms are more common. The linear form of these isotherms is shown as equation 5 (Langmuir) and 6 (Freundlich):

$$\frac{C_e}{q_e} = \frac{1}{k_1 q_0} + \frac{1}{q_0} C_e \qquad [5]$$

$$\ln q_e = \ln k_F + \frac{1}{n} \ln C_e \qquad [6]$$

where q_0 (mg/g) is the maximum adsorption capacity, q_e (mg/g) is the amount of HA adsorbed on the adsorbent, C_e (mg/l) is the equilibrium HA concentration, k_F and n are the Freundlich constants, and k_1 (l/mg) is the Langmuir constant. For the Langmuir model, the linear plot of 1/(X/m) versus 1/C, and for the Freundlich model, the linear plot of $\ln q_e$ versus $\ln C_e$ is drawn. The determination coefficient (R^2) is used to determine the goodness of fit of the models.

In this study, pseudo-first order and pseudo-second-order kinetics were used to describe the data. The pseudo-first order (equation 7) and the pseudo-second order (equation 8) are as follows:

$$\ln(q_e - q_t) = -K_1 t + \ln q_e \qquad [7]$$

$$\frac{t}{q_t} = \frac{1}{k_2 q_e^2} + \frac{1}{q_e} t \qquad [8]$$

where q_e and q_t are the amount of HA adsorbed on AC at time t and equilibrium time, respectively. K_1 and k_2 are constants of adsorption rate. For the pseudo-first order model, the plot of $\ln(q_e - q_t)$ versus t, and for the pseudo-second order model, the plot of t/q_t versus t is drawn. The determination coefficient (R^2) is used to determine the goodness of fit of the models.

Results and Discussion

Characterization of AC

Properties and morphology of AC were

determined using scanning electron microscopy (SEM) and energy-dispersive X-ray spectroscopy (EDS) analysis in the operating voltage of 20 keV (Figure 1). The electron image is magnified 9000 times. These analyses show the quantitative characteristics, such as particle size, shape/morphology, and surface area, of AC. The results of the analysis of SEM-EDS (Figure 2) show the elemental analysis of AC. As can be seen in figure 1, the two main elements in the AC were carbon and oxygen that included 90.39 and 9.61% by total weight, respectively. All these features show that AC has a high potential to absorb pollutants from water.

The XRD pattern of AC is illustrated in figure 3. In the pattern of AC, there was only one broad peak at 24.14 corresponding to amorphous carbon.[2]

Optimization of parameters for HA removal

Table 1 shows that there was a considerable variation in HA removal by AC at different values of selected parameters. Multiple regression analysis method based on equation 2 was used for analyzing the data. The predicted response Y for HA removal was obtained as following:

$$Y = 3.73 + 1.97X_1 + 0.52X_2 - 0.49X_3 - 0.2X_4 + 0.28 X_1X_2 - 0.23X_1X_3 - 0.004X_1X_4 + 0.11X_2X_3 + 0.021X_2X_4 - 0.029X_3X_4 - 0.41X_1^2 + 0.22X_2^2 + 0.39X_3^2 + 0.013X_4^2 \qquad [4]$$
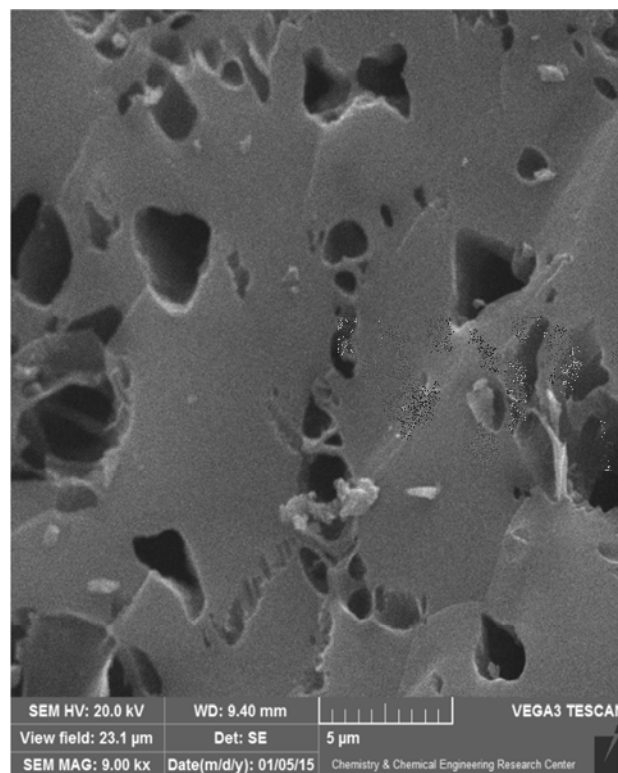

**Figure 1. Scanning electron microscopy (SEM) image of activated carbon (AC)**
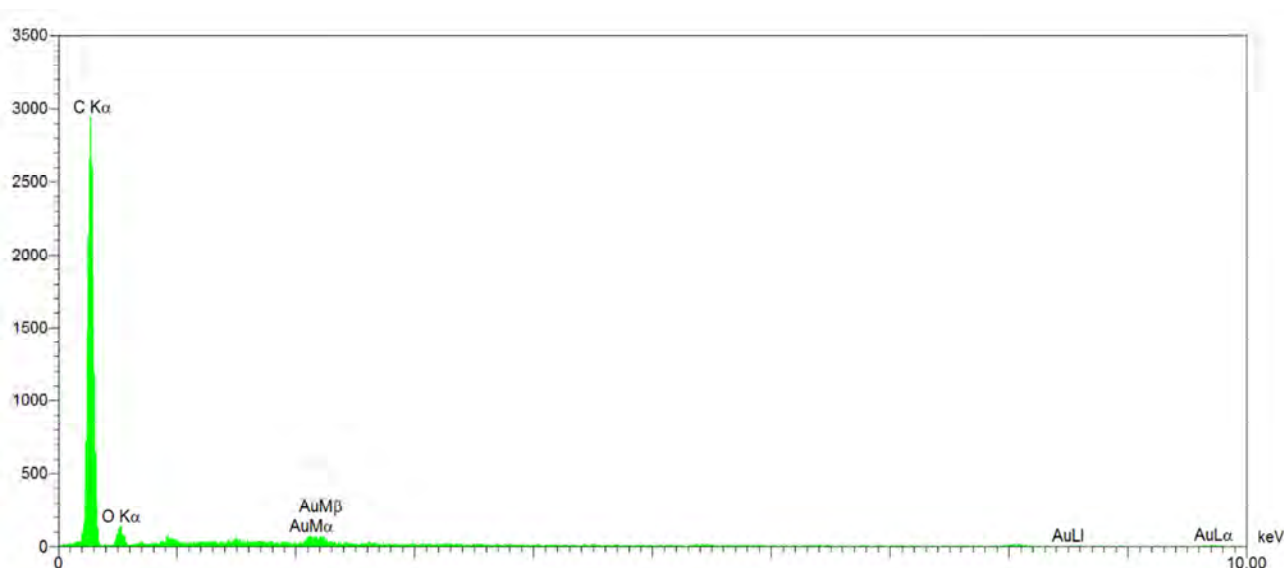
Figure 2. Energy-dispersive X-ray spectroscopy (EDS) diagrams of activated carbon (AC)
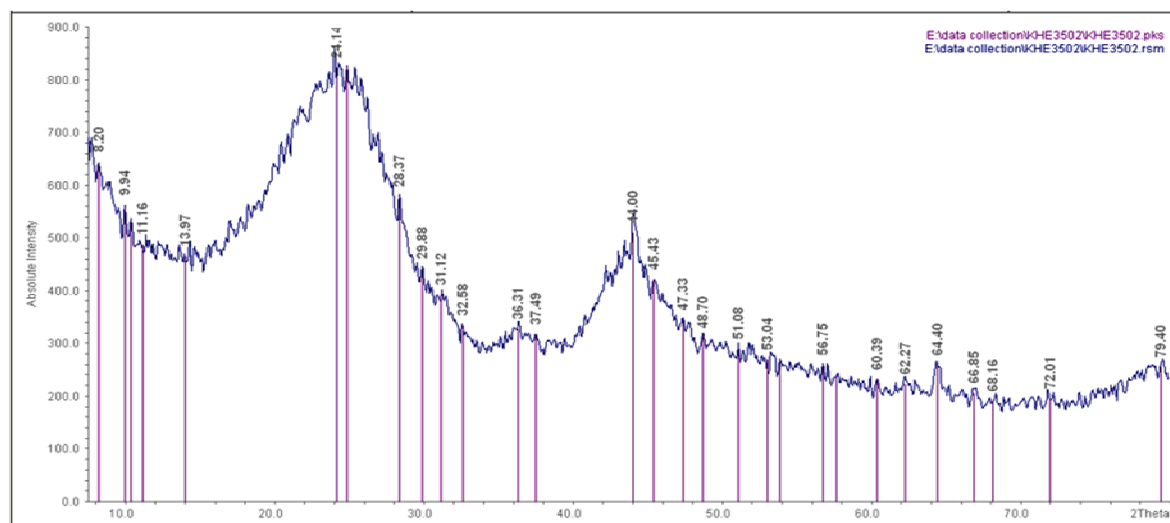
Figure 3. X-ray diffraction (XRD) patterns of activated carbon (AC)

Table 1. Box–Behnken factorial design (BBD) matrix in coded terms along with experimental and predicted values for humic acid (HA) removal

Runs	Independent variables (coded)				Humic acid removal (mg/l)	
	X_1	X_2	X_3	X_4	Experimental	Predicted
1	-1	-1	0	0	1.70	1.77
2	0	0	1	-1	13.36	13.55
3	1	0	1	0	26.19	24.67
4	1	0	0	-1	27.32	30.38
5	1	-1	0	0	23.18	22.24
6	0	-1	0	-1	12.16	12.12
7	0	0	0	0	12.37	12.36
8	-1	1	0	0	3.29	3.30
9	0	0	0	0	12.37	12.36
10	0	1	1	0	17.65	18.21
11	-1	0	1	0	2.00	2.19
12	0	1	0	-1	20.59	19.56
13	1	1	0	0	41.56	39.98
14	0	0	-1	1	18.57	17.84
15	0	0	0	0	12.37	12.36
16	0	-1	1	0	9.86	9.37
17	1	0	-1	0	42.83	41.11
18	-1	0	0	1	1.84	1.37
19	0	0	0	0	12.37	12.36
20	0	0	1	1	9.81	10.39
21	0	1	0	1	17.00	16.53
22	0	-1	0	1	8.94	9.25
23	-1	0	-1	0	3.68	4.06
24	1	0	0	1	24.33	26.50
25	0	0	0	0	12.37	12.36
26	0	-1	-1	0	17.23	17.86
27	0	1	-1	0	22.62	24.82
28	0	0	-1	-1	22.25	20.82
29	-1	0	0	-1	2.58	2.44

X_1 = Initial concentration of humic acid; X_2 = pH; X_3 = Time; X_4 = activated carbon dose

Table 2. Analysis of variance (ANOVA), regression coefficient estimate, and test of significance for humic acid (HA) removal

Factor	Sum of squares	Mean squares	Coefficient estimated ± S.E.	d.f.	F-value	P > F
Intercept	55.16	3.94	3.730 ± 0.072	14	154.00	< 0.0001
X_1	46.55	46.55	1.970 ± 0.046	1	1819.25	< 0.0001
X_2	3.21	3.21	0.520 ± 0.047	1	125.46	< 0.0001
X_3	2.89	2.89	-0.490 ± 0.047	1	112.99	< 0.0001
X_4	0.47	0.47	0.200 ± 0.047	1	18.36	0.0008
X_1X_2	0.32	0.32	0.280 ± 0.080	1	12.56	0.0032
X_1X_3	0.21	0.21	-0.230 ± 0.080	1	8.15	0.0127
X_1X_4	6.9×10^{-5}	6.9×10^{-5}	$(-4.13 \times 10^{-3}) \pm 0.08$	1	2.7×10^{-3}	0.9593
X_2X_3	0.05	0.051	0.110 ± 0.080	1	1.99	0.1804
X_2X_4	1.71×10^{-3}	1.71×10^{-3}	0.021 ± 0.080	1	0.07	0.8000
X_3X_4	3.46×10^{-3}	3.46×10^{-3}	-0.029 ± 0.08	1	0.14	0.7186
X_1^2	1.05	1.05	-0.410 ± 0.064	1	40.91	< 0.0001
X_2^2	0.33	0.33	0.220 ± 0.063	1	12.80	0.0030
X_3^2	1.01	1.01	0.390 ± 0.063	1	39.41	< 0.0001
X_4^2	1.14×10^{-3}	1.14×10^{-3}	0.013 ± 0.063	1	0.04	0.8359
Residual	0.36	0.03		14		
Corrected total	55.52			28		

X_1: Initial concentration of humic acid; X_2: pH; X_3: Time; X_4: Activated carbon dose

In this equation Y is the HA removal (mg/l), and X_1, X_2, X_3, and X_4 are initial concentration of HA, pH, contact time, and AC dose, respectively. The data obtained from Eq. 4 were verified by F value and the analysis of variance (ANOVA) in response surface quadratic model. All p-values below 0.05 were considered as significant. The linear effect of coefficients of initial concentration of HA (P < 0.0001), pH (P < 0.0001), contact time (P < 0.0001), and AC dose (P = 0.0008) were significant. Similarly, the interactive effects of initial concentration and pH (P = 0.0032), and initial concentration and time (P = 0.0127) were also significant. However, the interactive effect of initial concentration and dose (P = 0.9593), pH and time (P = 0.1804), pH and dose (P = 0.8), and time and dose was insignificant. The p-values of the quadratic terms, [initial concentration (X_1^2) (P < 0.0001), pH (X_2^2) (P = 0.003), and time (X_3^2) (P < 0.0001)] were significant. The F-value (154), R^2 value (0.99), probability (P < 0.0001), and coefficient of variation (C.V. = 4.32%) obtained through ANOVA for response surface quadratic model signify that the model is significant (Table 2). Statistical parameters listed in table 2 and the high value of the regression coefficient (R^2 = 0.98) suggest that the removal of HC by AC can be well described through this model. On the other hand, the F value showed that the model was significant. The F value in this study is equal to 82.32. Since the F parameter is higher than 18, the significance of the model for the removal of HC is clear.

As can be seen in table 1, experimental and predicted values for HA removal lie within a narrow interval. This also shows the outstanding degree of fitness for the model equation.

The main objective of the optimization is to determine the optimum values of variables for HA removal efficiency. In optimization, the desired aim in terms of HA removal efficiency was defined as achieving maximum removal efficiency. At optimum initial concentration (5.25 mg HA/l), pH (5.85), contact time (36.01 minutes), and dose (1.38g AC/l) the model predicted 1.90 mg HA/l or 67.52% removal efficiency.

The effect of the HA initial concentration and pH

Contour plots show the type of interaction between test variables and help to achieve the optimum conditions.[16] Figure 4 shows HA

removal as a result of interaction between initial concentration (5, 25, and 50 mg/l) and pH (3, 6, and 9). Colors for the contour plots represent the removal efficiency. For example, red means maximum removal, green medium, and blue minimum removal efficiency. With increased initial concentration, HA removal efficiency decreased, and maximum sorption (65.99%) was predicted at 5 mg HA/l. The results show that with increase in initial concentration, HA organic molecules are adsorbed on the surface of AC and these molecules can occupy greater number of active sites on the absorbent.[17] Thus, at lower concentration, a greater number of pores was available on the AC surface.

As the results verified, acidic conditions were more suitable for the removal of HA, and efficiency decreased when pH was greater than 5. Most of the organic contaminants were reduced effectively at lower pH values.[18] At low pH values, surface sites are closely coupled to H^+ ions; therefore, these sites become unavailable for other cations. Thus, HA could not be easily adsorbed onto AC. In alkaline conditions, HA is negatively charged and the efficiency slightly decreased.[15]

The effect of contact time and AC dosage

Removal efficiency for HA was investigated at contact time of 1, 30, and 60 minutes. The results showed that the optimum time for HA removal by AC was 60 minutes. Therefore, HA adsorption was found to increase with increase in time as shown in figure 5. The HA removal in the abovementioned time duration was attributed to the surface connection between active surface groups and HA ion. Furthermore, further sorption at the described times can be illustrated with an increased availability in the active boundary sites on the sorbent surface area.[19,20]
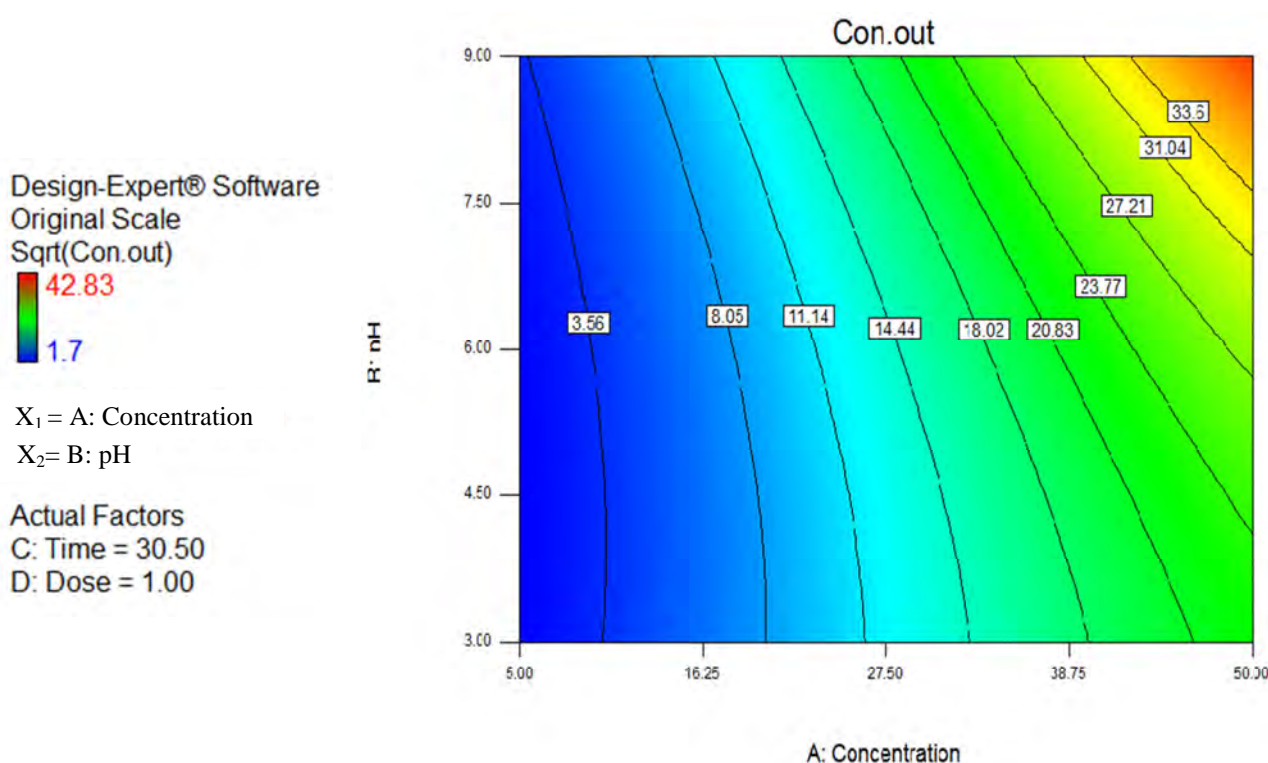

Figure 4. Response surface contour plots showing effect of initial concentration (mg HA/l) and pH on humic acid (HA) removal (mg/l)
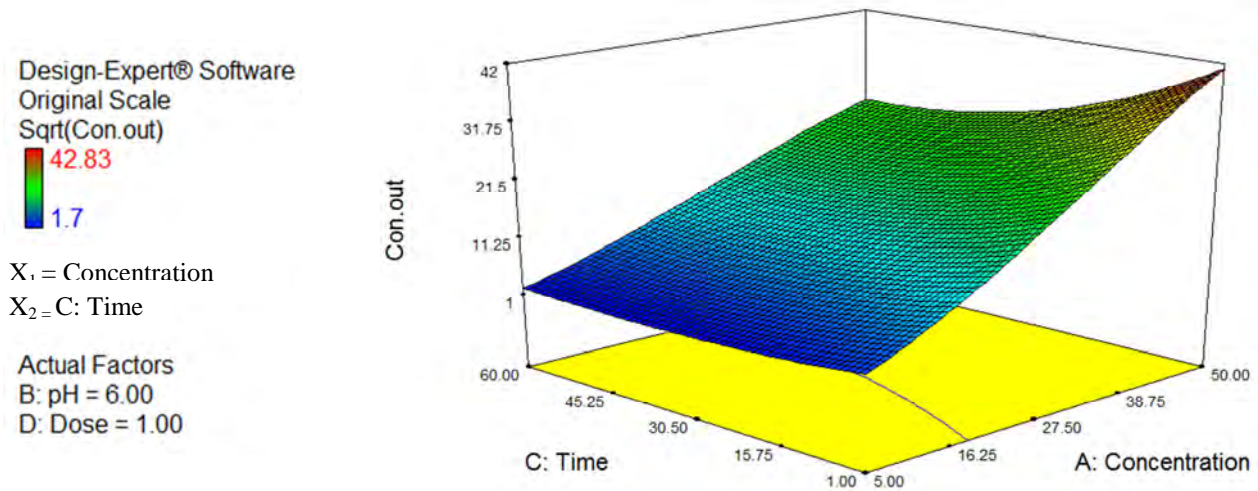
Figure 5. Response surface 3D plots showing effect of initial concentration (mg HA/l) and time on humic acid (HA) removal (mg/l)
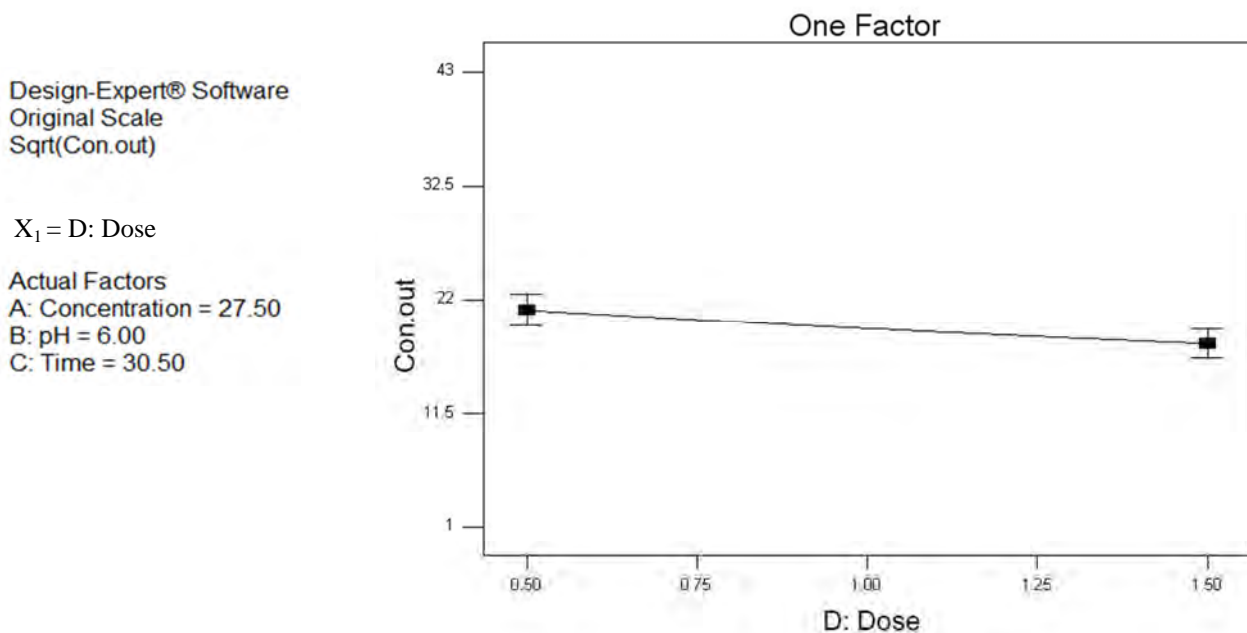

Figure 6. Response surface one factor plots showing effect of activated carbon (AC) dose (g AC/l) on humic acid (HA) removal (mg/l)

Consideration of the effect of one factor (AC dose) alone shows that its effect is in accordance with figure 6. As shown in figure 5, with increase in AC dosage, the removal efficiency also increased. The removal of organic compounds such as HA by AC implicates direct contact between the organic matter and cavity on the AC particle surface. ANOVA analysis showed the significant effect of adsorbent dosage on HA removal ($P < 0.0001$). Nevertheless, the interaction effects of these variables with other variables in this study (initial concentration, pH, and contact time) were not significant.

Isotherm and kinetic study

Equilibrium time is the primary result of absorption kinetics. If this parameter is specified, adsorption isotherms can be achieved. In this study, to obtain absorption equilibrium time, a 250 ml HA solution with concentration of 25 mg/l was prepared, and then, 125 mg of adsorbent was added to the container. The pH value of the solution was adjusted between 5.6 and 7. Mixing speed and temperature were 200 rpm and 25 °C, respectively. The sampling was conducted at specified intervals and after passing samples from a 0.45 µ filter, absorbed HA was measured using a spectrophotometer at a wavelength of 254 nm. The results of this phase were examined by drawing a diagram of the concentration versus time and when concentration changed over time and reached zero, it was recorded as the equilibrium time. As can be seen in figure 5, the equilibrium time in this study was 960 minutes (Figure 7).
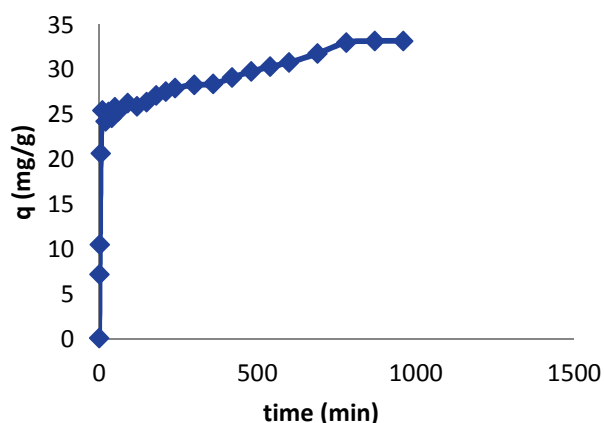

Figure 7. Equilibrium time curve of humic acid (HA) absorption on activated acid (AC)

Adsorption isotherms are equilibrium data used to describe the interaction between adsorbent and adsorbate. Isotherms also suggest the capacity of an adsorbent. The results of Langmuir and Freundlich isotherm models are shown in figures 8 and 9 and also in table 3. As is clear from the results and determination coefficient, the Freundlich isotherm model is able to better explain test results ($R^2 = 0.9971$). The empirical equation isotherm of Freundlich is based on multi-layer, non-homogeneous, and heterogeneous materials adsorbed on the adsorbent.[3]
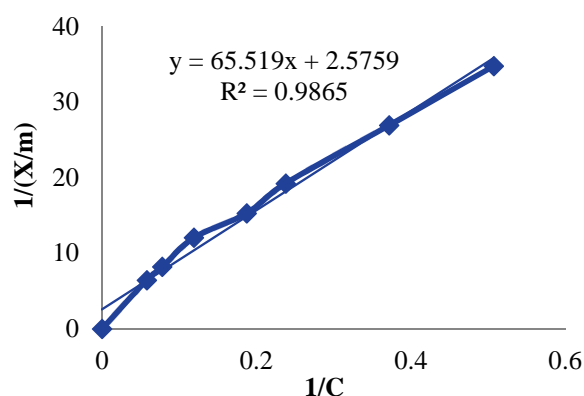
Figure 8. Langmuir model of humic acid (HA) absorption on activated acid (AC) (pH = 6-7.5, T = 25 ºC, mixing time for AC = 16 hours)
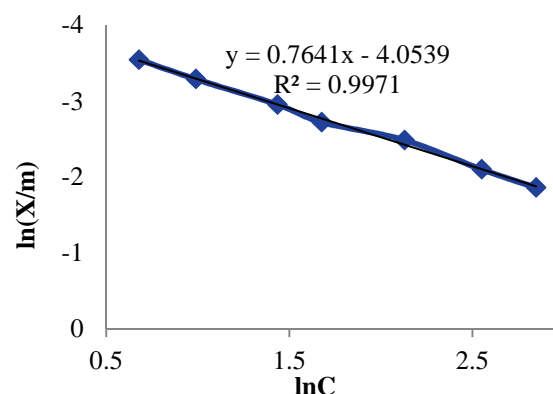
Figure 9. Freundlich model of humic acid (HA) absorption on activated carbon (AC) (pH = 6-7.5, T = 25 ºC, mixing time for AC = 16 hours)

Table 3 illustrates that the obtained value of n in the Freundlich model is 1.322; representing the average absorption of HA on AC.[9]

To investigate the factor influencing the reaction rate, it is necessary to study the kinetics of the process. Adsorption kinetics were studied in order to better understand the adsorption dynamic of HA on the adsorbent and produce a predictive model to estimate the amount of ions absorbed during the process.

Table 3. Parameters of Langmuir and Freundlich models in adsorption of humic acid (HA) on activated carbon (AC)

Langmuir			Freundlich		
b	q_m	R^2	k	n	R^2
0.2385	33.2	0.9865	0.0175	1.322	0.9971

Figures 10 and 11 show pseudo-first-order and pseudo-second-order kinetics curves, respectively. R^2 obtained for the pseudo-first- and pseudo-second-order models were 0.9855 and 0.9999, respectively. Therefore, the pseudo-second-order kinetic model is more acceptable for analysis of HA on AC.

Pesoudo first order reaction

$$y = -0.0054x + 0.6416$$
$$R^2 = 0.862$$
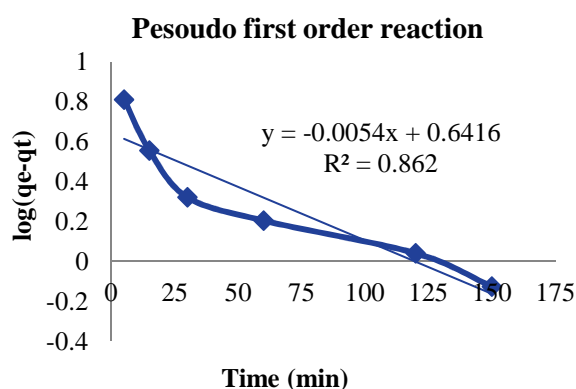
Figure 10. Pseudo-first-order kinetic model of humic acid (HA) absorption on activated carbon (AC) (initial concentration = 25 mg/l, pH = 6-7.5, T = 25 ºC

Pseudo-second-order kinetic model

$$y = 0.0377x + 0.0725$$
$$R^2 = 0.9999$$
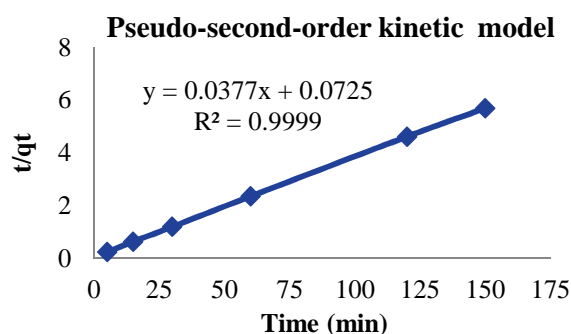
Figure 11. Pseudo-second-order kinetic model of humic acid (HA) absorption on activated carbon (AC) (initial concentration = 25 mg/l, pH = 6-7.5, T = 25 ºC

The pseudo-first-order kinetic model is based on absorbent capacity and is applied when adsorption, using diffusion mechanism, occurs within a boundary layer. While, the pseudo-second-order kinetic model shows that chemical adsorption is dominant and and shows the controlling mechanism in the process of adsorption.[21]

Conclusion

In the present study, RSM based on the four-factor-three-level BBD was employed as an experimental design tool to explain the effect of main operating parameters (including HA concentration, pH, contact time, and adsorbent dose) and their interactions on the removal of HA. RSM showed that HA removal efficiency was significantly affected by all the mentioned variables. AC is quite efficient in the removal of humic substances from solution. According to the ANOVA results, the model presents a high R^2 value (0.98) for HA removal efficiency. At optimum initial concentration (5.25 mg HA/l), pH (5.85), contact time (36.01 minutes), and dose (1.38 g AC/l) the model predicted 1.90 mg HA/l or 67.52% removal efficiency.

Conflict of Interests

Authors have no conflict of interests.

Acknowledgements

References

1. Khraisheh M, Al-Ghouti MA, Stanford CA. The application of iron coated activated alumina, ferric oxihydroxide and granular activated carbon in removing humic substances from water and wastewater: Column studies. Chemical Engineering Journal 2010; 161(1-2): 114-21.

2. Lorenc-Grabowska E, Gryglewicz G. Adsorption of lignite-derived humic acids on coal-based mesoporous activated carbons. J Colloid Interface Sci 2005; 284(2): 416-23.

3. Chang MY, Juang RS. Adsorption of tannic acid, humic acid, and dyes from water using the composite of chitosan and activated clay. J Colloid Interface Sci 2004; 278(1): 18-25.

4. Daifullah AAM, Girgis BS, Gad HMH. A study of the factors affecting the removal of humic acid by activated carbon prepared from biomass material. Colloids and Surfaces A: Physicochemical and Engineering Aspects 2004; 235(1-3): 1-10.

5. Doulia D, Leodopoulos C, Gimouhopoulos K, Rigas F. Adsorption of humic acid on acid-activated Greek bentonite. J Colloid Interface Sci 2009; 340(2): 131-41.

6. Wu FC, Tseng RL, Juang RS. Comparative adsorption of metal and dye on flake- and bead-types of chitosans prepared from fishery wastes. J Hazard Mater 2000; 73(1): 63-75.

7. Terdkiatburana T, Wang S, Tadé MO. Competition and complexation of heavy metal ions and humic acid on zeolitic MCM-22 and activated carbon. Chemical Engineering Journal 2008; 139(3): 437-44.

8. Wu FC, Tseng RL, Juang RS. Enhanced abilities of highly swollen chitosan beads for color removal and tyrosinase immobilization. J Hazard Mater 2001; 81(1-2): 167-77.

9. Lai CH, Chen CY. Removal of metal ions and humic acid from water by iron-coated filter media. Chemosphere 2001; 44(5): 1177-84.

10. Namasivayam C, Sangeetha D. Recycling of agricultural solid waste, coir pith: removal of anions, heavy metals, organics and dyes from water by adsorption onto ZnCl2 activated coir pith carbon. J Hazard Mater 2006; 135(1-3): 449-52.

11. Ndjeumi CC, Mãicãneanu A, Bike Mbah JB, Mouthe Anombogo GA, Kamga R. Assessment of physico-chemical parameters for humic acids adsorption on alumina. Chemistry Journal 2015; 1(4): 133-8.

12. Wang S, Zhu ZH. Humic acid adsorption on fly ash and its derived unburned carbon. J Colloid Interface Sci 2007; 315(1): 41-6.

13. Capasso S, Salvestrini S, Coppola E, Buondonno A, Colella C. Sorption of humic acid on zeolitic tuff: a preliminary investigation. Applied Clay Science 2005; 28(1-4): 159-65.

14. American Water Works Association. Water quality and treatment handbook. 5th ed. New York, NY: McGraw-Hill Professional; 1999.

15. Doddapaneni KK, Tatineni R, Potumarthi R, Mangamoori LN. Optimization of media constituents through response surface methodology for improved production of alkaline proteases by Serratia rubidaea. Journal of Chemical Technology and Biotechnology 2007; 82(8): 721-9.

16. Myers R, Montgomery DC. Response surface methodology: process and product optimization using designed experiments. 1st ed. New York, NY: John Wiley & Sons, Inc; 1995.

17. Babuponnusami A, Muthukumar K. Removal of phenol by heterogenous photo electro Fenton-like process using nano-zero valent iron. Separation and Purification Technology 2012; 98: 130-5.

18. Zhang WH, Quan X, Zhang ZY. Catalytic reductive dechlorination of p-chlorophenol in water using Ni/Fe nanoscale particles. J Environ Sci (China) 2007; 19(3): 362-6.

19. Tseng HH, Su JG, Liang C. Synthesis of granular activated carbon/zero valent iron composites for simultaneous adsorption/dechlorination of trichloroethylene. J Hazard Mater 2011; 192(2): 500-6.

20. Cheng W, Dastgheib SA, Karanfil T. Adsorption of dissolved natural organic matter by modified activated carbons. Water Res 2005; 39(11): 2281-90.

21. Han S, Kim S, Lim H, Choi W, Park H, Yoon J, et al. New nanoporous carbon materials with high adsorption capacity and rapid adsorption kinetics for removing humic acids. Microporous and Mesoporous Materials 2003; 58(2): 131-5.

Photocatalytic removal of Acid Red 88 dye using zinc oxide nanoparticles fixed on glass plates

Yahya Zandsalimi[1], Pari Teymouri[1], Reza Darvishi Cheshmeh Soltani[2], Reza Rezaee[1], Narmin Abdullahi[1], Mahdi Safari[1]

1 Environmental Health Research Center, Kurdistan University of Medical Sciences, Sanandaj, Iran
2 Department of Environmental Health, School of Health, Arak University of Medical Sciences, Arak, Iran

Original Article

Abstract

In this study, ZnO nanoparticles fixed on glass plates were employed as photocatalysts for the degradation of Acid Red 88 (AR88) dye in aquatic solution. ZnO nanoparticles were synthesized through coprecipitation method and fixed on glass plates. X-ray diffraction (XRD) and scanning electron microscopy (SEM) techniques were used for characterization of nanoparticle samples. A batch reactor equipped to UV lamps was used for photocatalytic experiments. The effect of pH, initial concentrations of AR88, radical scavengers, and enhancers were studied on photocatalytic removal efficiency of AR88. The results showed an increase in AR88 removal at the neutral pH of 7 (79%), but a decreased in acidic and alkaline pH values. It was also found that at lower initial concentration of dye the removal efficiency increases. Among different radical scavengers and enhancers, addition of CH_4O as radical scavenger and ethylenediaminetetraacetic acid (EDTA) as enhancer had the greatest effect on degradation efficiency. The photocatalysis process using fixed ZnO nanoparticles was shown to have good efficiency for removal of AR88 from aqueous solution. Therefore, it can be concluded that the photocatalysis process using fixed catalyst could be a promising method for treating wastewater of dye industries.

KEYWORDS: Acid Red 88, Photocatalytic Process, Nanoparticles, Zinc Oxide

Citation: Zandsalimi Y, Teymouri P, Darvishi Cheshmeh Soltani R, Rezaee R, Abdullahi N, Safari M. **Photocatalytic removal of Acid Red 88 dye using zinc oxide nanoparticles fixed on glass plates.** J Adv Environ Health Res 2015; 3(2): 102-10.

Introduction

Synthetic dyes are a group of organic pollutants that are widely used in the textile, paper, food, and plastic industries.[1] Wastewater from such industries is discharged into aquatic environments causing water pollution and environmental problems.[2] Among commercial dyes, the azo group is the largest and most important group, comprising up to 70% of dye compounds.[2] Azo dyes have nitrogen−nitrogen double bond (-N = N-) in their chemical structure, along with one or more aromatic system(s).[3] Worldwide production of azo dyes is about 500,000 tons per year, 1-20% of which is estimated to be discharged into the water bodies.[4] Therefore, such dyes are serious threats to the ecosystem.[5] These materials may reduce light penetration into the water, which affects the photosynthetic activity of plants. They may also cause eutrophication, depletion of dissolved oxygen in water, and increase in suspended solids and turbidity.[6] In addition, many dyes are resistant to biodegradation and oxidizing agents and are

---

Corresponding Author:
Mahdi Safari
Email: safari.m.eng@gmail.com

toxic and carcinogenic for humans and aquatics.[1,7] Therefore, it is essential to remove dyes from wastewater before it entering the environment.[8] Various methods have been used to remove dyes such as adsorption processes, chemical coagulation, chlorination, reverse osmosis, and nano-filtration.[1,9] However, the conventional processes for the purification of wastewater are not effective enough.[10] In such processes, only a change in the phase of dye occurs and the concentrated pollutants and generated secondary pollutants require advanced treatment processes.[11] Therefore, the appropriate option would be the application of processes, which lead to the removal of pollutants or their oxidation to harmless byproducts. Today, the integration of different advanced oxidation processes for the decomposition of organic pollutants has become more widespread.[12] For example, the integration of ultraviolet light and titanium dioxide (TiO_2) or zinc oxide (ZnO) catalysts for the removal of organic contaminants is a photocatalytic process with a more effective performance than other processes.[13] In general, advanced oxidation processes are oxidation and decomposition reactions in which free radicals, such as hydroxyl produced by UV light, breakdown organic matters into simpler inorganic compounds such as mineral acids, water, and CO_2.[14]

ZnO is a semiconductor photocatalyst with a high light sensitivity, high stability, and non-toxic nature and high efficiency in the production of electrons. Such characteristics make it a good candidate for the photocatalytic process.[15] The principal advantage of ZnO over TiO_2 is its capability to absorb a wide range of electromagnetic waves.[16,17] Catalysts in the photocatalytic processes are used in the fixed or suspension forms. The fixed catalysts are economical and functional because they do not need to be removed after large scale processes.[15] Acid Red 88 (AR88), is a mono azo dye and is widely used in the textile and food industries. It is resistant against optical, chemical, and biological decompositions and its byproducts (e.g., aromatic amines) have carcinogenic effects.[7] To the best of our knowledge, the use of ZnO nanoparticle fixed on glass plates as catalyst has not been reported for the removal of AR88 dye from aquatic solution. Therefore, this study investigated the efficiency of ZnO nanoparticles fixed on glass as catalyst in AR88 removal in the presence of UV light on a laboratory scale.

Materials and Methods

All chemicals used in this study were analytical grade and purchased from Merck Company (Germany). AR88 dye was purchased from Alvan Sabet Corporation, Iran. The characteristics of AR88 are presented in table 1.

ZnO nanoparticles have been synthesized through simple coprecipitation method. For the preparation of ZnO nanoparticles, 1.362 g $ZnCl_2$ was added to 50 ml deionized water. Then, 1 M NaOH solution was dropwise added to the abovementioned solution under magnetic stirring until the pH reached 10. The suspension was filtered and washed with absolute deionized water and ethanol and dried in an oven at 80 °C for two days.

Table 1. Characteristics of Acid Red 88

Dye	Chemical Structure	Molecular Formula	λmax (nm)	M_w (g/M)
Acid Red 88		$C_{20}H_{13}N_2NaO_4S$	505	400.38
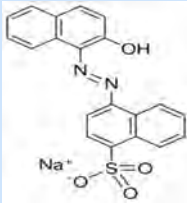
First, glass plates were kept in a solution of 50% NaOH for 24 hours. Then, 3% nanosuspension was prepared and mixed for 1 hour. It was placed in an ultrasonic bath until particles were dispersed. Subsequently, 5 ml of homogeneous solution was poured on the glass plates (3 × 15 cm) and kept for 24 hours at room temperature to dry slowly. Then, the glass plates were placed in an oven with a temperature of 450 °C for 3 hours for stabilization.[15]

A Plexiglas batch reactor with working volume of 500 ml was used for photocatalytic experiments. Moreover, 4 glass plates with fixed catalyst were placed on the inner surfaces of reactor walls. A 9-W low-pressure UVC lamp (Philips, Netherlands) with a quartz cover was used as the UV source. A magnetic stirrer (Heidolph, Germany) was used for mixing the solution (Figure 1).


1. UV lamp
2. Quartz tube
3. Glass plate
4. Stirrer bar
5. Magnetic stirrer
6. Power
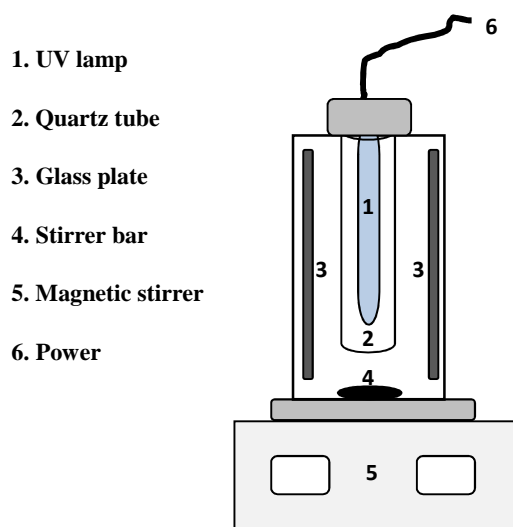
Figure 1. Photocatalytic reactor

Initially, AR88 dye stock solution (1000 mg/l) was prepared by dissolving 1 g of dye in 1000 ml of deionized water and the stock solution was kept in the refrigerator. Different concentrations of AR88 were prepared by the dilution of stock solution (1000 mg/l) and added to the reactor. The effect of different pH (3, 5, 7, 9, and 11), initial concentrations of AR88 (10, 25, 50, and 100 mg/l), and contact times (30, 60, 90, and 120 minutes) were studied on photocatalytic removal efficiency of AR88. Furthermore, the effects of radical scavengers (Na_2CO_3, NaCl, and CH_4O) and enhancers (H_2O_2, ethylenediaminetetraacetic acid (EDTA), and $FeSO_4$) were evaluated on the AR88 removal efficiency.

Equation (1) was used to calculate the percentage of dye removal.[18]

$$(1) \quad R = [\ C_0 - C_t\ /\ C_0\ ] \times 100$$

where, R is the removal percentage (%), and C_0 and C_t are dye concentrations at times of 0 and t, respectively.

The morphology of fixed ZnO nanoparticles was evaluated using a scanning electron microscope (SEM) (TESCAN, Czech Republic). The X-ray diffraction (XRD) patterns of synthesized ZnO nanoparticles were studied using a Cu anode XRD system (λ: 1.54056 Å) in 2θ range from 10 to 80° and step size of 0.026°/s. A DR-5000 UV-VIS spectrophotometer (HACH, USA) was employed for the measurement of AR88 at 505 nm (Determinate λ max). The pH of the solution was measured using a digital pH meter (Jenway, UK).

Results and Discussion

Structural analysis

SEM results

Figure 2 shows the SEM image of ZnO nanoparticles on glass plate. The fixed ZnO nanoparticles have relatively uniform spherical shape and uniform size distributions. The average size of ZnO nanoparticles is 20-50 nm with tangible agglomeration. It can be observed that the fixation of ZnO nanoparticles on a glass plate has been accomplished well.

XRD results

The crystal structure of synthesized ZnO nanoparticles was examined using XRD analysis and is shown in figure 3. The diffraction peaks analysis of the ZnO nanoparticles revealed peaks at 100, 002, 101,

102, 110, 103, and 112 planes, corresponding to the hexagonal wurtzite phase of ZnO.

Moreover, the sharp and intense peaks display the excellent crystal structure of synthesized ZnO nanoparticles. The crystallite size of ZnO nanoparticles was estimated using the Debye–Scherrer equation.[19] Accordingly, the average crystallite size of the ZnO nanoparticles was about 47.4 nm.
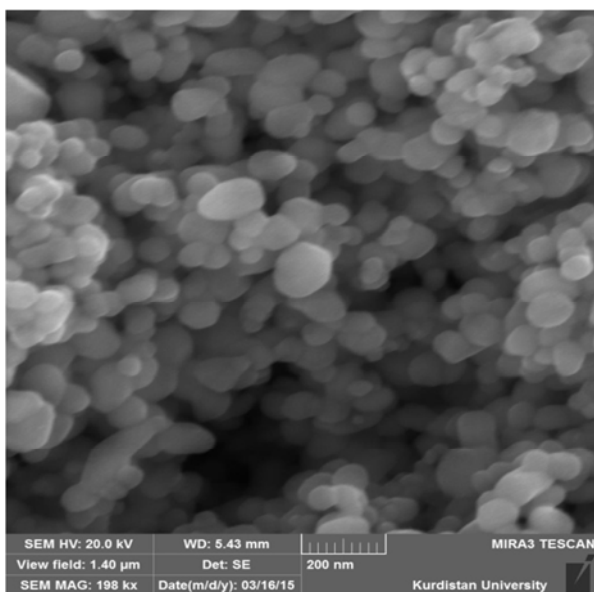

Figure 2. Scanning electron microscopy (SEM) image of fixed ZnO

Photocatalysis efficiency of AR88
Effect of pH
The pH of the solution may affect the surface charge of adsorbent, the degree of ionization of different contaminants, the separation of functional groups on the adsorbent active sites, and also the structure of dye molecules.[20] The effect of pH on the photocatalytic removal of AR88 from aqueous solutions was studied at the pH range of 3 to 11 and dye concentration of 50 mg/l (Figure 4). Samples were taken at 30-, 60-, 90-, and 120-minute time intervals and the removal (%) was calculated using equation 1. The highest removal efficiency (78%) was at neutral pH, and any increase or decrease from pH of 7 reduced the removal efficiency. A

similar result was also reported by Daneshvar et al. for Acid Orange 7, in which photocatalytic degradation was higher at neutral and alkaline pH values.[21] The presence of free hydroxyl anions in the solution is necessary for hydroxyl radical production. However, at the acidic pH values, there are no free hydroxyl anions in the solution.[15]
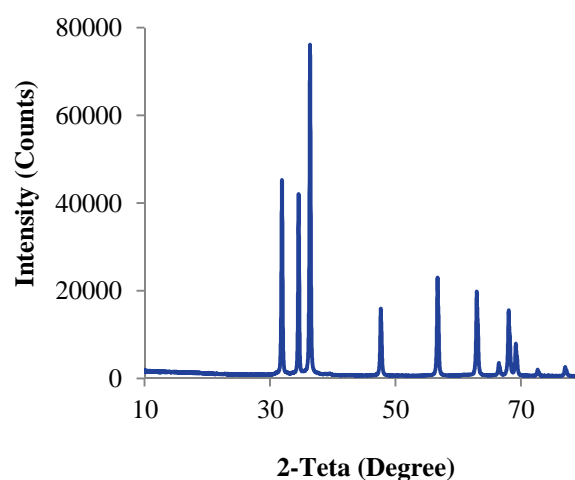
Figure 3. X-ray diffraction (XRD) pattern of ZnO nanostructures

Effect of initial dye concentration
The effect of initial dye concentration on the photocatalytic removal of AR88 in aqueous solutions is shown in figure 5. Samples with 10, 25, 50, and 100 mg/l of dye concentration and pH of 7 were provided and exposed to UV light for 120 minutes. The results showed that when the dye concentration increases from 10 to 100 mg/l, the removal efficiency decreases from 92% to 45% (Figure 5), meaning that their access to the catalyst surface is reduced. An important part of dye removal is performed by active hydroxyl radicals, generated by UV radiation on the catalyst surface. High concentration of dye molecules may act as an inhibitor of hydroxyl radical generation by absorbing light photons, which results in decreased dye removal efficiency.[21]

Grzechulska and Morawski studied the removal of azo acid black using a photocatalytic

process.[22] They reported that higher concentrations of dye cause the formation of multiple layers of dye molecules on the catalyst surface and prevent the direct contact of other molecules with the hydroxyl radicals, and thus, reduce the efficiency of the process. In addition, the increased numbers of dye molecules absorb light photons and inhibit them from reaching the catalyst surface and producing hydroxyl radicals.[22]
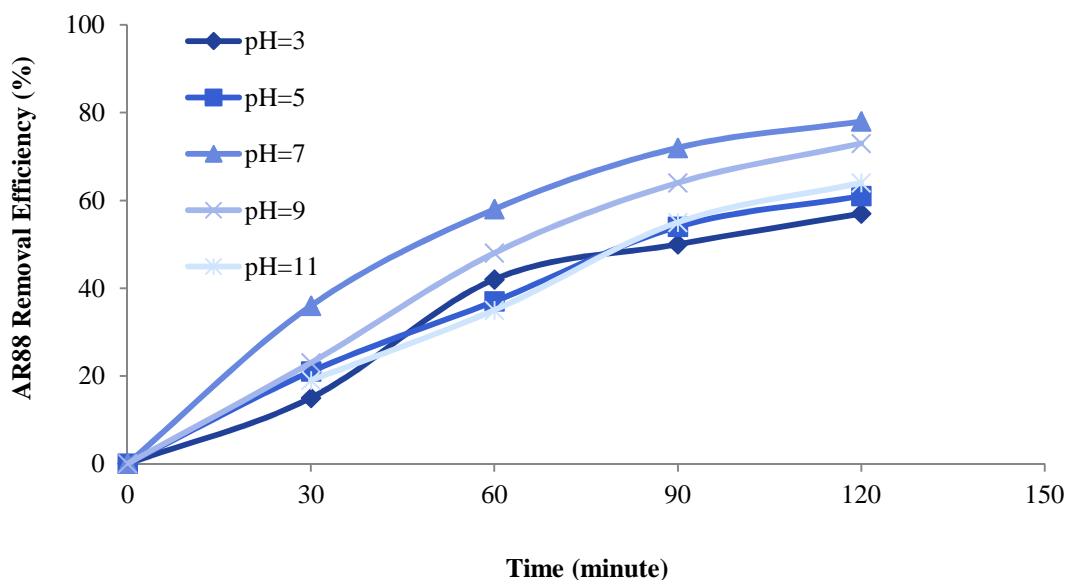

Figure 4. Effect of pH on the photocatalytic removal of Acid Red 88 (AR88) from aqueous solutions (initial dye concentration: 50 mg/l, time: 120 minutes)
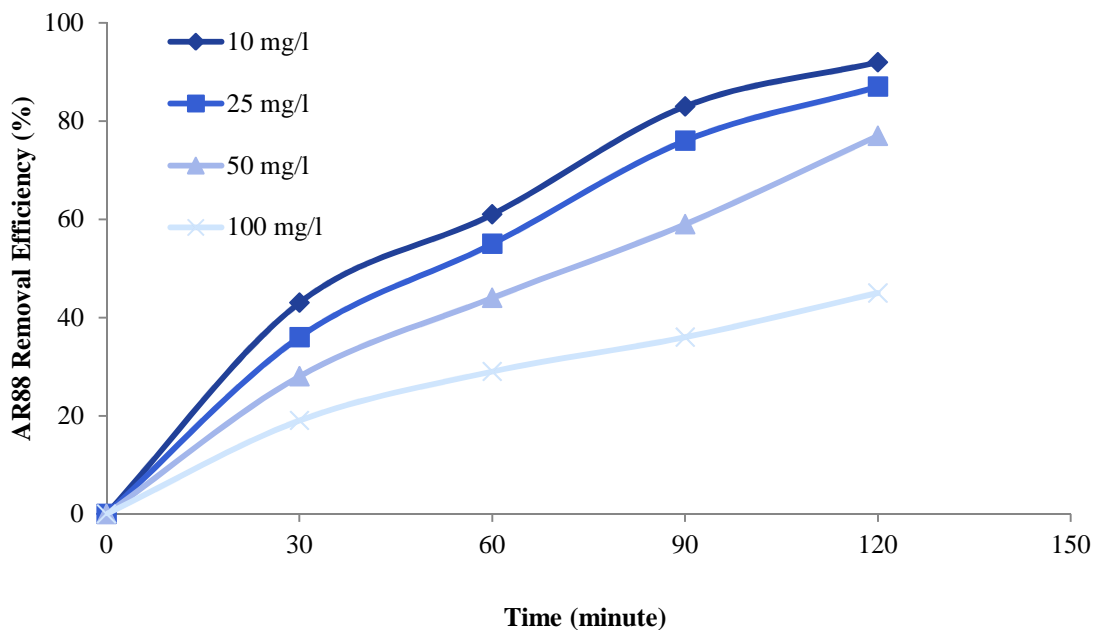

Figure 5. Effect of initial dye concentration on the photocatalytic removal of Acid Red 88 (AR88) from aqueous solutions (pH: 7, time: 120 minutes)

Effect of radical Scavengers

To evaluate the effect of interferences on the photocatalytic removal efficiency of dye, 1 mM of NaCl, Na_2CO_3, and CH_4O were separately added to the samples with a dye concentration of 50 mg/l and at neutral pH. Figure 6 shows the effect of radical scavengers on the photocatalytic removal of AR88 from aqueous solutions. After 120 minutes of contact time, the results showed that such interferences reduce the removal efficiency of the studied dye (Figure 6). The reaction of ions such as Cl^- and CO_3^{2-} with the hydroxyl free radicals reduces the free radicals, and thus, removal efficiency. Daneshvar et al. investigated the effect of operational parameters of Rhodamine B treatment.[23] They showed that Rhodamine B degradation decreased in the presence of Cl^-, HCO_3^-, and CO_3^{2-}, which was due to the scavenging of hydroxyl radicals.[23]
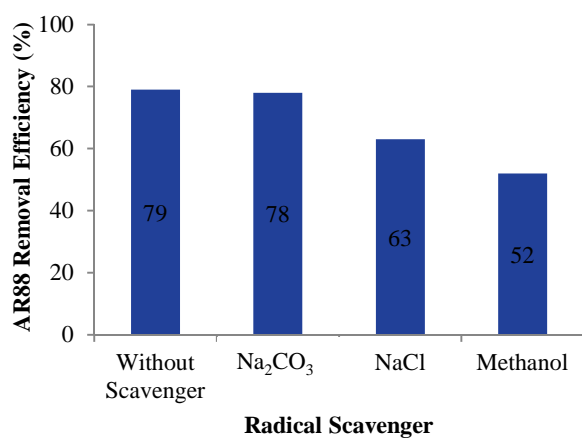

Figure 6. Effect of radical scavengers on the photocatalytic removal of Acid Red 88 (AR88) from aqueous solutions (initial dye concentration: 50 mg/l, pH: 7, time: 120 minutes)

Effect of Enhancers

In the present study, the effect of different enhancers, including H_2O_2, EDTA, and $FeSO_4$, on the photocatalytic removal of AR88 from aqueous solutions was investigated and the results are shown in figure 7. The results revealed that the addition of 1 mM H_2O_2, EDTA, and $FeSO_4$ into the dye solution (50 mg/l), at neutral pH and for 120 minutes, increases the removal efficiency of the dye by 97%, 99%, and 83%, respectively, from the constant removal of 79%. Subramonian and Wu, in their study on the effectiveness of enhancers on the photocatalytic process, showed that the addition of enhancers (H_2O_2 and $S_2O_8^{2-}$) results in the degradation of more dye molecules through the production of more hydroxyl radicals.[24] Similar results have been reported by other researchers.[25] A study on the removal and mineralization of reactive Yellow 86 dye showed that the presence of ferrous ions (Fe^{+2}) in the photo-Fenton process causes an increase in OH^0 generation, and therefore, increase in the photocatalytic decomposition of dye molecules.[26] In photocatalytic processes, EDTA acts as electron donor and scavenger of valence band holes and provides more radicals by delaying the electron-hole recombination on the particles and also enough time for photoactinic processes. The results of the study by Asgari and Ayati showed that photocatalytic removal of dye is faster in the presence of EDTA compared with its absence, which corresponds with the results of the present study.[27]
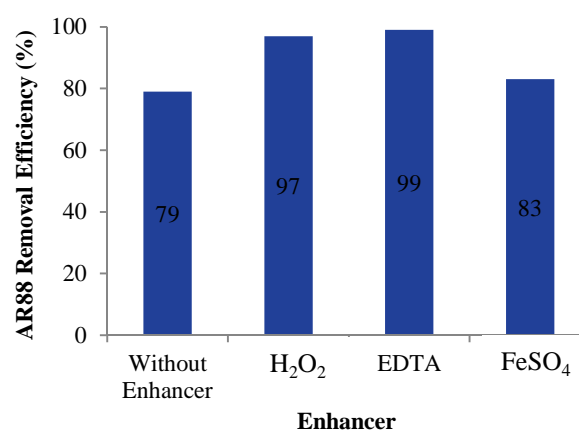

Figure 7. Effect of enhancers on the photocatalytic removal of Acid Red 88 (AR88) from aqueous solutions (initial dye concentration: 50 mg/l, pH: 7, time: 120 minutes)
EDTA: Ethylenediaminetetraacetic acid
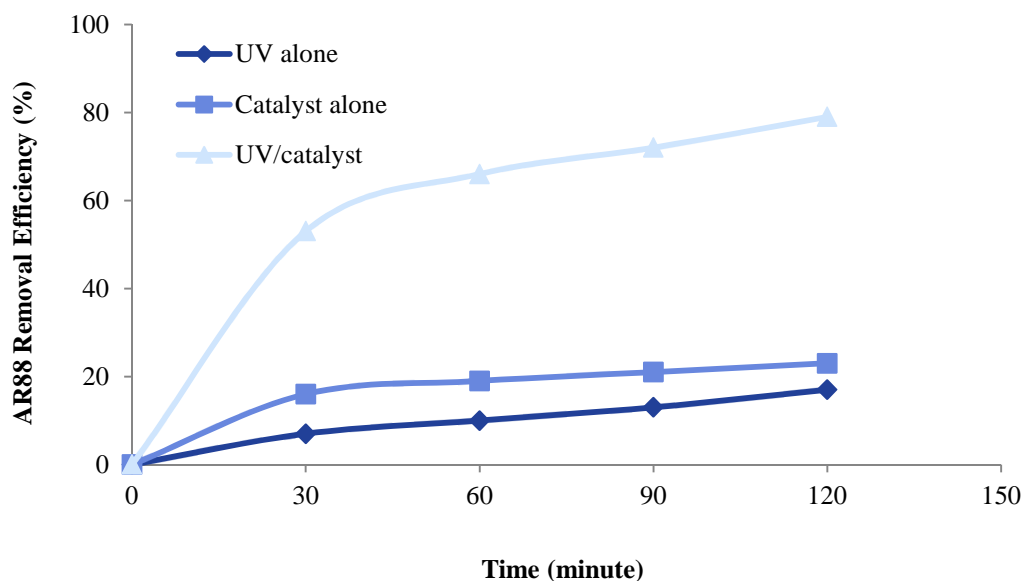
Figure 8. Comparison of photolysis, nanocatalyst alone, and photocatalysis processes in the removal of Acid Red 88 (AR88) from aqueous solutions (initial dye concentration: 50 mg/l, pH: 7, time: 120 minute)

Comparison of processes

To determine the effect of important parameters in photocatalytic decomposition of dye removal, adsorption, photolysis, and photocatalytic processes were studied using nanoparticles, UV light, and a combination of nanoparticles and UV light. Therefore, the experiments were performed on dye concentration of 50 mg/l, at pH of 7 and time intervals of 30, 60, 90, and 120 minutes. Figure 8 shows the comparison of photolysis, nanocatalyst alone, and photocatalysis processes in the removal of AR88 from aqueous solutions. The results indicate that the dye removal efficiency using photolysis process (without catalyst), catalyst alone, and the simultaneous use of both was 17, 23, and 79%, respectively. This finding could be attributed to the fact that the UV light or catalyst, separately, cannot produce enough hydroxyl radicals as the main dye degradation factor.[28] Shanthi and Kuzhalosai reported the same result for the removal of azo dye.[29] They reported that the use of photolysis, or the catalyst alone had little effect on the dye degradation, but the simultaneous application of both resulted in a high removal of dye.[29]

Conclusion

The removal of AR88 from aqueous solution using fixed ZnO photocatalysis under UV light irradiation was studied in the present research. The results showed that the highest removal efficiency was achieved at the neutral pH of 7 (79%). In acidic and alkaline pH, the removal efficiency decreased. By increasing the initial concentration of dye from 10 to 100 mg/l, the removal efficiency decreased from 92 to 45%. The addition of radical scavengers at optimum condition resulted in the decreasing of the removal efficiency, but with the addition of the enhancer the removal efficiency of AR88 was improved. The results of this study confirmed that photocatalysis using fixed ZnO nanoparticles is an efficient method for the removal of textile dyes from aqueous solution.

Conflict of Interests

Authors have no conflict of interests.

Acknowledgements

References

1. Darvishi Cheshmeh Soltani R, Khataee AR, Safari M, Joo SW. Preparation of bio-silica/chitosan nanocomposite for adsorption of a textile dye in aqueous solutions. International Biodeterioration & Biodegradation 2013; 85: 383-91.

2. Darvishi Cheshmeh Soltani R, Khataee AR, Safari M, Ghanadzadeh MJ, Rajaei MS. Response surface methodological evaluation of the adsorption of textile dye onto biosilica/alginate nanobiocomposite: thermodynamic, kinetic, and isotherm studies. Desalination and Water Treatment 2014; 1-14.

3. Behnajady MA, Modirshahla N, Hamzavi R. Kinetic study on photocatalytic degradation of C.I. Acid Yellow 23 by ZnO photocatalyst. J Hazard Mater 2006; 133(1-3): 226-32.

4. Sun JH, Shi SH, Lee YF, Sun SP. Fenton oxidative decolorization of the azo dye Direct Blue 15 in aqueous solution. Chemical Engineering Journal 2009; 155(3): 680-3.

5. Madhavan J, Sathish Kumar PS, Anandan S, Grieser F, Ashokkumar M. Degradation of acid red 88 by the combination of sonolysis and photocatalysis. Separation and Purification Technology 2010; 74(3): 336-41.

6. Noori Motlagh Z, Darvishi R, Shams Khoramabadi G, Godini H, Foroughi M. Study of Methylene Blue Using UV radiation in Study of the Effective Parameters on Decolorizationof Methylene Blue Using UV radiation in the Presence of Immobilized Catalyst. J Ilam Univ Med Sci 2013; 21(1): 36-46. [In Persian].

7. Konicki W, Pelech I, Mijowska E, Jasinska I. Adsorption Kinetics of Acid Dye Acid Red 88 onto Magnetic Multi-Walled Carbon Nanotubes-Fe3C Nanocomposite. CLEAN - Soil, Air, Water 2014; 42(3): 284-94.

8. Batool S, Akib Sh, Ahmad M, Balkhair KS, Ashraf MA. Study of modern nanoenhanced techniques for removal of dyes and water. Journal of Nanomaterials 2014; 2014: 20.

9. Masombaigi H, Rezaee A, Nasiri A. Photocatalytic Degradation of Methylene Blue using ZnO Nano-Particles. Iran J Health Environ 2009; 2(3): 188-95.

10. Mozia S, Tomaszewska M, Morawski AW. Photocatalytic degradation of azo-dye Acid Red 18. Desalination 2005; 185(1–3): 449-56.

11. Alqaragully MB. Removal of Textile Dyes (Maxilon Blue, and Methyl Orange) by Date Stones Activated Carbon. International Journal of Advanced Research in Chemical Science 2014; 1(1): 48-59.

12. Darvishi Cheshmeh Soltani R, Rezaee A, Rezaee R, Safari M, Hashemi H. Photocatalytic degradation of methylene blue dye over immobilized ZnO nanoparticles: Optimization of calcination conditions. J Adv Environ Health Res 2015; 3(1): 8-14.

13. Kamat PS, Huehn R, Nicolaescu R. Semiconductor Nanostructures for Simultaneous Detection and Degradation of Organic Contaminants in Water. J Photochem Photobiol A: Chem 2008; 42(573): 577.

14. Bayat Beed Koupeh R, Ebrahimi M, Keyvani B. Removal of Acid red 206 Dye in Pollutant Water by ZnFe2O4/Bentonite as a Nanophotocatalyst in Batch Reactor Using Taguachi Method. Journal of water and wastewater 2013; 24(3): 128-35. [In Persian].

15. Darvishi Cheshmeh Soltani R, Rezaee A, Safari M, Khataee AR, Karimi B. Photocatalytic degradation of formaldehyde in aqueous solution using ZnO nanoparticles immobilized on glass plates. Desalination and Water Treatment 2015; 53(6): 1613-20.

16. Behnajady MA, Modirshahla N, Daneshvar N, Rabbani M. Photocatalytic degradation of C.I. Acid Red 27 by immobilized ZnO on glass plates in continuous-mode. J Hazard Mater 2007; 140(1-2): 257-63.

17. Mekasuwandumrong O, Pawinrat P, Praserthdam P, Panpranot J. Effects of synthesis conditions and annealing post-treatment on the photocatalytic activities of ZnO nanoparticles in the degradation of methylene blue dye. Chemical Engineering Journal 2010; 164(1): 77-84.

18. Al-Ghouti MA, Khraisheh MA, Allen SJ, Ahmad MN. The removal of dyes from textile wastewater: a study of the physical

characteristics and adsorption mechanisms of diatomaceous earth. J Environ Manage 2003; 69(3): 229-38.

19. Patterson AL. The Scherrer Formula for X-Ray Particle Size Determination. Phys Rev 1939; 56(10): 978-82.

20. Uzun I. Kinetics of the Adsorption of Reactive Dyes by Chitosan. Dyes and Pigments 2006; 70(2): 76-83.

21. Daneshvar N, Rasoulifard MH, Khataee AR, Hosseinzadeh F. Removal of C.I. Acid Orange 7 from aqueous solution by UV irradiation in the presence of ZnO nanopowder. J Hazard Mater 2007; 143(1-2): 95-101.

22. Grzechulska J, Morawski AW. Photocatalytic decomposition of azo-dye acid black 1 in water over modified titanium dioxide. Applied Catalysis B: Environmental 2002; 36(1): 45-51.

23. Daneshvar N, Behnajady MA, Mohammadi MKA, Dorraji MSS. UV/H2O2 treatment of Rhodamine B in aqueous solution: Influence of operational parameters and kinetic modeling. Desalination 2008; 230(1−3): 16-26.

24. Subramonian W, Wu TY. Effect of Enhancers and Inhibitors on Photocatalytic Sunlight Treatment of Methylene Blue. Water, Air, & Soil Pollution 2014; 225(4): 1922.

25. Abo-Farha SA. Photocatalytic Degradation of Monoazo and Diazo Dyes in Wastewater on Nanometer-Sized TiO2. Journal of American Science 2010; 6(11): 130-42.

26. Surana M, Mehta P, Pamecha K, Kabra BV. The decolourization and mineralization of azo dye reactive yellow 86 in aqueous solution by photo-Fenton Reagent, D. Pharma Chemica 2011; 3(2): 39-47.

27. Asgari R, Ayati B. Using the EDTA Hole Scavenger to Accelerate Decolorization in the Immobilized Photocatalytic Process. Journal of Water & Wastewater 2015; 26(97): 19-27. [In Persian].

28. Rahmani Z, Kermani M, Mohammad Mahmoudi N. Performance Evaluation of advanced Photochemical Oxidation (UV/H2O2) and UV in BV16 and RR120 Dye Removal from aqueous solution. The Journal of Toloo-e-Behdasht 2014; 12(4): 135-49. [In Persian].

29. Shanthi M, Kuzhalosai V. Photocatalytic degradation of an azo dye, Acid Red 27, in aqueous solution using nano ZnO. Indian Journal of Chemistry-Section A 2012; 51(3): 428-34.

Acute toxicity of titanium dioxide nanoparticles in Daphnia magna and Pontogammarus maeoticus

Seyed Ali Johari[1], Saba Asghari[1]

1 Department of Fisheries, School of Natural Resources, University of Kurdistan, Sanandaj, Iran

Original Article

Abstract

Titanium dioxide nanoparticles (nTiO$_2$) are the world's second most widely consumed nanomaterial and large quantities of this material enters the aquatic ecosystem annually. Therefore, understanding the effects of nTiO$_2$ on aquatic organisms is very important. The present study used Daphnia magna as a model freshwater organism and Pontogammarus maeoticus as a brackish water organism to evaluate short term toxicity of a well characterized nTiO$_2$ suspension. According to the results, acute exposure of D. magna and P. maeoticus to nTiO$_2$ concentrations ranging from 0.1 to 200 mg/l did not cause any mortality; therefore, lethal concentrations could not be calculated [lethal concentrations (LC) > 200 mg/l]. Observations showed that the TiO$_2$ nanoparticles were trapped on the surface of the body, under the carapace, and in the gut of the D. magna. Although the results of the present acute toxicity experiment did not show nTiO$_2$ to be toxic to the tested aquatic organisms in an environmentally relevant concentration, further studies are needed on the chronic effects of lower concentrations of this nanomaterial in simulated natural ecosystems.

KEYWORDS: Acute, Amphipoda, Cladocera, Nanoparticles, Titanium Dioxide, Toxicity

Citation: Johari SA, Asghari S. **Acute toxicity of titanium dioxide nanoparticles in Daphnia magna and Pontogammarus maeoticus.** J Adv Environ Health Res 2015; 3(2): 111-9.

Introduction

The increasing use of engineered nanomaterials in human life and industrial applications is currently showing inventory listings of 1628 nanotechnology-based consumer products.[1] According to estimations, the worth of nanoproducts will be about $3 trillion by 2020.[2] The 3 most common nanomaterial mentioned in consumer product inventories are silver, titanium, and carbon with 383, 179, and 87 products, respectively.[1]

Nanomaterials have many advantages in terms of life and livelihood improvement, but they may also cause risks to humans and the environment. That is why it is important to recognize the adverse effects of nanomaterials, an issue which is addressed in "nanotoxicology". In addition, part of the engineered nanomaterials produced globally will reach water bodies; 0.4–7% according to Keller et al.[3] Thus, understanding the effect of these substances on aquatic organisms is very important, an issue which is addressed in "aquatic nanotoxicology". Titanium dioxide nanoparticles (nTiO$_2$) is important because of its application in self-cleaning windows, coatings, paints, UV-absorbent cosmetics, and also antimicrobial and antifouling coatings.[4,5] According to estimates, it appears that the

Corresponding Author:
Seyed Ali Johari
Email: a.johari@uok.ac.ir

http://jaehr.muk.ac.ir

concentration of nano-TiO$_2$ in aquatic environment is between 0.7 to 16.8 micrograms per liter.[6,7] Moreover, an estimated 15600 tons of nano-TiO$_2$ enter aquatic ecosystems annually worldwide.[3] Therefore, understanding the effects of nano-TiO$_2$ on aquatic organisms is critical.

Daphnia magna is very sensitive to pollutants and is a suitable aquatic organism through which to evaluate the toxic effects of chemicals in freshwater environment. Therefore, standard toxicity test methods on this aquatic animal have been developed by organizations such as the Organization for Economic Cooperation and Development (OECD), US Environmental Protection Agency (EPA), and International Standards Organization (ISO).[8,9]

There are several recent publications about the toxic effects of some nanomaterials on amphipods.[10-20] Most of these studies show that these sediment-dwelling organisms are likely to have a high potential for exposure to nanomaterial, are highly susceptible to the effects of nanomaterial, and should be considered in the risk assessment of these substances. Gammaridae is a family of amphipods that lives in a wide range of salinities in sea coasts as well as brackish and freshwater environments and generally feed on detritus and herbal materials. Pontogammarus maeoticus is distributed in the Ponto-Caspian region including the Caspian, Azov, and Black Seas.[21] This benthic infauna specie can be found in abundance in the brackish water of Iranian coasts of the Caspian Sea, and usually feeds on detritus.[22] This aquatic organism itself is an important prey for important commercial fish of the Caspian Sea, including sturgeons. To our knowledge, only two studies on nano-TiO$_2$ toxicity in gammarids have been conducted on a freshwater gammarus (Gammarus fossarum) and there is no information on nano-TiO$_2$ toxicity in brackish water gammarids.[11,17]

Therefore, in the present study, we used D. magna as a standard freshwater organism and Pontogammarus maeoticus as a brackish water organism to evaluate the short term toxicity of nano-TiO$_2$ suspension.

Materials and Methods

Powdered TiO$_2$ nanoparticles (nTiO$_2$) were purchased from US Research Nanomaterials, Inc. (Houston, USA). According to information provided by the manufacturer, this white powder consists of more than 99% pure anatase TiO$_2$ nanoparticles with average size of 10-25 nm. A stock suspension of 400 mg/l was prepared by dispersing 40 mg of this powder in 100 ml distilled deionized water following vigorous vortex (Thermo Scientific M37610) for 30 minutes at room temperature, and then, sonication for 6 hours in a bath-type sonicator (Branson 8510EXT-0011). This suspension was not very stable; therefore, it was sonicated for a further 15 minutes before every use. The pH of the final suspension was 6.02.

Transmission electron microscopy (TEM) analyses of the dry nTiO$_2$ powder and its suspension were performed using an H-7100FA transmission electron microscope (Hitachi, Japan) with an acceleration voltage of 125 kV. For each type, the diameters of 80 randomly selected particles were measured at magnifications of 100,000 using Axio Vision digital image processing software (Release 4.8.2.0, Carl Zeiss Micro Imaging GmbH, Germany). Energy dispersive X-ray (EDX) analyses of dry nTiO$_2$ powder and its suspension were performed using an EX200 energy-dispersive X-ray analyzer (Horiba, Japan). Absorption spectral measurements of nTiO$_2$ suspension were obtained using a Spectra-MAX-PLUS 384 UV–visible spectrophotometer (Molecular Devices, USA) in a range of 190-1000 nm.

Daphnia acute toxicity tests

Acute (48 hours) toxicity experiments were performed according to the "Daphnia Sp. acute immobilization test" (OECD test guideline

number 202).[8] The M4 media was used as exposing media and all exposure solutions were prepared immediately before starting the tests through diluting the nano-TiO$_2$ stock in fully aerated M4 media. The concentrations used for daphnia acute toxicity tests were 0.1, 0.5, 1, 2.5, 5, 10, 25, 50, 100, 150, and 200 mg/l nano-TiO$_2$ and M4 media without the addition of nanoparticles in the control groups. After adding appropriate amounts of stock to M4 media, the stock mixtures were continuously stirred with a magnetic stirrer to distribute the suspension at stable concentration to the extent possible. For each concentration, 10 randomly selected neonates, which were younger than 24 hours old, were placed in glass beakers containing 100 ml of exposing media in triplicate. The animals were not fed during the experiments, and all tests were conducted in a water bath system with a constant temperature (20 ± 2 °C) and 16-hour light/8-hour dark photoperiods. After 24 and 48 hours of exposure, any immobilization and mortality of the daphnids in test beakers were assessed according to Annex 1 of OECD 211 based upon which an animal can be taken as dead when it is immobile (i.e., when it is not able to swim) or there is no observed movement of post-abdomen or appendages within 15 seconds after gentle agitation of the test container.[23] It should be noted that, for greater certainty of the results, the tests were continued for 2 more days (a total of 96 hours). Furthermore, the visible adsorption and uptake of TiO$_2$ particles by D. magna were observed and recorded using a microscope (Olympus CX41) equipped with a digital camera (DIXI 3000 mega pixel, NEK Corp., Germany).

Gammarus acute toxicity tests

The samples of the gammarid specie of P. maeoticus were collected 1 week before the beginning of the experiment from the coast of the Caspian Sea near Noor city, Iran, far from any settlement and agricultural activity (36° 35' 1.8" N, 52° 2' 32.8" E). In the laboratory, gammarids were kept in aerated sea water with a salinity of 12 g/l (salinity of their living area in the South of the Caspian Sea) at a constant temperature of 20 ± 1 °C. They were fed lettuce leaves ad libitum until the beginning of the experiment. Only adults with a body length between 8 and 10 mm were used for toxicity experiments. This range was selected to minimize the effect of body size on the results of the experiments.

Test organisms were placed in 200 ml glass beakers containing 10 organisms and 150 ml of freshly prepared test solution. All the tests were conducted in a water bath system with a constant temperature (20 ± 1 °C) and 16-hour light/8-hour dark cycles. Feeding of organisms was stopped 6 hours before the beginning of toxicity tests and the animals were not fed during the bioassays. In this study, fully aerated sea water was used as the exposure media and the test solutions were prepared immediately prior to use by diluting the nano-TiO$_2$ stock in the sea water. After adding appropriate amounts of the stock to the sea water, the stock mixtures were stirred using a magnetic stirrer to distribute the suspension at as stable a concentration as possible. The concentration used for gammarus acute toxicity tests were 0.1, 0.5, 1, 2.5, 5, 10, 25, 50, 100, 150, and 200 mg/l nano-TiO$_2$. Each bioassay included a completely random design, consisting of treatments and controls in triplicate. To evaluate the toxicity of each chemical, the mortality of the gammarids in each test beaker were assessed after 24, 48, 72, and 96 hours of exposure.

Results and Discussion

Particle characterization

In the case of dry nTiO$_2$ powder observed by TEM, most of the particles were needle shaped (Figure 1. A). Moreover, 86.23% of the particles had diameters between 5 and 30 nm (Figure 2.), and only 5.07% of the particles had diameters of more than 50 nm with a maximum diameter of

81 nm. The count median diameter (CMD) for the particles was 13.90 nm (Figure 3). Furthermore, the geometric mean diameter (GMD) and geometric standard deviation (GSD) of dry $nTiO_2$ powder were 17.50 nm and 1.71, respectively. In the case of $nTiO_2$ suspension, TEM images showed that in an aqueous environment the nanoparticles clump and form large aggregates (Figure 1. B). About 28.47% of

these clumps were 15 to 100 nm, 52.55% were 100 to 500 nm, and 18.98% were above 500 nm. As seen in figure 4, EDX analysis confirmed that only elemental titanium was presented in $nTiO_2$ powder. Spectral scans of the sonicated $nTiO_2$ suspension gave the typical profile expected with a distinct peak at about 330 nm (Figure 5) and was similar to previous reports for TiO_2 nanoparticles.[24,25]
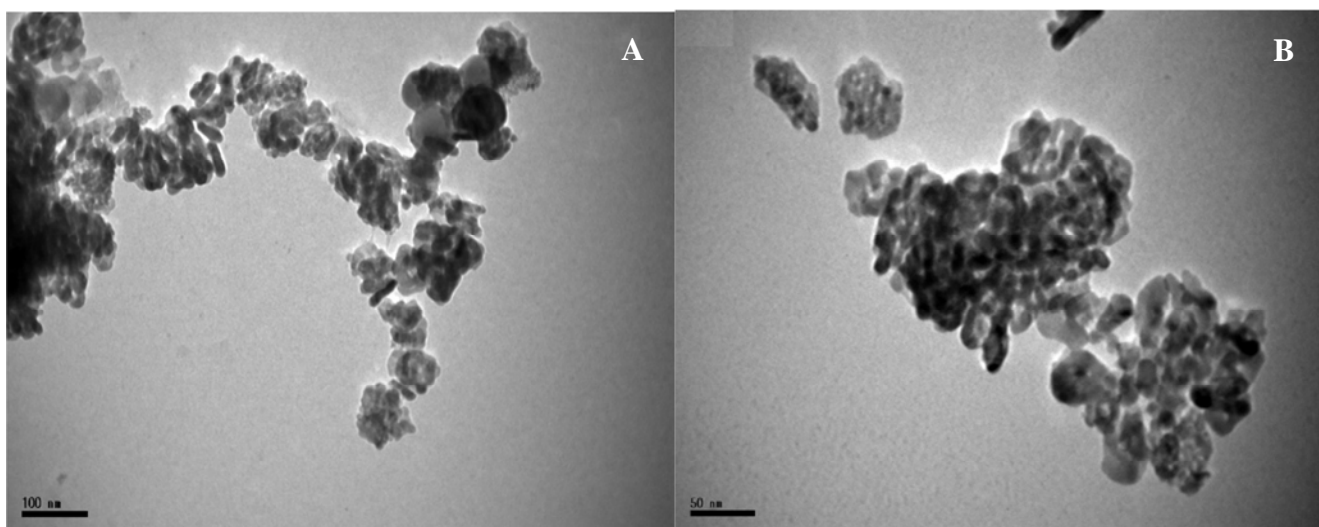
Figure 1. Transmission electron micrographs of dry titanium dioxide nanoparticles (nTiO₂) powder (A) and aqueous suspension of nTiO₂ (B)
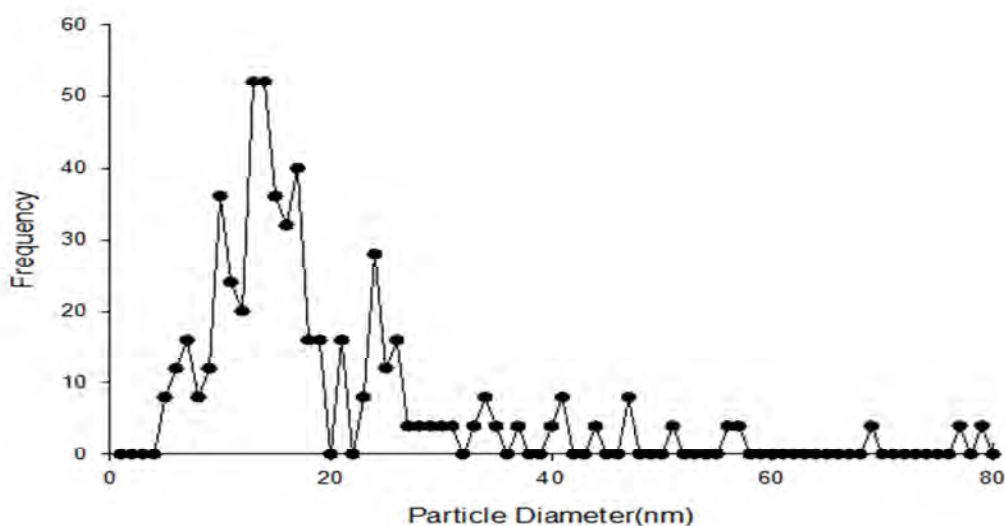
Figure 2. Size distribution of particles based on number frequency determined from transmission electron microscope data in dry titanium dioxide nanoparticles (nTiO₂) powder
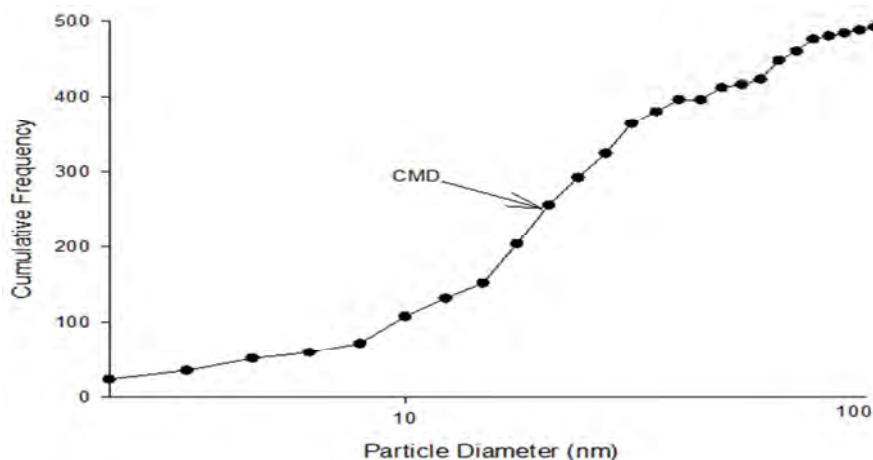
Figure 3. Size distribution of particles based on cumulative frequency determined from transmission electron microscope data in dry titanium dioxide nanoparticles (nTiO₂) powder
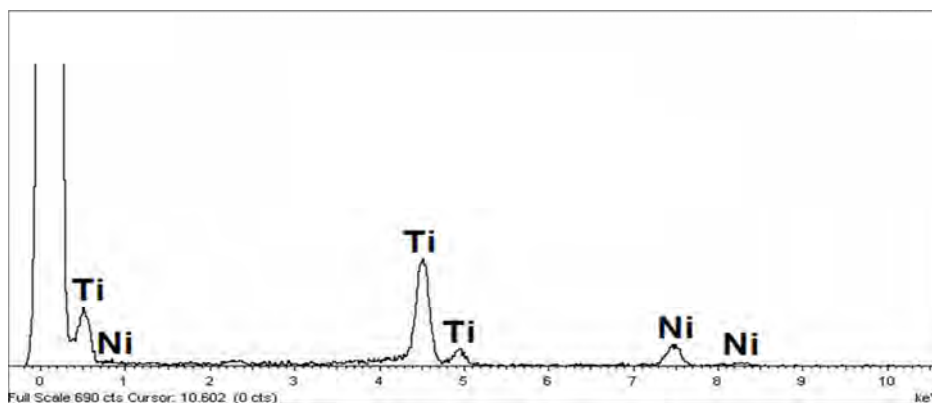
Figure 4. Energy dispersive X-ray (EDX) spectrometer patterns of dry titanium dioxide nanoparticles (nTiO₂) powder [Ni signals in EDX spectrometer are from transmission electron microscopy (TEM) grid]
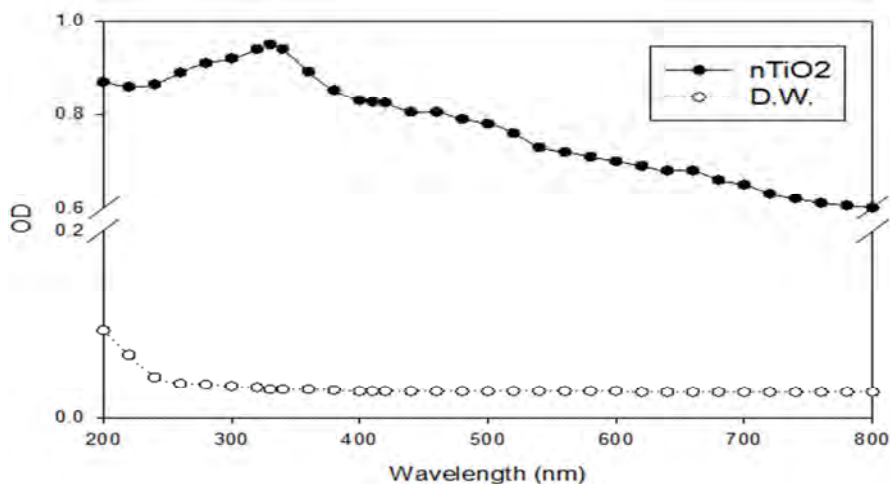
Figure 5. UV–VIS absorption spectra of suspensions of titanium dioxide nanoparticles (nTiO2) and distilled water (D.W.)

Effects of TiO2 nanoparticles on daphnids and gammarids

During the experiments, the mean ± SD of the water pH and dissolved oxygen in the exposure vessels of daphnids were 7.81 ± 0.13 and 7.44 ± 0.19 mg/l, respectively. Moreover, the mean ± SD of the water pH and dissolved oxygen in the exposure vessels of gammarids were 8.3 ± 0.1 and 8.4 ± 0.3 mg/l, respectively. Both in the freshwater (daphnia medium) and brackish water (gammarus medium), sediments of aggregated TiO$_2$ nanoparticles became gradually visible at the bottom of the test beakers with time lapse. During the exposure period, the rate of mortalities in the control groups of daphnids and gammarids was less than 5% and 10%, respectively. According to the results of this study, short term exposure of D. magna to nTiO$_2$ concentrations ranging from 0.1 to 200 mg/l did not cause any mortality even after a longer testing time of up to 96 hour. Thus, we could not calculate lethal concentration of nTiO$_2$ for daphnids [lethal concentrations (LC) > 200 mg/l]. In addition, similar results were obtained in toxicity experiments on P. maeoticus within 96 hours of exposure to nTiO$_2$. Therefore, nTiO$_2$ suspension prepared by sonication in this study did not cause any mortality in D. magna and P. maeoticus during 96 hours of exposure, and therefore, median lethal concentrations (LC$_{50}$s) were estimated to be greater than 200 mg/l. Generally, LC$_{50}$ data provides a good baseline for toxicity tests. According to the US EPA toxicity categories, European Union legislation, and European Union Council Directive 67/548/EEC of 27 June 1967, any substance with a short term LC$_{50}$ of greater than 100 mg/l must be classified as "practically non-toxic" to aquatic organisms.[26,27] Furthermore, according to the Globally Harmonized System of Classification and Labelling of Chemicals (GHS), any substance with a short term LC$_{50}$ of greater than 100 mg/l must be classified as "category

acute 4" to aquatic organisms and may have long lasting harmful effects on aquatic life.[28] The results of several studies on the acute toxicity of different nTiO$_2$ in Daphnia magna are summarized in table 1. As can be seen, most of these studies found acute effect levels of nTiO$_2$ at greater than 100 mg/l, and this is in agreement with our results. The only studies in which the calculated LC$_{50}$ values were less than 100 mg/l were those by Garcia et al.[29] who had used a laboratory synthesized nano-TiO$_2$ which stabilized using tetramethylammonium hydroxide (TMAOH), and Lovern and Klaper [24] who examined the toxicity of nano-TiO$_2$ suspension after filtration. However, in another study by Wiench et al.,[30] the calculated LC$_{50}$ of nTiO$_2$ was greater than 100 mg/l even after filtration. As mentioned before, no information is available on the acute toxicity of nTiO$_2$ on gammarids. Nevertheless, in the case of amphipods, acute toxicity of nano-TiO$_2$ was evaluated in Hyalella azteca by Li et al.[18] According to their results, under a laboratory light, nano-TiO$_2$ showed low toxicity in H. azteca (LC$_{50}$ = 631 mg/l). However, in the presence of simulated solar radiation, nano-TiO$_2$ toxicity in this amphipod showed a 21-fold increase compared to a standard laboratory light (LC$_{50}$ = 29.9 mg/l). Although this increase did not make nano-TiO$_2$ toxic to H. azteca in an environmentally relevant concentration, but this shows the importance of conducting toxicity experiments in natural conditions.

After exposing daphnia to nTiO$_2$ suspensions, some pigmentation was visible in parts of the brood chamber which was not observable in controls (Figure 6). These pigments can be a sign of nanoparticle accumulation under the carapace. Moreover, at higher concentrations, aggregates of nanoparticles were attached to the external surface and appendages of D. magna (Figure 6). In addition, large amounts of dark material were found in the gut tract of daphnia after nanoparticle exposure.

Consequently, the nTiO₂ tested in this study can clearly be ingested by D. magna, and therefore, an accumulation could occur in the gut. In some cases, the ingestion of particles was enough to prevent movement of the daphnia through the water column and caused them to sink to the bottom of the beakers. Similar results were observed in our previous study on toxicity of silver nanoparticles in D. magna.[31] These results suggest that exposure of aquatic organisms to such nanoparticles could pose a risk of bioaccumulation, especially for filter-feeding copepods such as D. magna.

Table 1. A summary of the results of several studies on acute toxicity of titanium dioxide nanoparticles (nTiO₂) in Daphnia magna

Average size of TiO₂ particles in exposure media	Source of nanoparticles	Suspension/preparation method	48-hour LC₅₀ (mg/l)	Reference
15 to 100 nm (28.47%) 100 to 500 nm (52.55%) > 500 nm (18.98%)	Commercial powder	Sonication	> 200	Present study
10 nm	Synthesized in the lab	Stabilizer (TMAOH)	16	29
> 580	Commercial powder	Sonication	> 100	32
n.d.	Commercial powder	Shaking	143.4	33
n.d.	Commercial powder	Sonication	> 250	34
< 100 nm to clumps larger than 200 μm	Commercial powder	Stirring, sonication, or filtration	> 100	30
140 nm	n.d.	Not specified	> 100	35
30 nm	Commercial powder	Filtration	5.5	24
Larger clumps (100 to 500 nm)	Commercial powder	Sonication	> 500	24

n.d. = Not determined; TMAOH: Tetramethylammonium hydroxide; LC₅₀: Lethal concentrations
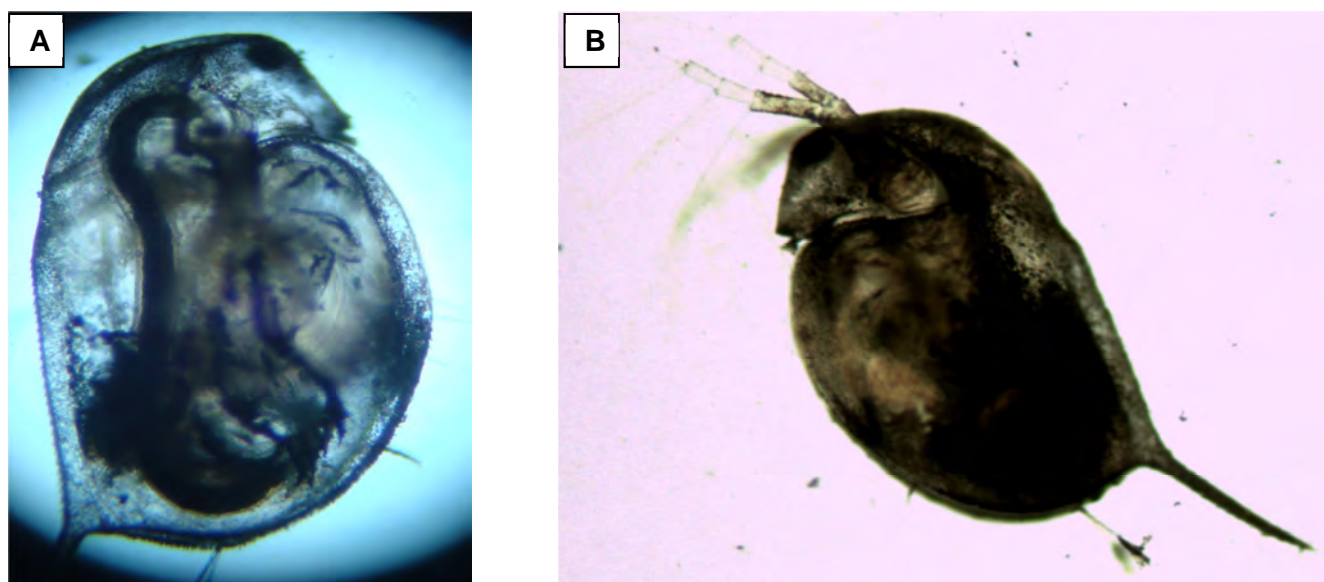
**Figure 6. The uptake and adsorption of titanium dioxide (TiO₂) particles by Daphnia magna 24 hours after exposure to aqueous suspension of Titanium dioxide nanoparticles (nTiO₂) (100 mg/l) (Particles of nTiO₂ are observable on the whole body surface, in the brood chamber, and carapace. In addition, the dark appearance of the gut tract shows that nTiO₂ can be ingested by daphnia.)**

Conclusion

As mentioned in the introduction, the estimated concentration of nano-TiO$_2$ in aquatic environments is currently less than 0.02 mg/l. Therefore, according to the results of the present lab scale study, it seems that this nanomaterial is not an acute hazard for aquatic ecosystems. However, it should be noted that this nanomaterial may have chronic toxic effects on aquatic organisms at low concentrations as it is currently present in the aquatic environment. Therefore, more studies are needed to evaluate the chronic aquatic toxicity of nTiO$_2$ in environmentally relevant concentrations. In addition, toxicity evaluation of this nanomaterial in a simulated natural ecosystem is required.

Conflict of Interests

Authors have no conflict of interests.

Acknowledgements

References

1. Wilson Database. Consumer Products Inventory: An inventory of nanotechnology-based consumer products introduced on the market [Online]. [cited 2015]; Available from: URL: http://www.nanotechproject.org/cpi/
2. Roco MC. The long view of nanotechnology development: the National Nanotechnology Initiative at 10 years. Journal of Nanoparticle Research 2011; 13(2): 427-45.
3. Keller AA, McFerran S, Lazareva A, Suh S. Global life cycle releases of engineered nanomaterials. Journal of Nanoparticle Research 2013; 15: 1692.
4. Parkin IP, Palgrave RG. Self-cleaning coatings. J Mater Chem 2005; 15: 1689-95.
5. Huang Z, Maness PC, Blake DM, Wolfrum EJ, Smolinski SL, Jacoby WA. Bactericidal mode of titanium dioxide photocatalysis. Journal of Photochemistry and Photobiology A: Chemistry 2000; 130(2-3): 163-70.
6. Mueller NC, Nowack B. Exposure modeling of engineered nanoparticles in the environment. Environ Sci Technol 2008; 42(12): 4447-53.
7. O'Brien N, Cummins E. Ranking initial environmental and human health risk resulting from environmentally relevant nanomaterials. J Environ Sci Health A Tox Hazard Subst Environ Eng 2010; 45(8): 992-1007.
8. OECD. OECD Guidelines for the Testing of Chemicals OECD Guidelines for the Testing of Chemicals Fifteenth Addendum No: 202. Paris, France: OECD Publishing; 2004.
9. Baun A, Hartmann NB, Grieger K, Kusk KO. Ecotoxicity of engineered nanoparticles to aquatic invertebrates: a brief review and recommendations for future toxicity testing. Ecotoxicology 2008; 17(5): 387-95.
10. Kennedy AJ, Hull MS, Steevens JA, Dontsova KM, Chappell MA, Gunter JC, et al. Factors influencing the partitioning and toxicity of nanotubes in the aquatic environment. Environ Toxicol Chem 2008; 27(9): 1932-41.
11. Bundschuh M, Zubrod JP, Englert D, Seitz F, Rosenfeldt RR, Schulz R. Effects of nano-TiO(2) in combination with ambient UV-irradiation on a leaf shredding amphipod. Chemosphere 2011; 85(10): 1563-7.
12. Mwangi JN, Wang N, Ritts A, Kunz JL, Ingersoll CG, Li H, et al. Toxicity of silicon carbide nanowires to sediment-dwelling invertebrates in water or sediment exposures. Environ Toxicol Chem 2011; 30(4): 981-7.
13. Fabrega J, Tantra R, Amer A, Stolpe B, Tomkins J, Fry T, et al. Sequestration of zinc from zinc oxide nanoparticles and life cycle effects in the sediment dweller amphipod Corophium volutator. Environ Sci Technol 2012; 46(2): 1128-35.
14. Jackson BP, Bugge D, Ranville JF, Chen CY. Bioavailability, toxicity, and bioaccumulation of quantum dot nanoparticles to the amphipod Leptocheirus plumulosus. Environ Sci Technol 2012; 46(10): 5550-6.
15. Hanna SK, Miller RJ, Zhou D, Keller AA, Lenihan HS. Accumulation and toxicity of metal oxide nanoparticles in a soft-sediment estuarine amphipod. Aquat Toxicol 2013; 142-143: 441-6.
16. Poynton HC, Lazorchak JM, Impellitteri CA, Blalock B, Smith ME, Struewing K, et al. Toxicity and transcriptomic analysis in Hyalella azteca suggests increased exposure and susceptibility of epibenthic organisms to zinc oxide nanoparticles. Environ Sci Technol 2013; 47(16): 9453-60.
17. Kalcikova G, Englert D, Rosenfeldt RR, Seitz F, Schulz R, Bundschuh M. Combined effect of UV-irradiation and TiO(2)-nanoparticles on the predator-

prey interaction of gammarids and mayfly nymphs. Environ Pollut 2014; 186: 136-40.

18. Li S, Wallis LK, Ma H, Diamond SA. Phototoxicity of TiO(2) nanoparticles to a freshwater benthic amphipod: are benthic systems at risk? Sci Total Environ 2014; 466-467: 800-8.

19. Li S, Wallis LK, Diamond SA, Ma H, Hoff DJ. Species sensitivity and dependence on exposure conditions impacting the phototoxicity of TiO(2) nanoparticles to benthic organisms. Environ Toxicol Chem 2014; 33(7): 1563-9.

20. Park S, Woodhall J, Ma G, Veinot JG, Cresser MS, Boxall AB. Regulatory ecotoxicity testing of engineered nanoparticles: are the results relevant to the natural environment? Nanotoxicology 2014; 8(5): 583-92.

21. Barnard JL, Barnard CM. Freshwater Amphipoda of the World: Handbook and bibliography, Volume 2. Vernon, VA: Hayfield Associates; 1983.

22. Mirzajania AR. A study on the population biology of Pontogammarus maeoticus (Sowinsky, 1894) in Bandar Anzali, southwest Caspian Sea. Zoology in the Middle East 2003; 30(1): 61-8.

23. OECD. OECD Guidelines for the Testing of Chemicals / Section 2: Effects on Biotic Systems Test No. 211: Daphnia magna Reproduction Test. Paris, France: OECD Publishing; 2008.

24. Lovern SB, Klaper R. Daphnia magna mortality when exposed to titanium dioxide and fullerene (C60) nanoparticles. Environ Toxicol Chem 2006; 25(4): 1132-7.

25. Federici G, Shaw BJ, Handy RD. Toxicity of titanium dioxide nanoparticles to rainbow trout (Oncorhynchus mykiss): gill injury, oxidative stress, and other physiological effects. Aquat Toxicol 2007; 84(4): 415-30.

26. Directive 1999/45/EC. General classification and labeling requirements for dangerous substances and preparations (Annex VI) [Online]. [cited 1999]; Available from: URL: ec.europa.eu/environment/archives/dansub/pdfs/annex6_en.pdf

27. EUR-Lex. Regulation (EC) No 1272/2008 of the European Parliament and of the Council of 16 December 2008 on classification, labelling and packaging of substances and mixtures, amending and repealing Directives 67/548/EEC and 1999/45/EC, and amending Regulation (EC) No 1907/2006 [Online]. [cited 2008 Dec 12]; Available from: URL: http://eur-lex.europa.eu/legal-content/EN/TXT/?uri=celex:32008R1272

28. UNECE. Globally Harmonized System of Classification and Labelling of Chemicals (GHS, Rev.4). New York, NY: United Nations; 2011.

29. Garcia A, Espinosa R, Delgado L, Casals E, Gonzalez E, Puntes V, et al. Acute toxicity of cerium oxide, titanium oxide and iron oxide nanoparticles using standardized tests. Desalination 2011; 269(1-3): 136-41.

30. Wiench K, Wohlleben W, Hisgen V, Radke K, Salinas E, Zok S, et al. Acute and chronic effects of nano- and non-nano-scale TiO(2) and ZnO particles on mobility and reproduction of the freshwater invertebrate Daphnia magna. Chemosphere 2009; 76(10): 1356-65.

31. Asghari S, Johari SA, Lee JH, Kim YS, Jeon YB, Choi HJ, et al. Toxicity of various silver nanoparticles compared to silver ions in Daphnia magna. J Nanobiotechnology 2012; 10: 14.

32. Zhu X, Chang Y, Chen Y. Toxicity and bioaccumulation of TiO2 nanoparticle aggregates in Daphnia magna. Chemosphere 2010; 78(3): 209-15.

33. Zhu X, Zhu L, Chen Y, Tian S. Acute toxicities of six manufactured nanomaterial suspensions to Daphnia magna. Journal of Nanoparticle Research 2008; 11(1): 67-75.

34. Strigul N, Vaccari L, Galdun C, Wazne M, Liu X, Christodoulatos C, et al. Acute toxicity of boron, titanium dioxide, and aluminum nanoparticles to Daphnia magna and Vibrio fischeri. Desalination 2009; 248(1-3): 771-82.

35. Warheit DB, Hoke RA, Finlay C, Donner EM, Reed KL, Sayes CM. Development of a base set of toxicity tests using ultrafine TiO2 particles as a component of nanoparticle risk management. Toxicol Lett 2007; 171(3): 99-110.

Adsorption of 4-chlorophenol from aqueous solution using activated carbon synthesized from aloe vera green wastes

Yusef Omidi-Khaniabadi[1], Ali Jafari[1], Heshmatollah Nourmoradi[2], Fatemeh Taheri[1], Seddigheh Saeedi[1]

1 Department of Environmental Health Engineering, School of Health, Lorestan University of Medical Sciences, Khorramabad, Iran
2 Department of Environmental Health Engineering, School of Health, Ilam University of Medical Sciences, Ilam, Iran

Original Article

Abstract

In this study, activated carbon synthesized from Aloe vera green wastes was used as a sorbent to remove 4-chlorophenol (4-CP) from aqueous solutions. The influence of contact time (0-100 minutes), pH (2-8), adsorbent dosage (1-9 g/l), and initial 4-CP concentration (10-60 mg/l) in batch system was investigated on the sorption. The sorbent was specified using scanning electron microscopy (SEM). Equilibrium for 4-CP sorption was reached at contact time of 40 minutes. The pH of 2 was also found to be the optimum pH in the sorption process. Fitting the experimental data to different kinetic and isotherm models illustrated that the experimental data was well fitted by pseudo-second order kinetic ($R^2 > 0.98$) and Freundlich isotherm ($R^2 > 0.99$) models. According to the results, activated carbon prepared from Aloe vera green wastes is a low-cost effective option for the sorption of 4-CP from aqueous solutions.

KEYWORDS: Adsorption, Aloe Vera, 4-chlorophenol, Kinetics

Citation: Omidi-Khaniabadi Y, Jafari A, Nourmoradi H, Taheri F, Saeedi S. **Adsorption of 4-Chlorophenol from Aqueous Solution using Activated Carbon Synthesized from Aloe Vera Green Wastes.** J Adv Environ Health Res 2015; 3(2): 120-9.

Introduction

Water pollution due to industrial activities has been considered as one of the most important problems in the current century, especially in developing countries.[1] Phenol and phenolic compounds have been listed as priority pollutants in water and wastewater because of their high toxicity and low biodegradability.[2-4] The principal sources of environmental pollution with chlorophenols are effluent from petrochemical units, coal gasification sites, oil refineries, and pharmaceutical industries.[5] A phenolic compound recognized as a priority pollutant by the United States Environmental Protection Agency (USEPA) due to its toxicity, carcinogenicity, and mutagenicity to living organisms is 4-chlorophenol (4-CP).[5-7] The maximum permissible limit of 4-CP in potable water is 0.5 mg/l.[5] Normally, 4-CP is not degraded through biological treatment in aqueous media. Therefore, many techniques such as electrochemical oxidation, photocatalytic degradation, ultra-filtration, wet oxidation, solvent extraction, and membrane separation and adsorption have been used to remove 4-CP from aqueous solutions.[8-10] Among the physicochemical methods, adsorption process has been widely applied as a treatment technique for organic pollutants.[11,12] This method is one of the best treatment alternatives

Corresponding Author:
Yusef Omidi-Khaniabadi
Email: yusef_omidi@yahoo.com

for the removal of pollutants like 4-CP from water and wastewater, because it is possible to recover the sorbent and adsorbate. Adsorption onto activated carbon due to its simple application and high sorption capacity is the most commonly used technique for the removal of toxic organic pollutants. However, sorption by commercial activated carbon is expensive. Therefore, researches on the production of activated carbon from cheap, local, agricultural wastes, especially due to its low-cost have gained attention worldwide.[13,14] In addition to activated carbon, use of some adsorbents such as carbon black[8], XAD-4 resin[15], surfactant-modified natural zeolite[16], immobilized soybean peroxidase[17], chitosan[18], pumice treated with cationic surfactant[19], Amberlite XAD-16 resin[20], perlite[21], bentonite[21] and Azolla filiculoides biomass[22] has been reported for 4-CP removal from aqueous solutions. The Aloe vera plant is grown in warm tropical areas such as India, United States, Mexico, Australia, Africa, South America, and Iran. Aloe vera green waste is the by-product of the agricultural industry and its original material is used in the production of latex and drugs.[23] In this study, Aloe vera green waste was used as a low-cost sorbent in the production of activated carbon for the removal of 4-CP from synthetic wastewater. The influence of parameters such as contact time, pH, adsorbent dosage, and initial concentration was investigated on the sorption.

Materials and Methods

All Aloe vera green waste used in this study was collected from suburban farms of Ahvaz, Iran. 4-CP, H_2SO_4, and NaOH were purchased from Merck Co. (Germany). Through the addition of 0.1 N H_2SO_4 or NaOH, the solution pH was adjusted using a pH meter (50-pp-sartorious model). All of the other chemical substances used were of analytical grade. The stock solution of 4-CP (1000 mg/l) was prepared by dissolving 1 g of 4-CP in 1 l deionized water and the working solutions were prepared by dilution of the stock solution. 4-CP has a chemical formula of C_6H_5ClO and molecular weight of 128.56 g/mol.[11] The suspension of sorbent and adsorbate was agitated using a rotary shaker (Behdad-Rotomix Model) at 200 rpm.

Elemental analysis of samples of Aloe vera green waste-based activated carbon was conducted using a Heraeus Elemental Analyzer (Jobin-Yvon Ultima ICP-AES, USA). The surface morphology of the sorbent before and after adsorption process was characterized by a scanning electron microscope (SEM, Jeol Model Jsm-T330, Japan). The concentration of 4-CP in the solution was measured by an UV-Vis spectrophotometer (PG Instrument Limited Model) at maximum absorbance wavelength of 280 nm.

Aloe vera green wastes were thoroughly washed with deionized water for the removal of impurities and dried in an oven at 150 °C for 24 hours. Then, it was crushed using a Thomas-Wiley Laboratory Mill and sieved. The activated carbon with particle sizes of 300-600 μm was carbonized in a furnace at 550 °C for 20 minutes and sieved (mesh no = 40) for later experiments.

Batch sorption experiments were conducted to determine the influence of parameters such as contact time (0-100 minutes), pH (2-8), adsorbent dosage (1-9 g/l), and adsorbate concentration (10-60 mg/l) on the sorption of 4-CP from aqueous solutions using activated carbon from Aloe vera green wastes. All of the adsorption experiments were carried out at room temperature (25 °C) and shaken (200 rpm) with 100 ml 4-CP solution in a 250 ml Erlenmeyer flask. After agitation, the suspension was filtered using fiberglass paper and the sample absorbance was measured to determine 4-CP content. The experiments were duplicated and the average values were considered. The adsorption capacity of 4-CP was calculated using equation (1):

$$q_e = \frac{(C_0 - C_e)\, V}{m} \qquad (1)$$

Where q_e (mg/g) is the sorption capacity of Aloe vera green waste-based activated carbon, C_0 and C_e (mg/l) are the initial and equilibrium adsorbate concentrations, V (l) is the volume of the solution and m (g) is the mass of adsorbent.

Results and Discussion

Characterization

Chemical composition of activated carbon derived from Aloe vera green waste showed that O, Ca, K, and Mg formed 92.7% of the total weight (wt%) of the sorbent. Other minor compounds included Na (5.92%) and Cl (1.35%).

Figures 1 (a) and (b) illustrate the surface morphology of the sorbent before and after the sorption. As seen in figure 1 (a), before the sorption, the surface morphology of activated carbon has uneven cavities and fine open pores. A regular structure and developed pores can be seen after the sorption in figure 1 (b), which shows a smoother surface of activated carbon. The development of pores can be due to the effect of 4-CP that has filled the pores.

Effect of contact time

The sorption data versus contact time for the uptake of 4-CP by Aloe vera green waste-based activated carbon is indicated in figure 2 (a). It can be seen that at first initial adsorption of 4-CP occurred rapidly. Equilibrium was obtained at contact time of 40 minutes (q_e = 5.59 mg/g), and then, gradually reached a fixed state during the remaining time of up to 100 minutes. The fast uptake of 4-CP molecules at the beginning of the adsorption time can be due to the availability of large numbers of vacant sites on the sorbent surface. With the increasing of contact time these vacant sites were saturated with 4-CP and adsorption capacity was gradually increased. Similar results were obtained for the removal of 4-CP by various adsorbents.[5,16,18]

Zazouli et al. reported that the optimum contact time for removal of 4-CP from aqueous solution by Azolla filiculoides biomass was obtained at 75 minutes.[22] Bilgili showed that the sorption of 4-CP from aqueous media by XAD-4 resin reached equilibrium at contact time of 120 minutes.[15] Therefore, in this study, the contact time of 40 minutes was selected for the subsequent experiments.
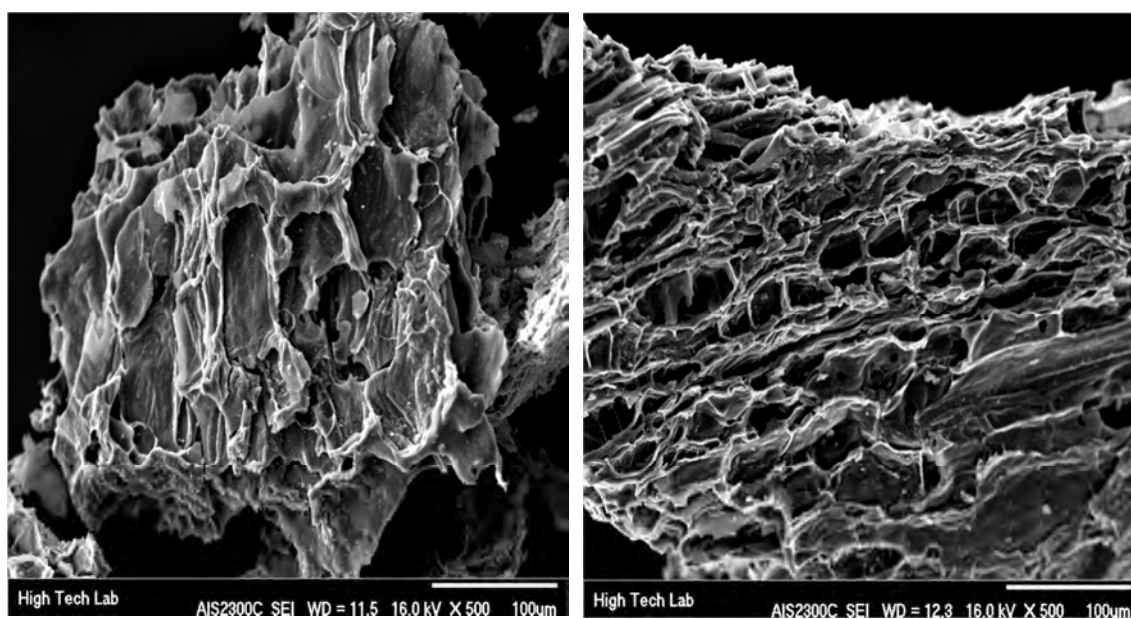

Figure 1. The scanning electron microscopy (SEM) image of activated carbon (a) before and (b) after the uptake process

Kinetic study

Kinetic models are suitable for designating the sorption mechanism of 4-CP on the adsorbent surface. In this study, the experimental data was fitted by pseudo-first order and pseudo-second order kinetic models in order to attain a better understanding from the sorption process and the results are presented in table 1. The pseudo-first order kinetic model [24-26] can be illustrated by equation (2):

$$\ln(q_e - q_t) = \ln q_e - k_1 t \qquad (2)$$

Where q_e and q_t (mg/g) are the values of 4-CP adsorbed onto the activated carbon surface at equilibrium and at time t (minute), respectively. Moreover, K_1 (1/minute) is the rate constant of the pseudo-first order kinetic model. K_1 and q_e were determined from linear plot of $\ln(q_e - q_t)$ versus time (minute), which are obtained from the slope and intercept, respectively.

The experimental data of 4-CP sorption was also analyzed using pseudo-second order kinetic model.[24,27] This sorption kinetic model can be shown by the following equation:

$$\frac{t}{q_t} = \frac{1}{k_2 q_e^2} + \frac{t}{q_e} \qquad (3)$$

Where q_e and q_t (mg/g) are similar to the pseudo-first order kinetic model, and K_2 (g/mg. minute) is the rate constant of the pseudo-second order kinetic. K_2 and q_e can be obtained from the intercept and slope of $\frac{t}{q_t}$ against time in equation 3, respectively.

Figures 2 (b) and (c) show the pseudo-first order and pseudo-second order kinetic models for the adsorption of 4-CP from aqueous solutions by activated carbon obtained from Aloe vera green waste. The higher liner correlation coefficient ($R^2 > 0.98$) of the pseudo-second order kinetic model showed that the pseudo-second order kinetic model fitted the experimental data better than other kinetic models described earlier. Ahmed and Theydan showed that the removal of 4-CP from aqueous solution using activated carbon from Albizia lebbeck seed pods followed the pseudo-second order kinetic model.[5] Zazouli et al. also illustrated that the equilibrium data of 4-CP removal using Azolla filiculoides biomass was well described by the pseudo-second orde kinetic model.[22] These results are in agreement with those reported by Tseng and Tseng[28] and Wu et al.[29] for 4-CP adsorption on activated carbons prepared from different agricultural precursors.

Effect of solution pH and adsorbent dosage

The solution pH is a substantial parameter in the sorption system.[30] The solution pH has a control effect on the ionization, dissociation, nature, and surface properties of the sorbent.[31]
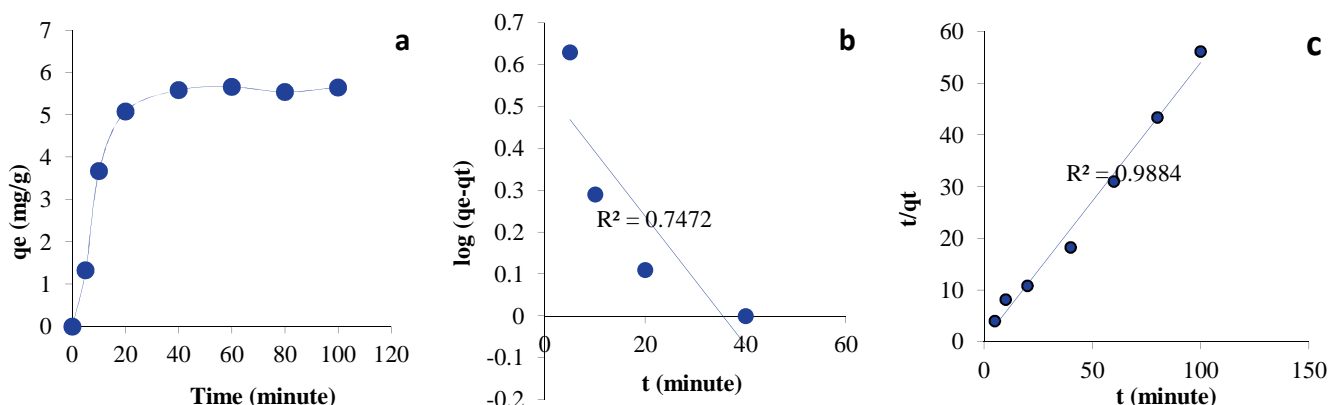

Figure 2. (a) Effect of contact time on the sorption of 4-CP (adsorbent dosage = 3 g/l, and initial concentration = 20 mg/l at the initial solution pH), and (b) pseudo-first order and (c) pseudo-second order kinetic models

Table 1. Parameters of pseudo-first order kinetic and pseudo-second order kinetic models

| Adsorbate	Pseudo-first order			Pseudo-second order				
	q_e, experimental (mg/g)	K_1 (1/minute)	R^2	q_e, experimental (mg/g)	K_2 (g/mg.minute)	h (g/mg.minute)	q_e, calculated (mg/g)	R^2
4-CP	5.85	0.0069	0.74	6.59	0.49	0.41	6.3	0.98
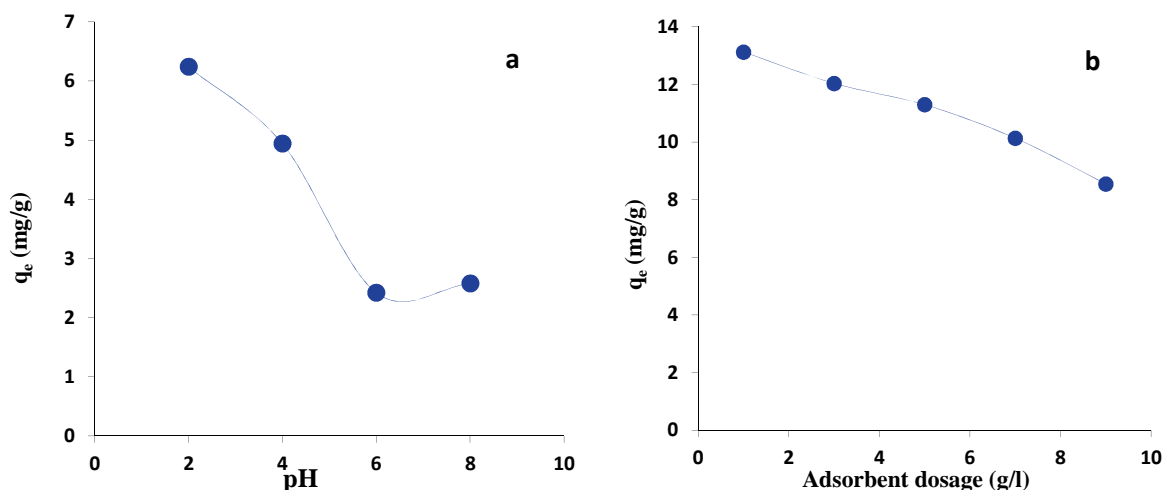
Figure 3. (a) Effect of pH on the adsorption of 4-CP (contact time = 40 minutes, adsorption dosage = 3 g/l, and initial concentration = 20 mg/l) and (b) effect of adsorbent dosage on the adsorption of 4-CP (contact time = 40 minutes, initial concentration = 20 mg/l, and pH = 2)

The influence of pH on the removal of 4-CP was investigated and the results are illustrated in figure 3 (a). As can be seen, the increasing of solution pH had a significant effect on the decreasing of 4-CP sorption by activated carbon. This result may be due to change in surface charge of 4-CP molecules and functional groups of the sorbent. The isoelectric point of the natural sorbent was found to be at pH of 11.3. At the lower pH values of the isoelectric point, there is a positive charge on the sorbent surface which will promote reaction with 4-CP. Radhika and Palanivelu reported that at a pH of 2, the adsorbent surface has more positively charged sites, but with the increase in solution pH, the sorption of 4-CP decreases.[32] Thus, the optimum pH for the removal of 4-CP by carbon in this study was chosen as a pH of 2.

The effect of different dosages of Aloe vera green waste-based activated carbon was evaluated in an initial 4-CP concentration of 20 mg/l at room temperature and the results are

presented in figure 3(b). It was observed that with increasing the adsorbent dosage from 1 g/l to 9 g/l, the adsorption capacity was reduced. The decrease in the sorption value of 4-CP in higher dosages of Aloe vera green waste activated carbon may be due to the unavailability of the pollutant molecules and their inability to cover all the active sites on the adsorbent surface. In other words, a large number of the surface active sites of the adsorbent cannot reach saturation state at high Aloe vera green waste activated carbon dosages. Therefore, a 1 g/l dose of Aloe vera green waste activated carbon was chosen as the optimum dosage for the next stages. Bilgili illustrated that the sorption of 4-CP from aqueous media remained almost constant at sorbent dosages greater than 10 g/l.[15]

Effect of initial concentrations of 4-CP

The influence of initial concentrations of 4-CP on the sorption capacity was investigated and the results are illustrated in figure 4 (a). It is

evident that the sorption capacity of activated carbon prepared from Aloe vera green waste rapidly increased with the increasing of 4-CP in the solution. This can be due to accessibility of vacant sites of the adsorbent surface and increase in the driving force of 4-CP including the van der Waals force to the active sites of the adsorbent; this state can occur at higher 4-CP concentrations.

Isotherm study

When the sorption process reaches an equilibrium state, the study of adsorption isotherms is necessary in order to explain the distribution of adsorbate molecules between liquid and solid phases. Moreover, the isotherms can provide information about the heterogeneity and homogeneity of the adsorbent surface.[33] In this study, the experimental data were analyzed by Langmuir, Freundlich, and Tempkin isotherms in initial concentration of 10-100 mg/l at contact time of 12 hours and the results are presented in table 2.

The Langmuir isotherm assumes that monolayer uptake occurs at binding sites with homogenous energy levels.[13] This isotherm model predicts the maximum sorption capacity of 4-CP on the homogenous surface of Aloe vera green waste-based activated carbon. The Langmuir isotherm can be linearized using equation (4):

$$\frac{C_e}{q_e} = \left(\frac{1}{bQ_m}\right) + \frac{C_e}{Q_m} \qquad (4)$$

Where C_e (mg/l) is the equilibrium concentration of 4-CP, q_e (mg/g) the sorption capacity of Aloe vera green waste activated carbon in during the equilibrium time. Q_m (maximum adsorption capacity, mg/g) and b (the Langmuir constant, l/mg) are obtained from the slope and intercept of linear plots of C_e/q_e versus C_e, respectively.

The essential property of the Langmuir isotherm model is a dimensionless constant separation factor, R_L, or equilibrium parameter[34,27] and is defined by equation (5):

$$R_L = \frac{1}{1 + bC_0} \qquad (5)$$

Where b is the Langmuir constant and C_0 is initial adsorbate concentration (Langmuir isotherm). The value of R_L demonstrates that the sorption system is unfavorable ($R_L > 1$), irreversible ($R_L = 0$), liner ($R_L = 1$), or favorable ($0 < R_L < 1$). Based on the value of R_L (0.92), the sorption system of 4-CP on the activated carbon was favorable.

The Freundlich isotherm model can be applied for non-ideal adsorption on aheterogeneous surface of sorbent.[35] The Freundlich isotherm model can be described by equation (6):

$$\ln q_e = \ln K_f + \left(\frac{1}{n}\right) \ln C_e \qquad (6)$$

Where q_e is the sorption capacity, C_0 is initial adsorbate concentration (Langmuir isotherm), K_f (l/g) and n are constants of the isotherm and illustrate the capacity and intensity of the adsorption, respectively. In this isotherm model, n demonstrates the adsorption intensity. K_f and n are obtained from the intercept and slope of plotting ln q_e versus ln C_e, respectively. The values of n higher than 1 illustrate that the sorption bonds between pollutant and adsorbent surface have been powerfully formed. An n value higher than 1 and less than 10 shows that the adsorption process is suitable. In this study, the value of n calculated using the Freundlich model was 1.13. Therefore, the value of n illustrated that the adsorption bonds between 4-CP and Aloe vera green waste activated carbon was appropriately strong. Figures 4 (b) and (c) show the Langmuir and Freundlich isotherm models plot for the adsorption of 4-CP on the activated carbon surface.

Tempkin illustrates the influence of some indirect sorbate/adsorbate interactions on the adsorption isotherm.[36,37] The Tempkin isotherm is applied through equation (7):

$$q_t = B_1 \ln K_t + B_1 \ln C_e \qquad (7)$$

Where q_e (mg/g) is the adsorption capacity at equilibrium time, C_e (mg/l) is the equilibrium concentration of 4-CP, and B_1 and K_1 are Tempkin constants. Amounts of B_1 and K_t are calculated from the plot of q_e versus ln C_e. Figure 4 (d) shows the Tempkin isotherm model plot for the sorption of 4-CP. The adsorption isotherm model of 4-CP by Aloe

vera green waste activated carbon was well described by the Freundlich isotherm. Similar results were reported by Radhika and Palanivelu for the removal of 4-CP from aqueous solution using coconut shell activated carbon.[32] Kuleyin reported that the experimental data of 4-CP removal using surfactant-modified natural zeolite are well described by the Freundlich isotherm model.[16]
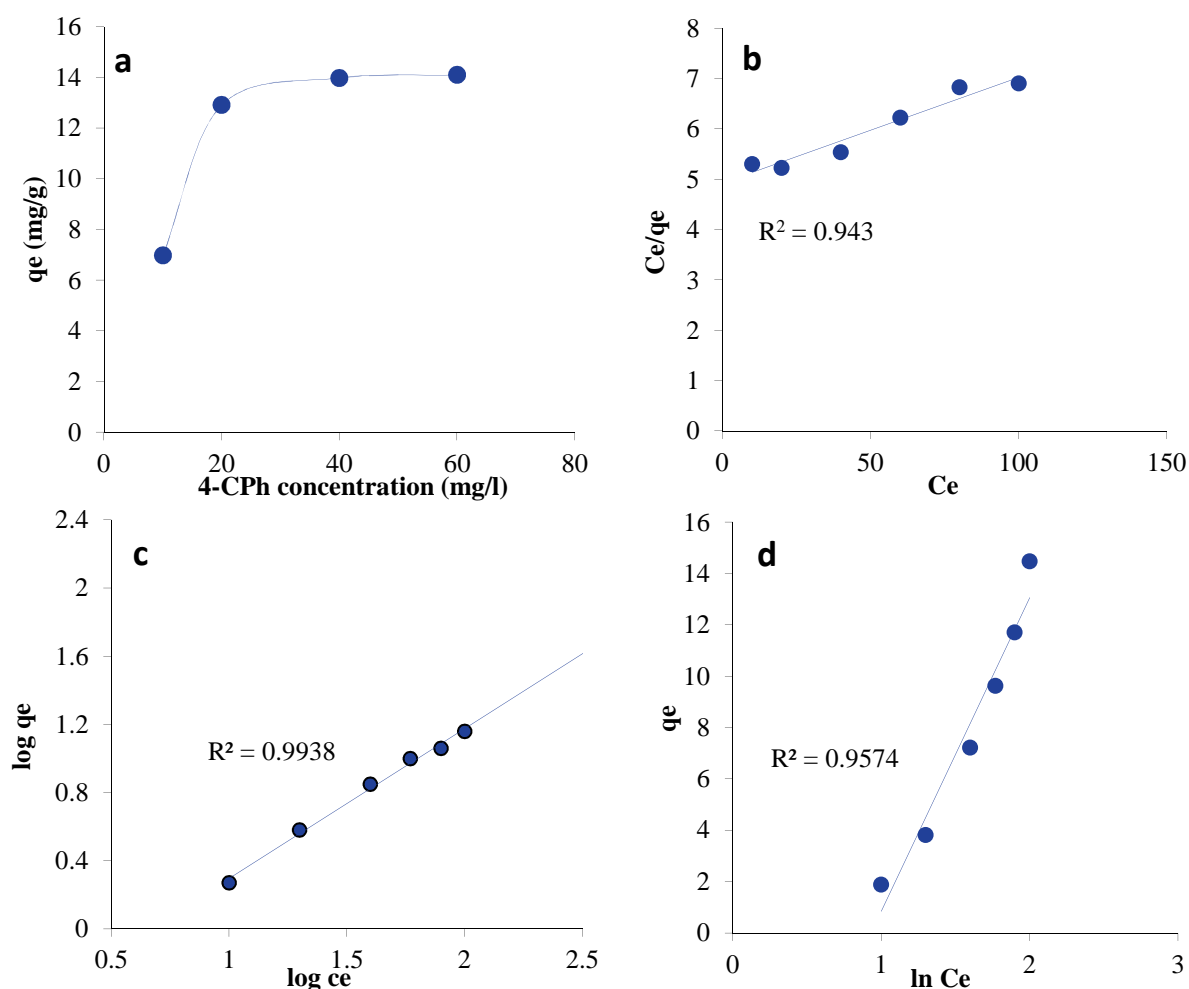
Figure 4. (a) Effect of initial concentration on the adsorption of 4-CP (contact time = 40 minutes, adsorption dosage = 1 g/l, and pH = 2) and (b) Langmuir, (c) Freundlich, and (d) Tempkin isotherms

Table 2. Parameters of Langmuir, Freundlich, and Tempkin isotherms

Adsorbate	Langmuir				Freundlich			Tempkin		
	q_m (mg/g)	b (l/g)	R^2	R_L	K_f (l/g)	n	R^2	B_1	K_t (l/g)	R^2
4-CP	47.6	0.0042	0.94	0.92	0.23	1.13	0.99	11.37	0.029	0.95

Table 3. Comparison of the maximum monolayer adsorption capacities of 4-CP with activated carbon from various adsorbents

Adsorbent	Maximum sorption capacity (mg/g)	Contact time (h)	Temperature (°k)	Ref.
Aloe vera green waste-based activated carbon	47.60	12.00	298	This study
Zeolit	12.70	8.00	293	16
Azolla filiculoides biomass	8.24	1.15	298	22
Rice husk	44.64	2.00	288	38
Cork	93.84	168.00	298	39
Chitosan	20.49	-	303	18

Comparison with other studies

The maximum adsorption capacity of 4-CP by activated carbon in this study was 47.6 mg/g. This value has been compared with q_m obtained in the literature for activated carbons prepared from various agricultural and industrial wastes (Table 3). It can be observed in table 3 that the activated carbon prepared from Aloe vera green waste can be considered as an effective adsorbent for uptake of 4-CP from aqueous media.

Conclusion

In this batch study, Aloe vera green waste activated carbon was used as an adsorbent for the uptake of 4-CP from aqueous solutions. The optimum contact time for the removal of 4-CP by carbon was 40 minutes. Moreover, the optimum pH acquired was 2. The Freundlich isotherm model and pseudo-second order kinetic model described the data better than other isotherm and kinetic models. It can be concluded from this study that Aloe vera green waste-based activated carbon can be employed as a low-cost adsorbent for the removal of 4-CP from aqueous solution.

Conflict of Interests

Authors have no conflict of interests.

Acknowledgements

References

1. Jourvand M, Shams Khorramabadi G, Omidi Khaniabadi Y, Godini H, Nourmoradi H. Removal of methylene blue from aqueous solutions using modified clay. Journal of Basic Research in Medical Sciences 2015; 2(1): 32-41.
2. Nguyen AT, Juang RS. Photocatalytic degradation of p-chlorophenol by hybrid H(2)O(2) and TiO(2) in aqueous suspensions under UV irradiation. J Environ Manage 2015; 147: 271-7.
3. Nourmoradi H, Avazpour M, Ghasemian N, Heidari M, Moradnejadi K, Khodarahmi F, et al. Surfactant modified montmorillonite as a low cost adsorbent for 4-chlorophenol: Equilibrium, kinetic and thermodynamic study. Journal of the Taiwan Institute of Chemical Engineers 2015.
4. Sun Y, Chen J, Li A, Liu F, Zhang Q. Adsorption of resorcinol and catechol from aqueous solution by aminated hypercrosslinked polymers. Reactive and Functional Polymers 2005; 64(2): 63-73.
5. Ahmed MJ, Theydan SK. Adsorption of p-chlorophenol onto microporous activated carbon from Albizia lebbeck seed pods by one-step microwave assisted activation. Journal of Analytical and Applied Pyrolysis 2013; 100: 253-60.
6. Sze MF, McKay G. An adsorption diffusion model for removal of para-chlorophenol by activated carbon derived from bituminous coal. Environ Pollut 2010; 158(5): 1669-74.
7. Sze MF, McKay G. Enhanced mitigation of para-chlorophenol using stratified activated carbon adsorption columns. Water Res 2012; 46(3): 700-10.
8. Dominguez-Vargas JR, Navarro-Rodriguez JA, de Heredia JB, Cuerda-Correa EM. Removal of chlorophenols in aqueous solution by carbon black low-cost adsorbents. Equilibrium study and influence of operation conditions. J Hazard Mater 2009; 169(1-3): 302-8.

9. Zhihui A, Peng Y, Xiaohua L. Degradation of 4-chlorophenol by microwave irradiation enhanced advanced oxidation processes. Chemosphere 2005; 60(6): 824-7.

10. Sarkar M, Acharya PK. Use of fly ash for the removal of phenol and its analogues from contaminated water. Waste Manag 2006; 26(6): 559-70.

11. Nourmoradi H, Nikaeen M, Khiadani H. Removal of benzene, toluene, ethylbenzene and xylene (BTEX) from aqueous solutions by montmorillonite modified with nonionic surfactant: Equilibrium, kinetic and thermodynamic study. Chemical Engineering Journal 2012; 191: 341-8.

12. Babaei AA, Alaee Z, Ahmadpour E, Ramazanpour-Esfahani A. Kinetic modeling of methylene blue adsorption onto acid-activated spent tea: A comparison between linear and non-linear regression analysis. Journal of Advances in Environmental Health Research 2014; 2(4): 197-208.

13. de Luna MD, Flores ED, Genuino DA, Futalan CM, Wan MW. Adsorption of Eriochrome Black T (EBT) dye using activated carbon prepared from waste rice hullsΓÇöOptimization, isotherm and kinetic studies. Journal of the Taiwan Institute of Chemical Engineers 2013; 44(4): 646-53.

14. Dehestaniathar A, Rezaee A. Adsorption of nitrate from aqueous solution using activated carbon-supported Fe0, Fe2 (SO4)3, and FeSO4. Journal of Advances in Environmental Health Research 2014; 2(3): 181-8.

15. Bilgili MS. Adsorption of 4-chlorophenol from aqueous solutions by xad-4 resin: isotherm, kinetic, and thermodynamic analysis. J Hazard Mater 2006; 137(1): 157-64.

16. Kuleyin A. Removal of phenol and 4-chlorophenol by surfactant-modified natural zeolite. J Hazard Mater 2007; 144(1-2): 307-15.

17. Gomez M, Matafonova G, Gomez JL, Batoev V, Christofi N. Comparison of alternative treatments for 4-chlorophenol removal from aqueous solutions: use of free and immobilized soybean peroxidase and KrCl excilamp. J Hazard Mater 2009; 169(1-3): 46-51.

18. Li JM, Meng XG, Hu CW, Du J. Adsorption of phenol, p-chlorophenol and p-nitrophenol onto functional chitosan. Bioresour Technol 2009; 100(3): 1168-73.

19. Akbal F. Sorption of phenol and 4-chlorophenol onto pumice treated with cationic surfactant. J Environ Manage 2005; 74(3): 239-44.

20. Abburi K. Adsorption of phenol and p-chlorophenol from their single and bisolute aqueous solutions on Amberlite XAD-16 resin. J Hazard Mater 2003; 105(1-3): 143-56.

21. Koumanova B, Peeva-Antova P. Adsorption of p-chlorophenol from aqueous solutions on bentonite and perlite. J Hazard Mater 2002; 90(3): 229-34.

22. Zazouli M, Balarak D, Mahdavi Y. Application of Azolla for 2-Chlorophenol and 4-Chrorophenol Removal from Aqueous Solutions. Iranian Journal of Health Sciences 2013; 1(2): 43-55.

23. Malakootian M, Mansoorian HJ, Yari A. Removal of reactive dyes from aqueous solutions by a non-conventional and low cost agricultural waste: adsorption on ash of Aloe Vera plant. Iranian Journal of Health, Safety & Environment 2014; 1(3): 117-25.

24. Liu Q, Yang B, Zhang L, Huang R. Adsorption of an anionic azo dye by cross-linked chitosan/bentonite composite. Int J Biol Macromol 2015; 72: 1129-35.

25. Karaca S, Gürses A, Acisli O, Hassania A, Kiransan M, Yikilmaz K. Modeling of adsorption isotherms and kinetics of Remazol Red RB adsorption from aqueous solution by modified clay. Desalination & Water Treatment 2013; 51(13-15): 2726-39.

26. Chen D, Chen J, Luan X, Ji H, Xia Z. Characterization of anionΓÇôcationic surfactants modified montmorillonite and its application for the removal of methyl orange. Chemical Engineering Journal 2011; 171(3): 1150-8.

27. Chaari I, Feki M, Medhioub M, Bouzid J, Fakhfakh E, Jamoussi F. Adsorption of a textile dye "Indanthrene Blue RS (C.I. Vat Blue 4)" from aqueous solutions onto smectite-rich clayey rock. J Hazard Mater 2009; 172(2-3): 1623-8.

28. Tseng RL, Tseng SK. Pore structure and adsorption performance of the KOH-activated carbons prepared from corncob. J Colloid Interface Sci 2005; 287(2): 428-37.

29. Wu FC, Tseng RL, Hu CC. Comparisons of pore properties and adsorption performance of KOH-activated and steam-activated carbons. Microporous and Mesoporous Materials 2005; 80(1−3): 95-106.

30. DiazGomez-Trevino AP, Martinez-Miranda V, Solache-Rios M. Removal of remazol yellow from aqueous solutions by unmodified and stabilized iron modified clay. Applied Clay Science 2013; 80–81: 219-25.

31. Laszlo K. Adsorption from aqueous phenol and aniline solutions on activated carbons with different surface chemistry. Colloids and Surfaces A: Physicochemical and Engineering Aspects 2005; 265(1−3): 32-9.

32. Radhika M, Palanivelu K. Adsorptive removal of chlorophenols from aqueous solution by low cost adsorbent−Kinetics and isotherm analysis. Journal of Hazardous Materials 2006; 138(1): 116-24.

33. Almeida CA, Debacher NA, Downs AJ, Cottet L, Mello CA. Removal of methylene blue from colored effluents by adsorption on montmorillonite clay. J

Colloid Interface Sci 2009; 332(1): 46-53.

34. Radaee E, Alavi Moghaddam MR, Arami M. The Study of the Adsorption of Reactive Blue 19 Dye by Activated Carbon from Pomegranate Residue. Journal of Water & Wastewater 2014; 25(92): 27-34.

35. Noorimotlagh Z, Darvishi Cheshmeh Soltani R, Khataee AR, Shahriyar S, Nourmoradi H. Adsorption of a textile dye in aqueous phase using mesoporous activated carbon prepared from Iranian milk vetch. Journal of the Taiwan Institute of Chemical Engineers 2014; 45(4): 1783-91.

36. Elmoubarki R, Mahjoubi FZ, Tounsadi H, Moustadraf J, Abdennouri M, Zouhri A, et al. Adsorption of textile dyes on raw and decanted Moroccan clays: Kinetics, equilibrium and thermodynamics. Water Resources and Industry 2015; 9: 16-29.

37. Ghaedi M, Khajesharifi H, Hemmati Yadkuri A, Roosta M, Sahraei R, Daneshfar A. Cadmium hydroxide nanowire loaded on activated carbon as efficient adsorbent for removal of Bromocresol Green. Spectrochimica Acta Part A: Molecular and Biomolecular Spectroscopy 2012; 86: 62-8.

38. AL-Doury MM, Ali SS. Removal of Phenol and Parachlorophenol from Synthetic Wastewater Using Prepared Activated Carbon from Agricultural Wastes. International Journal of Sustainable and Green Energy 2015; 4(3): 92-101.

39. Mouruo PAM, Carrott PJM, Ribeiro Carrott MML. Application of different equations to adsorption isotherms of phenolic compounds on activated carbons prepared from cork. Carbon 2006; 44(12): 2422-9.

Optimization of ammonia removal in an integrated fix-film activated sludge using response surface methodology

Hooshyar Hossini[1], Abass Rezaee[1], Reza Barati-Roshvanlo[1]

1 Department of Environmental Health, School of Medicine, Tarbiat Modares University, Tehran, Iran

Original Article

Abstract

In this work, removal of ammonia from synthetic wastewater using integrated fixed-film activated sludge (IFAS) process was optimized using response surface methodology (RSM). The main operating parameters such as ammonia concentration rate (ALR) and hydraulic retention time (HRT) were optimized to acquire the maximum removal efficiency. The linear, 2FI, quadratic, mean, and cubic models were utilized for modeling of the parameters. Residual nitrate and nitrite were determined as the byproducts. The results showed that the actual data fitted well with the predicted results. The maximum ammonia removal achieved using mean, linear, 2FI, quadratic, and cubic models were 59.88, 79.05, 79.32, 77.11, and 78.65%, respectively. Nitrate and nitrite were determined in ammonia concentrations of higher than 100 mg/l. The obtained results showed that RSM is a suitable technique for the optimization of conditions for the maximum removal of ammonia.

KEYWORDS: Ammonia, Wastewater, Optimization, Biofilms, Optimization

Citation: Hossini H, Rezaee A, Barati-Roshvanlo R. **Application of response surface methodology for optimization of ammonia removal in integrated fixed-film activated sludge.** J Adv Environ Health Res 2015; 3(2): 130-8.

Introduction

Nitrogen compounds such as ammonium/ammonia ions are the main pollutants in water and wastewater. Discharge of ammonia into environmental resources can lead to various health and environmental problems such as eutrophication, oxygen depletion, and toxicity.[1] Water and wastewater containing large quantities of ammonium/ammonia ions can have adverse effects on human health (metabolic diseases) and the environment (such as eutrophication and overgrowth of plants).[2] Ion exchange, electrodialysis (ED), reverse osmosis, electrocoagulation, and biological treatments are proposed for the removal of ammonia from aqueous sources.[3] Among the proposed techniques, biological processes have various advantages such as their low cost, low operation handling, reliability, and efficacy, and being environmentally friendly. Conventional biological removal of nitrogenous compounds is performed using a two-step process involving nitrification and denitrification.[4] The two-step nitrification–denitrification process using ammonia and nitrite oxidizing biomass is preformed via conversion of ammonium (NH_4^+) to nitrate (NO_3^-), and finally, to N_2 gas.[5-7] These two stages are illustrated as the following reactions:

$$NH_4^+ + \frac{3}{2}O_2 \xrightarrow{\text{Ammonia oxidiziers biomass}} NO_2^- + 2H^+ + H \quad (1)$$

$$No_2^- + \frac{1}{2}O_2 \xrightarrow{\text{Nitrite oxidiziers biomass}} NO_3^- + 2H^+ + H \quad (2)$$
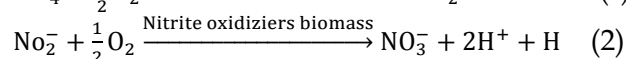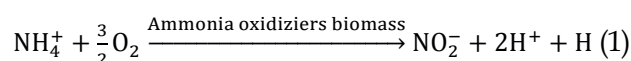
**Corresponding Author:**
Abbas Rezaee
Email: rezaee@modares.ac.ir

Denitrification pathway can be summarized by the following reactions:

$$\frac{1}{5}No_3^- + \frac{5}{6}H^+ + e^- \xrightarrow{\text{Denitifying biomass}} \frac{1}{10}N_2 + \frac{3}{5}H_2O \quad (3)$$

$$\frac{1}{3}No_2^- + \frac{4}{3}H^+ + e^- \xrightarrow{\text{Denitifying biomass}} \frac{1}{6}N_2 + \frac{2}{5}H_2O \quad (4)$$
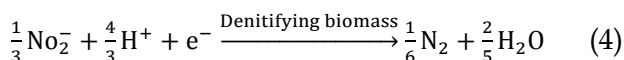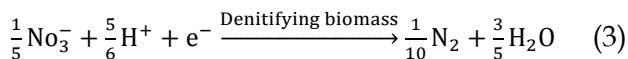
Reactions 3 and 4, respectively, show anoxic growth on nitrate and anoxic growth on nitrite. Nitrification and denitrification are conducted simultaneously for nitrogen removal, but efficient and reliable nitrogen removal requires long solid residence time. Fixed-film processes such as integrated fixed-film activated sludge (IFAS) or moving bed biofilm reactors (MBBR) have been shown to be successful in simultaneous nitrification and denitrification.[8] The enhanced removal of chemical oxygen demand (COD) and biological nutrient (nitrogen and phosphorus) removal have been well demonstrated using IFAS.[9] Optimization of operating parameters is an important method in various fields of sciences. Presently, response surface methodology (RSM) is applied successfully in many scientific fields such as biology, chemistry, medicine, and economy.[10] RSM was proposed by Box et al. in the 1950s.[11] RSM is based on an experimental design with the final goal of evaluating optimal functioning of industrial facilities, using minimum experimental effort.[10]. The aim of the present study was to optimize ammonia concentration and hydraulic retention time (HRT) for the determination of the best conditions of ammonia removal through IFAS process. To the best our knowledge and according to the literature review, the optimization of operating factors of ammonia removal through IFAS process has not been reported.

Materials and Methods

Bench-scale experiments were conducted using a plexiglass reactor with total volume of 13 l (100 × 10 × 15 cm dimensions) (Figure 1). All chemicals used in this work were analytical

reagent grade and they were used without further purification. A general medium containing 500 mg/l dextrose, 12 mg/l potassium dihydrogen phosphate, 16 mg/l dipotassium phosphate, 18 mg/l calcium chloride, and 24 mg/l magnesium sulfate was used at the start-up. The synthetic wastewater was continuously pumped to the reactor for 42 days. The HRT of the reactor was adjusted at 12 hours. The pH was adjusted normally at 7 ± 0.2. The mixed liquor suspended solids (MLSS) was adjusted at 2.5 g/l with HRT of 24 hours start-up period. All experiments were performed at room temperature (25 ± 1 °C). Ammonia, nitrite, nitrate, and COD were analyzed according to standard methods. Nitrate was determined using spectrophotometer at λmax of 220 nm. The Nitrite content was analyzed through colorimetric method and sulfanilamide and naphthylethylendiamine dihydrochloride regents at λmax of 543 nm. The determination of ammonia content was conducted through phenate method.
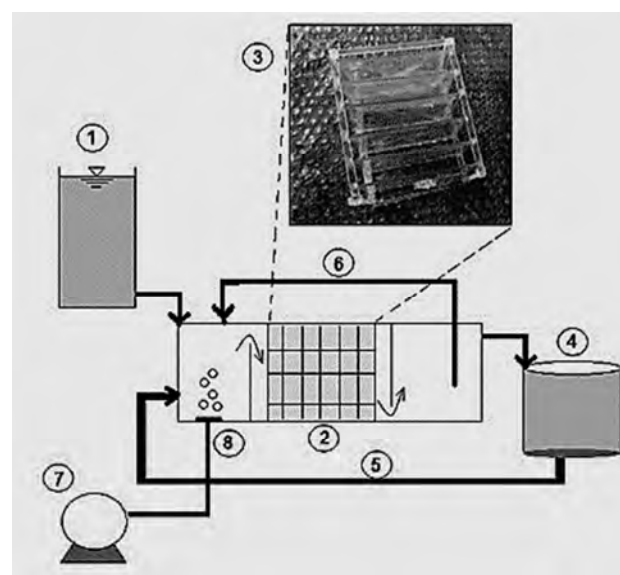

Figure 1. Schematic representation of experimental setup for integrated fixed-film activated sludge (IFAS) process [1] feed tank, 2) fixed film, 3) media, 4) sedimentation tank, 5) returne active sludge, 6) internal recirculation, 7) blower, 8) air diffuser]

RSM offers an empirical relationship between the response function and the independent variables. In this study, the coefficients of the response functions for various dependent variables were determined with the response functions using the Design-Expert regression software (trial version, Stat-Ease Inc., Minneapolis, MN, USA) regression program. The least squares technique was used to evaluate polynomial approximation. The central composite design (CCD) was used to analyze the main parameters (x_1: ammonia concentration, x_2: HRT). Wastewater was prepared with COD of 500 mg/l and different concentrations of ammonia (20, 43, 60, 88, and 100 mg-N/l). According to the primary design, HRT was adjusted in 4, 5.75, 10, 14.25, and 16 hours for -α, -1, 0, +1, +α, respectively. Based on the experimental runs, a total of 13 runs of the CCD experimental design and response are presented in table 1.

Results and Discussion

During the start-up period, ~89.5% ammonia removal was achieved at a constant ammonia load of about 32 mg-N/l and HRT of 16 hours. The percentage of COD removal was determined between 66.8 to 94.86% during 42 days since the start-up.

Based on the experimental runs, a total of 13 runs of the CCD experimental design were

conducted. The coefficient of variation (CV) is the value of the reproducibility of the model and should be lower than 10%. The predicted R-squared amount was agreed with the adjusted R-squared. The difference between R-squared and adjusted R-squared values should not be more than 0.2. The analysis of variables with statistical values and constant are presented in table 2. A significant lack of fit implies that there may be some systematic variation unaccounted for in the hypothesized model.[12] Ammonia removal efficiency was predicated based on the final equation for coded and actual factors. The final first-order and second-order (polynomial) regression in terms of coded and actual factors for all applied models are represented by the following equations.

Final equations in terms of coded factors:

$$Ra_{Mean} = +66.06 \tag{5}$$

$$Ra_{Linear} = +66.06 - (2.50 \times x_1) + (13.25 \times x_2) \tag{6}$$

$$Ra_{2FI} = +66.06 - (2.50 \times x_1) + (13.25 \times x_2) + (2.28 \times x_1 \times x_2) \tag{7}$$

$$Ra_{Quadratic} = +65.79 - (2.50 \times x_1) + (13.25 \times x_2) + (2.28 \times x_1 \times x_2) - (0.32 \times x_12) + (0.76 \times x_22) \tag{8}$$

$$Ra_{Cubic} = +65.79 - (1.82 \times x_1) + (10.77 \times x_2) + (2.28 \times x_1 \times x_2) - (0.32 \times x_12) + (0.76 \times x_22) + (4.96 \times x_12 \times x_2) - (1.35 \times x_1 \times x_22) \tag{9}$$

Table 1. The central composite design (CCD) using natural and coded factors

Run	Precedence	Ammonia concentration (mg-N/L)	HRT (hour)	X1	X2
1	11	88	5.75	1	-1
2	4	60	10	0	0
3	5	60	10	0	0
4	12	88	14.25	1	1
5	13	100	10	2	0
6	10	60	16	0	2
7	6	60	10	0	0
8	7	60	4	0	-2
9	3	32	14.25	-1	1
10	8	60	10	0	0
11	9	60	10	0	0
12	2	32	5.75	-1	-1
13	1	20	10	-2	0

HRT: Hydraulic retention time; X1: Minimum level; X2: Maximum level

Table 2. Statistical analysis of models

Type	Source	df	F-Value	P-value Prob > F	Result
Mean	Model	0	-	-	-
	Lack of Fit	8	46.04	0.0011	
	R2			0	
	Adjusted R2			0	
	Predicted R2			-0.17	Significant
	Adequate Precision			-	
	SD			11.46	
	C.V. %			17.35	
Linear	Model	2	58.87	< 0.0001	Significant
	Lack of Fit	6	4.19	0.0934	
	R2			0.92	
	Adjusted R2			0.90	
	Predicted R2			0.84	Not Significant
	Adequate Precision			22.19	
	SD			3.51	
	C.V. %			5.32	
2FI	Model	3	43.04	< 0.0001	Significant
	Lack of Fit	5	4.05	0.0999	
	R2			0.93	
	Adjusted R2			0.91	
	Predicted R2			0.78	Not Significant
	Adequate Precision			19.98	
	SD			3.38	
	C.V. %			5.11	
Quadratic	Model	5	21.24	0.0004	Significant
	Lack of Fit	3	6.34	0.0532	
	R2			0.93	
	Adjusted R2			0.89	
	Predicted R2			0.62	Not Significant
	Adequate Precision			14.92	
	SD			3.73	
	C.V. %			5.65	
Cubic	Model	7	24.51	0.0014	Significant
	Lack of Fit	1	6.54	0.0628	
	R2			0.97	
	Adjusted R2			0.93	
	Predicted R2			-0.14	Not Significant
	Adequate Precision			16.12	
	SD			2.99	
	C.V. %			4.52	

Final equations in terms of actual factors:

$$Ra_{Mean} = +66.065 \qquad (10)$$

$$Ra_{Linear} = +40.15 - (0.088 \times \text{ammonia concentration}) + (3.12 \times HRT) \qquad (11)$$

$$Ra_{2FI} = +51.52 - (0.28 \times \text{ammonia concentration}) + (1.98 \times HRT) + (0.019 \times \text{ammonia concentration} \times HRT) \qquad (12)$$

$$Ra_{Quadratic} = +54.06 - (0.23 \times \text{ammonia concentration}) + (1.14 \times HRT) + (0.019 \times \text{ammonia concentration} \times HRT) - (3.94 \text{ E-004} \times \text{ammonia concentration2}) + (0.042 \times HRT2) \qquad (13)$$

$$Ra_{Cubic} = \text{Not available for aliased models.} \qquad (14)$$

Predicated efficiencies were calculated using equations 4-14. It was found that the calculated values were similar to experimental

removal data. According to the obtained results, a uniform removal efficiency pattern was provided for each run (Figure 2).

The adequacy of a model can be evaluated by diagnostic plots such as a normal probability plot of the studentized residuals and a plot of predicted versus actual values.[10]

Figure 3 illustrates three dimensional graphics response surface plots of the main parameters and their interactions for ammonia removal efficiency.

The mean model did not change in efficiency for different amounts of ammonia concentration and HRT (Figure 4a). However, in the other models, the ammonia efficiency increased with the increasing of HRT at lower ammonia concentrations (Figures 4b-e). To create favorable conditions for nitrification and denitrification, continuous operation and a relatively long HRT are required.[13] HRT is the main operating variable for biological stabilization. Moreover, solid retention time (SRT) is one of the major factors that contribute to different treatment performances and biomass characteristics.[13] It has been reported that complete nitrification occurred when HRT was longer than 3 hours. The total nitrogen

removal rate was low at HRT of less than 3 hours due to limited partial nitrification.[14] Rostron et al. similarly reported low nitrification at HRT of less than 3 hours. In this condition, very little nitrate was produced.[15] In the numerical optimization, a minimum and a maximum level have to be provided for each parameter.[16] The level of all parameters within the range of investigation was optimized for maximum ammonia removal. Under optimal conditions, maximum ammonia removal was predicted for each model.

In the numerical optimization, a minimum and a maximum level must be provided for each parameter. For several responses, the goals are combined into an overall desirability function.[16] Desirability is defined as an objective function that ranges from zero (0.00), outside of the limits, to one (1.00), at the goal. The program seeks to maximize this function. By starting from several points in the design space, chances for finding the best local maximum improve.[17] Level of all parameters within the range of investigation was set for maximum ammonia removal. With regard to numerical optimization, at optimal conditions, the maximum ammonia removal value was predicted for each model (Table 3).
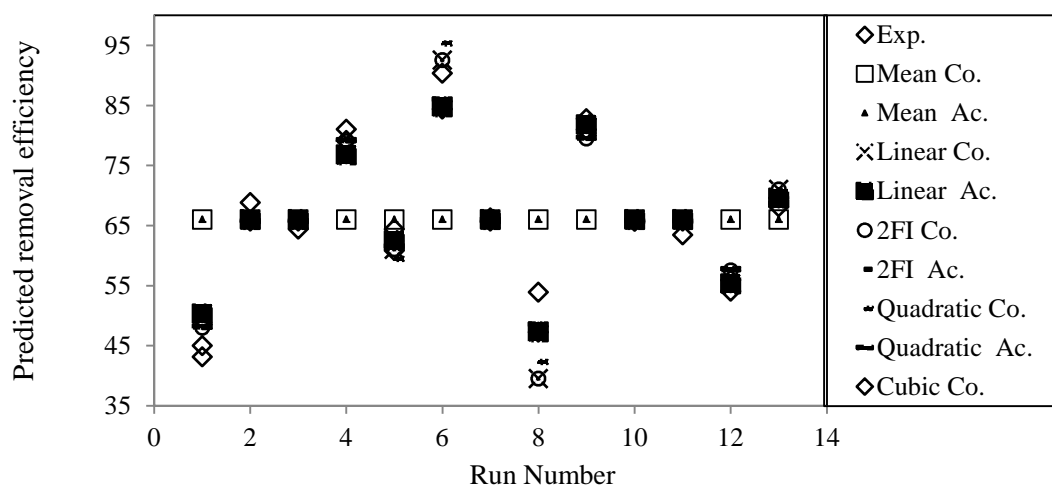

**Figure 2. Ammonia removal efficiency pattern for applied models**
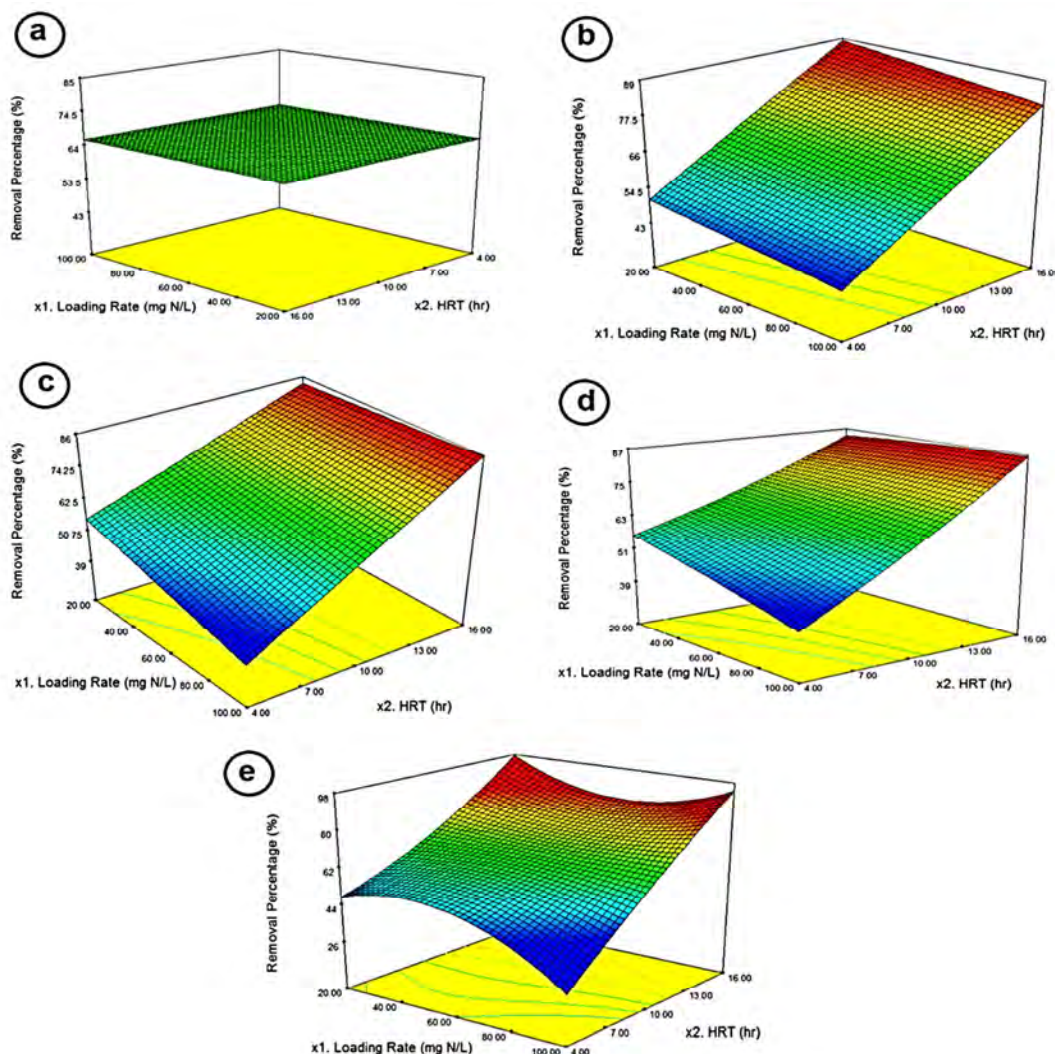
Figure 3. Ammonia byproducts from integrated fixed-film activated sludge (IFAS) process at different loading rates of ammonia

To approve the validity of the optimized points, an experiment was carried out with the parameters suggested by the model. The obtained result shows 95% similarity. The results confirmed the validity of the model, and the experimental values were determined and found to be quite close to the predicted values. Under these conditions, the experimental value for ammonia removal was found to be 59.88, 79.05, 79.32, 77.11, and 78.65% for mean, linear, 2FI, quadratic, and cubic models, respectively. The obtained results showed that an efficient nitrification

potential (79.32% for 2FI model) is provided by IFAS reactor. Similar to the current study, many researchers have studied the potential of nitrification using different biosystems that can be seen in table 4.[15, 18-21]

In order to monitor ammonia conversion to N_2 gas and nitrate, residual nitrate/nitrite (sum of NO_2^- and NO_3^-) was determined for high ammonia concentrations (20-100 mg-N/l) and HRT of 14.25 hours. High amounts of byproducts were seen at 100 mg-N/l of ammonia (Figure 3). At this ammonia concentration, nitrate and nitrite values were
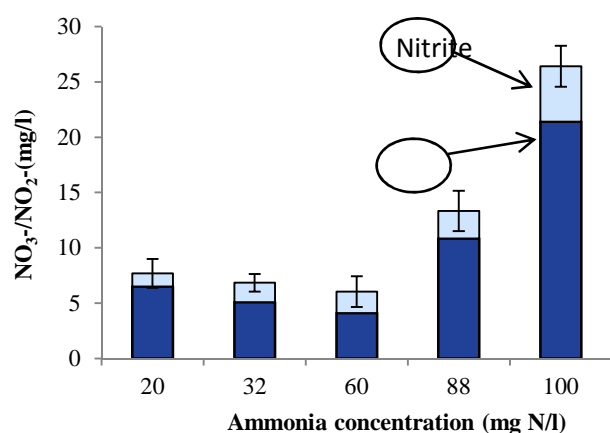
Figure 4. Three-dimensional graphics of response surface for ammonia removal efficiency in (a) mean, (b) linear, (c) 2FI, (d) quadratic, and (e) cubic models

determined at ~26.42 mg/l. In most wastewater treatment plants, nitration is presented by nitrogen oxidizing bacteria such as the genus Nitrospira and Nitrobacter.[7] From the results it can be seen that a long HRT is required to treat the higher ammonium concentrations. This can occur due to the very slow growth of autotrophic nitrifiers. In the case of Nitrobacter sp. (as a dominant species

of nitrite oxidizing bacteria), generation times have been reported at about 18 and 69 hours, and this can provide a low cell yield.[2] On the other hand, during short HRTs, a small amount of ammonia is converted to nitrite and other intermediates, which implies that the denitrifying bacteria has limited access to electron sources.[2]

Conclusion

The results of this study showed that maximum ammonia removal was acquired at 59.88, 79.05, 79.32, 77.11, and 78.65% in the mean, linear, 2FI, quadratic, and cubic models, respectively. High correlation coefficient (r^2) was observed for linear (0.92), 2FI (0.93), quadratic (0.93), and cubic models (0.97). Therefore, the actual data fitted well with the predicted results. A higher amount of ammonia byproducts were observed at 100 mg-N/l of ammonia. At this ammonia concentration, total concentrations of nitrate/nitrite were determined at about 26.42 mg/l.

Conflict of Interests

Authors have no conflict of interests.

Table 3. Numerical optimal conditions and maximum predicted removal

Model	Ammonia concentration (mg-N/l)	HRT (h)	Removal Efficiency (%)	Desirability
Mean	60	8.06	66.06	0.55
Linear	32	14.25	81.81	0.93
2FI	32	14.25	79.53	0.88
Quadratic	50	14.25	79.84	0.89
Cubic	32	14.25	82.86	0.96

HRT: Hydraulic retention time

Table 4. Literature review

Wastewater type	Reactor	Nitrification rate (%)	References
Synthetic feed	IFAS	79.32 for 2FI% model	Current study
Synthetic feed	Linpor and Kaldnes	35-40%	Rostron et al.[15]
Refinery wastewater	Activated sludge	over 90%	Fang et al.[18]
Synthetic feed	Activated sludge	nearly 100%	Campos et al.[19]
Synthetic feed	Activated sludge	98%	Ruiz et al.[21]
Domestic wastewater	IFAS	over 87%	Regmi et al.[20]

IFAS: Integrated fixed- film activated sludge

References

1. Van Hulle SWH, Vandeweyer HJP, Meesschaert BD, Vanrolleghem PA, Dejans P, Dumoulin A. Engineering aspects and practical application of autotrophic nitrogen removal from nitrogen rich streams. Chemical Engineering Journal 2010; 162(1): 1-20.

2. Hossini H, Rezaee A, Ayati B, Mahvi AH. Simultaneous nitrification and denitrification using a polypyrrole/microbial cellulose electrode in a membraneless bio-electrochemical system. RSC Adv 2015; 5(89): 72699-708.

3. Li M, Feng C, Zhang Z, Yang S, Sugiura N. Treatment of nitrate contaminated water using an electrochemical method. Bioresour Technol 2010; 101(16): 6553-7.

4. Virdis B, Rabaey K, Rozendal RA, Yuan Z, Keller J. Simultaneous nitrification, denitrification and carbon removal in microbial fuel cells. Water Res 2010; 44(9): 2970-80.

5. Kaelin D, Manser R, Rieger L, Eugster J, Rottermann K, Siegrist H. Extension of ASM3 for two-step nitrification and denitrification and its calibration and validation with batch tests and pilot scale data. Water Res 2009; 43(6): 1680-92.

6. Iacopozzi I, Innocenti V, Marsili-Libelli S, Giusti E. A modified Activated Sludge Model No. 3 (ASM3) with two-step nitrification-denitrification. Environmental Modelling & Software 2007; 22(847): 861.

7. Francis CA, Roberts KJ, Beman JM, Santoro AE, Oakley BB. Ubiquity and diversity of ammonia-oxidizing archaea in water columns and sediments of the ocean. Proc Natl Acad Sci U S A 2005; 102(41): 14683-8.

8. Onnis-Hayden A, Majed N, Schramm A, Gu AZ. Process optimization by decoupled control of key microbial populations: distribution of activity and abundance of polyphosphate-accumulating organisms and nitrifying populations in a full-scale IFAS-EBPR plant. Water Res 2011; 45(13): 3845-54.

9. Rosso D, Lothman SE, Jeung MK, Pitt P, Gellner WJ, Stone AL, et al. Oxygen transfer and uptake, nutrient removal, and energy footprint of parallel full-scale IFAS and activated sludge processes. Water Res 2011; 45(18): 5987-96.

10. Jiménez-Contreras E, Bailón-Moreno R, Torres-Salinas D, Ruiz-Baños R, Ruiz-Pérez R, Moneda-Corrochano DL. Response Surface Methodology and its Application in Evaluating Scientific activity. Scientometrics 2009; 79(1): 201-18.

11. Box GE, Wilson KB. On the Experimental Attainment of Optimum Conditions. Journal of the Royal Statistical Society 1951; 13(1): 1-45.

12. Bashir MJK, Aziz HA, Yusoff MS, Adlan M. Application of response surface methodology (RSM) for optimization of ammoniacal nitrogen removal from semi-aerobic landfill leachate using ion exchange resin. Desalination 2010; 254(1−3): 154-61.

13. Kim YM, Park D, Jeon CO, Lee DS, Park JM. Effect of HRT on the biological pre-denitrification process for the simultaneous removal of toxic pollutants from cokes wastewater. Bioresour Technol 2008; 99(18): 8824-32.

14. Cho S, Fujii N, Lee T, Okabe S. Development of a simultaneous partial nitrification and anaerobic ammonia oxidation process in a single reactor. Bioresour Technol 2011; 102(2): 652-9.

15. Rostron WM, Stuckey DC, Young AA. Nitrification of high strength ammonia wastewaters: comparative study of immobilisation media. Water Res 2001; 35(5): 1169-78.

16. Mourabet M, El Rhilassi A, El Boujaady H, Bennani-Ziatni M, El Hamri R, Taitai A. Removal of fluoride from aqueous solution by adsorption on hydroxyapatite (HAp) using response surface methodology. Journal of Saudi Chemical Society 2012.

17. Mirazimi SMJ, Rashchi F, Saba M. Vanadium removal from roasted LD converter slag: Optimization of parameters by response surface methodology (RSM). Separation and Purification Technology 2013; 116: 175-83.

18. Fang HY, Chou MS, Huang CW. Nitrification of ammonia-nitrogen in refinery wastewater. Water

http://jaehr.muk.ac.ir

Research 1993; 27(12): 1761-5.

19. Campos JL, Mosquera-Corral A, Sanchez M, Mendez R, Lema JM. Nitrification in saline wastewater with high ammonia concentration in an activated sludge unit. Water Res 2002; 36(10): 2555-60.

20. Regmi P, Thomas W, Schafran G, Bott C, Rutherford B, Waltrip D. Nitrogen removal assessment through nitrification rates and media biofilm accumulation in an IFAS process demonstration study. Water Res 2011; 45(20): 6699-708.

21. Ruiz G, Jeison D, Chamy R. Nitrification with high nitrite accumulation for the treatment of wastewater with high ammonia concentration. Water Res 2003; 37(6): 1371-7.

Potential human health risk assessment of heavy metals in the flesh of mallard and pochard in the South Eastern Caspian Sea region of Iran

Mohammad Hosein Sinkakarimi[1], Ali Reza Pourkhabbaz[1], Mehdi Hassanpour[2], Jeffrey M. Levengood[3], Seyed Mahmoud Ghasempouri[4]

1 Department of Environmental Science, School of Natural Resources, Birjand University, Birjand, Iran
2 Department of Environment, Provincial Directorate of Environment Protection, Gorgan, Iran
3 Illinois Natural History Survey, University of Illinois at Urbana-Champaign, Illinois, USA
4 Department of Environmental Sciences, School of Natural Resources and Marine Science, Tarbiat Modares University, Noor, Iran

Brief Communication

Abstract

Every year, migratory waterfowl are hunted and consumed by people in Golestan Province of Iran. Due to the heavy metal contamination of wintering habitats, an estimation of the human health risks associated with the consumption of these ducks is necessary. Therefore, this study was conducted to estimate the health risks of exposure to cadmium (Cd), total chromium (Cr), iron (Fe), lead (Pb), and zinc (Zn) due to the consumption of pectoral muscle of mallard (Anas platyrhynchos) and pochard (Aythya ferina) harvested and hunted in the South-Eastern Caspian Sea region of Iran. The mean values of these metals in the pectoral muscle of mallards and pochards were used to calculate estimated daily intake (EDI), estimated weekly intake (EWI), and target hazard quotients (THQ). The EDI (µg/day/70 kg body weight) for Cd, Cr, Fe, Pb, and Zn in mallard were 0.2, 0.04, 58, 1.1, and 12.8, respectively. The EDI (µg/day/70 kg body weight) for Cd, Cr, Fe, Pb, and Zn in pochard were 0.8, 0.1, 69, 0.8, and 13.4, respectively. The estimated total THQ (higher than 1) indicated that heavy metal levels in pochard flesh were unsafe for consumption. The EDI and EWI of the metals examined were below those recommended by the Joint FAO/WHO Expert Committee on Food Additives (JECFA) and oral doses suggested by the United States Environmental Protection Agency (USEPA). There appears to be little risk of exposure to metals associated with the consumption of mallard and pochard in this region.

KEYWORDS: Heavy Metals, Risk, Ducks, Food Additives, Humans

Introduction

Contamination of the environment with metals is increasing, and may pose a threat to some species and populations. They may exert beneficial or harmful effects on plant, animal, and human life depending upon the concentration.[1] These elements are introduced into the environment through various routes, such as smelting processes, fuel combustion, and industrialization.[1] They make their way into aquatic systems through atmospheric fallout, dumping of wastes, accidental leaks, runoff from terrestrial systems (industrial and domestic effluents), and geological weathering.[2] Birds obtain heavy metals from their food and the surrounding environment, and their body burdens represent a balance between rates of intake and elimination.[3]

Corresponding Author:
Mohammad Hosein Sinkakarimi
Email: mh_sinkakarimi@yahoo.com

Heavy metals discharged into the aquatic environment can damage both aquatic species diversity and ecosystems, due to their toxicity and accumulative behaviour.[4] Inorganic contaminants such as Cd, Cr, and Pb are among the most studied metal contaminants. These metals react with diffusing ligands, macromolecules, and ligands present in membranes, which mostly cause bioaccumulation and biomagnification in the food chain, persistence in the environment, and disorders in the metabolic processes of living organisms.[5]

High concentrations of metals in the Gomishan and Miankaleh Wetlands of North-Eastern Iran are of great concern due to their potential effects on wildlife and human health.[6] These two wetlands are under the protection of the Ramsar Convention. With the rapid industrialization and economic development in the watershed, pollution has become widespread in these areas.[6]

The objectives of this study were to determine the concentrations of cadmium (Cd), chromium (Cr), iron (Fe), lead (Pb) and zinc (Zn) in the pectoral muscle of mallard and pochard from Miankaleh and Gomishan International wetlands and to assess the potential human health risk for hunters' family members via consumption of the ducks. To our knowledge, this is the first study of the metal exposure risk from consumption of flesh of ducks wintering in the South Eastern Caspian Sea region, Iran.

Materials and Methods

During the winter of 2012, 30 mallard (15 males and 15 females) and 30 pochard (15 males and 15 females) ducks were shot in the Miankaleh (36° 20' N, 53° 43' E) and Gomishan (54° 53' N, 37° 9' E) International Wetlands under license of the Environmental Protection Agency of Golestan, Iran. These sites are among the important wetlands and wintering areas for birds in the Middle East (Figure 1).
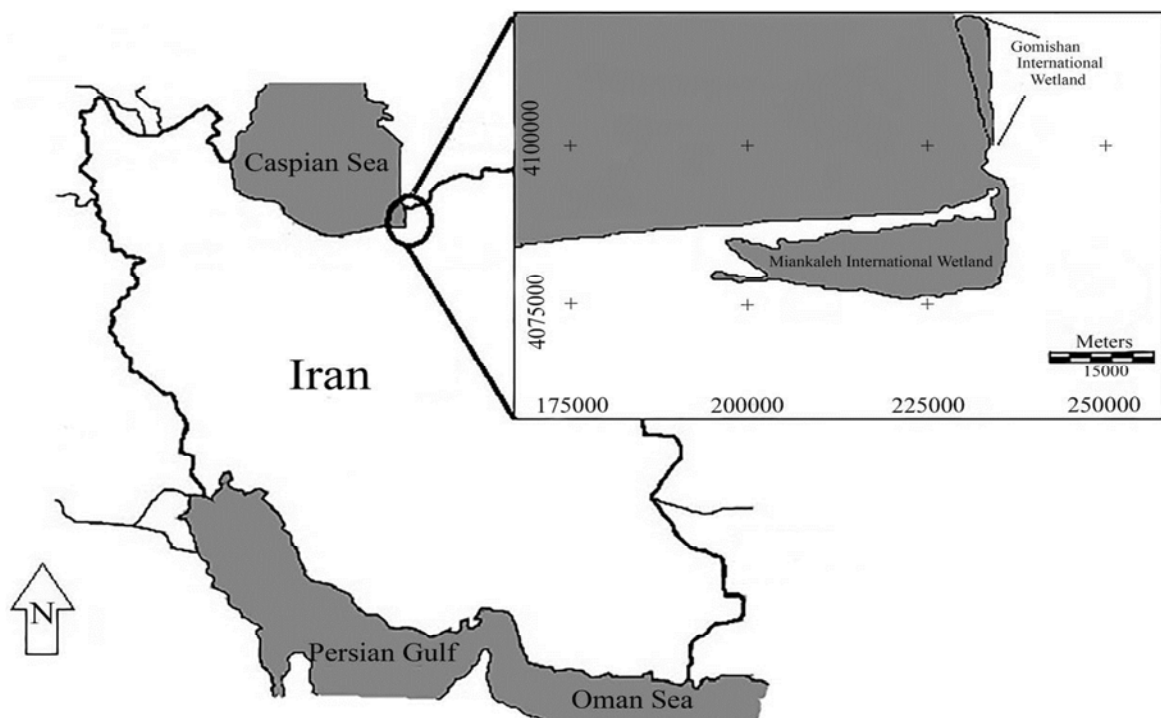

Figure 1. Sampling sites in the South East of the Caspian Sea

Upon collection, specimens were immediately transported to a laboratory where pectoral muscles were excised and samples frozen for later analysis. Median body mass and total length of mallard were 1.178 kg and 55.95 cm and of pochard were 0.924 kg and 44.1 cm, respectively. Approximately 5 g of wet tissue of pectoral muscle was placed in a porcelain crucible and dried at 135 °C for 2 hours. Samples were then transferred to a cool muffle furnace and the temperature was slowly raised to 450-500 °C overnight. After cooling, 2 ml of HNO_3 were added and the sample was then heated on a hot plate until dry. The sample was returned to the cooled furnace and the temperature was raised to 450-500 °C for an hour. After cooling, 10 ml of 1N HCL were added and heated on the hot plate to dissolve the ash. Digested samples were filtered and diluted to 25 ml in 1N HCL.[7] Metal concentrations were determined using an atomic absorption spectrophotometer (GFS97, Thermo Electron, Cambridge, UK). The accuracy of the analysis was confirmed by measuring certified reference material tissue (DORM-2; National Research Council, Canada). Recoveries ranged from 95 to 105%. Detection limits (µg/g) were 0.004 for Cd, 0.03 for total Cr, 0.05 for Fe, 0.001 for Pb, and 0.005 for Zn. The concentrations of metals in samples were expressed as microgram per gram wet weight (µg/g ww).

THQ was calculated according to the guidelines of the United States Environmental Protection Agency (USEPA).[8] Based on the USEPA guidance, we assumed that the adsorbed contaminant dose was equal to the ingestion dose and that cooking had no effect on the contaminants.[8] Furthermore, because of the unavailable oral reference dose (R_fD_o) of Pb, the value is specified as the permissible tolerable daily intake (PTDI) suggested by the Joint FAO/WHO Expert Committee on Food Additives (JECFA) 2013.[9]

THQ was calculated using the following equation:

$$THQ = (EF \times ED \times MS \times C)/(R_fD_o \times BW \times AT) \times 10^{-3} \tag{1}$$

where THQ is the Target Hazard Quotient, which indicates the ratio between exposure and reference dose. A THQ of higher than 1 means that the THQ is higher than the daily reference dose and systemic effects may occur.[10] In general, the R_fD_o is an estimate (with uncertainty spanning perhaps an order of magnitude) of the daily exposure of the human population (including sensitive subgroups) that is likely to be without an appreciable risk of deleterious effects during a lifetime. EF is the exposure frequency or number of exposure events per year of exposure (about 182.5 days) and ED is the exposure duration (72 years).[11] MS is the meal size of 95 g; Sinkakarimi et al. indicated that a Golestan province hunter's family members consume about 95 g/day of waterfowl.[6] C is the metal concentration (µg/g w.wt). R_fD_o is the oral reference dose (µg/g/day); the R_fD_o values used in this study were 1×10^{-3} for Cd, 7×10^{-1} for Fe, 4×10^{-3} for Pb, and 3×10^{-1} for Zn.[9,12] BW is the body weight of 70 kg,[8] and AT is the averaging time (it is equal to EF × ED).

In this study, total THQ is treated as the arithmetic sum of the individual metal THQ values, obtained using the method of Chien et al.[13]

$$Total\ THQ\ (TTHQ) = THQ\ (toxicant\ 1) + THQ\ (toxicant\ 2) + \dots \dots + THQ\ (toxicant\ n) \tag{4}$$

The estimated daily intake (EDI) and estimated weekly intake (EWI) depend on both the metal concentration in food and the daily and weekly food consumption. In addition, body weight influences the tolerance to contaminant exposure. The EDI and EWI account for these factors and are calculated as follows:

$$EDI\ (µg/g/daily) = (MS \times C)/BW \tag{2}$$

$$EWI\ (µg/g/week) = (MS \times C)/BW \tag{3}$$

Results and Discussion

Concentrations of metals

The concentration of metals in the pectoral muscle tissue of mallard and pochard follows the sequence Fe > Zn > Pb > Cd > Cr (Table 1). Lead is a non-essential element and it is well documented that Pb can cause neurotoxicity, nephrotoxicity, and many other adverse health effects.[14] The maximum permitted concentration of Pb in food proposed by both the Australian National Health and Medical Research Council (ANHMRC) and Spanish legislation are 2.0 µg/g as wet weight basis.[15,16] Moreover, the United Kingdom has a legislated permissible level for Pb in food of 1.0 µg/g.[17] In our study, the concentrations of Pb in mallard and pochard flesh were lower than these thresholds (Table 1). In contrast, the European Commission (EC) and Institute of Turkish Standards for Food (ITSF) considered 0.1 and 0.5 µg/g w.w, respectively, as the permissible threshold for Pb in food.[18,19] The flesh of mallard and pochard we examined clearly exceeded this lower threshold and, according to these guidelines, pose health risks to humans consuming them. In a similar study in Poland, Binkowski examined Pb levels in the flesh of mallard and coot (Fulica atra), and concluded that their flesh was unfit for human consumption.[20] The mean concentration of Pb (µg/g w.w) in our study was higher than that in common teal (Anas crecca) (0.32) from Northern Iran (Sinkakarimi et al.,[6] Unpublished data), and mallard (0.23), garganey (Anas querquedula) (0.48), and tufted duck (Aythya fuligula) (0.15) from Warmia and Mazury, Poland.[21] It was also higher than that in mallard (0.04) and coot (0.06) from Zator, in Southern Poland,[20] scaup (Aythya marila) (0.55) from Szczecin Lagoon, Poland,[22] and gadwall (Anas strepera) (0.92) from Northern Iran (Sinkakarimi et al.,[6] Unpublished data).

The mean Cd concentrations we observed in mallard and pochard did not exceed the maximum permitted concentration of the ANHMRC (2 µg/g), Western Australian authorities (5.5 µg/g), and Spanish legislation (1 µg/g).[15,16] On the other hand, observed concentrations of Cd in the pectoral muscle of mallards and pochards were greater than the EC threshold (0.05 µg/g ww) for Cd in food.[15,17,18] Similarly, Binkowski reported that the flesh of mallard and coot from Poland was unfit for human consumption due to its Cd content.[20]

The mean concentration of Cd in our study was greater than that of common teal (0.13) from Northern Iran (Sinkakarimi et al.,[6] Unpublished data), mallard (0.01) and coot (0.02) from Zator, in Southern Poland,[20] and scaup (0.06) from Szczecin Lagoon, Poland.[22]

Although naturally occurring, most Cr to which biota are exposed originate from anthropogenic activities involved in pigments, municipal sewage, mining, and refining.[23] The Cr concentrations we observed were lower than the Western Australian Food and Drug Regulations' stated concentration of 5.5 µg/g for Cr in seafood for consumption.[15]

Iron and Zn are essential elements that are regulated through normal homeostatic mechanisms.[24] The concentrations of Zn we observed in pochard and mallard flesh were below the acceptable limit (1000 µg/g) in food set by the ANHMRC and WHO.[15,25] The mean concentrations of Fe and Zn in this study were within the ranges normally found in other ducks in other regions.[21,26,27]

THQ

The health risk of heavy metals in seafood is usually estimated by the THQ.[28] The THQ does not provide a quantitative estimate of the probability of an exposed population experiencing an adverse health effect, but it does offer an indication of the risk level due to pollutant exposure. The THQ of each metal we examined was lower than 1, suggesting that people would not experience health risks from consumption of mallards and pochards from

the wetlands of the South East of the Caspian Sea (Table 2). On the other hand, values of the THQ index for total exposure were higher than 1 for pochard, indicating that the estimated exposure is a major health concern.

Dietary intake

An important aspect in assessing risk to human health from potentially harmful chemicals in food is the knowledge of the dietary intake of such substances that must remain within the determined safety limits. In the present study, we have shown that the estimated daily intakes of Cd, Fe, Pb, and Zn through the consumption of mallard and pochard by adults are lower than the acceptable daily intake recommended by the JECFA (Table 3).[9] With respect to Cr, the JECFA does not set a provisional tolerable intake limit. However, comparing the estimated intake with the oral reference dose suggested by the USEPA (equal to 3 and 1500 µg/g/day for Cr VI and Cr III, respectively), our results indicate that daily intake was lower than this

reference dose (Table 1). Furthermore, our results for Cd, Zn, and Fe were lower than the oral reference dose (µg/g/day) suggested by the USEPA (Cd: 1, Zn: 300, and Fe: 700). No oral reference dose has been suggested by the USEPA for Pb or total Cr.[8]

Conclusion

Prior to this study, no published information existed on the risks of consuming the flesh of these popular waterfowl from the Caspian Sea region. The results of this study indicated that the estimated provisional permissible tolerable weekly intake (PTWI) and PTDI values for Cd, total Cr, Fe, Pb, and Zn in the pectoral muscle of mallard and pochard were lower than the values established by various authorities.[29-32] In addition, THQ indices for total exposure in pochard were higher than 1.0; thus, consumption of the pectoral muscle of this species wintering in the South Eastern Caspian Sea region was a human health concern.

Table 1. Metal concentrations (mean ± Standard deviation) in the pectoral muscle of mallard and pochard collected from wetlands in the South Eastern region of the Caspian Sea

Species	N	Pb	Cd	Cr	Zn	Fe
Mallard	30	0.83 ± 0.32	0.21 ± 0.09	0.03 ± 0.01	9.46 ± 2.51	43.05 ± 12.46
Pochard	30	0.62 ± 0.40	0.59 ± 0.37	0.09 ± 0.06	9.92 ± 3.14	50.88 ± 17.18

Table 2. Estimated target hazard quotients (THQ) for individual metals and total THQ from consumption of the pectoral muscle of mallard and pochard from the South Eastern region of the Caspian Sea

Species	Pb	Cd	Cr	Zn	Fe	TTHQ
Mallard	0.281	0.285	-	0.043	0.083	0.692
Pochard	0.210	0.801	-	0.045	0.045	1.101

TTHQ: Total target hazard quotients

Table 3. The estimated daily and weekly intakes for mallard and pochard flesh by adult humans in the South East of the Caspian Sea

Metal	PTWI	PTWI*	PTDI	Mallard EWI (EDI)	Pochard EWI (EDI)
Pb	25	1750	250	7.9 (1.10)	5.9 (0.8)
Cd	6	420	60	2.0 (0.20)	5.6 (0.8)
Cr	-	-	-	0.3 (0.04)	0.9 (0.1)
Zn	7000	490000	70000	89.9 (12.80)	94.3 (13.4)
Fe	5600	392000	56000	409 (58.40)	483.4 (69.0)

Mean daily waterfowl consumption in Iran is 95 g per person
PTWI: Provisional permissible tolerable weekly intake in µg/week/kg body weight; * PTWI per 70 kg body weight of adults (µg/week/70 kg body weight); PTDI: Permissible tolerable daily intake (µg/day/70 kg body weight); EWI: Estimated weekly intake (µg/week/70 kg body weight); EDI: Estimated daily intake (µg/day/70 kg body weight)

Conflict of Interests

Authors have no conflict of interests.

Acknowledgements

References

1. Frstner U, Wittmann GT. Metal Pollution in the Aquatic Environment. Berlin, Germany: Springer-Verlag; 1981. p. 486.
2. Eisler R. Trace metal concentrations in marine organisms. London, UK: Pergamon Press; 1981.
3. Evans PR, Moon SJ. Heavy metals in shorebirds and their prey in Northeast England. In: Say PJ, Whitton BA, Editors. Heavy Metals in Northern England: Environmental and Biological Aspects. Durham, UK: Department of Botany, University of Durham; 1981.
4. Matta J, Milad M, Manger R, Tosteson T. Heavy metals, lipid peroxidation, and ciguatera toxicity in the liver of the Caribbean barracuda (Sphyraena barracuda). Biol Trace Elem Res 1999; 70(1): 69-79.
5. Morgano MA, Rabonato LC, Milani RF, Miyagusku L, Balian SC. Assessment of trace elements in fishes of Japanese foods marketed in Sao Paulo (Brazil). Food Control 2011; 22(5): 778-85.
6. Sinkakarimi MH, Pourkhabbaz RR, Hassanpour M. The study of waterfowl organs as bioindicators of metals pollution in southeastern Caspian Sea [MSc Thesis]. Birjand, Iran: Department of Environment, University of Birjand; 2013.
7. Horwitz W. Official Methods of Analysis of the Association of Official Analytical Chemists. Gaithersburg, MD: The Association p. 2200; 2000.
8. Environmental Protection Agency. Assessing human health risks from chemically contaminated fish and shellfish: a guidance manual. Washington, DC: U.S. Environmental Protection Agency; 1989.
9. World Health Organization. Evaluations of the Joint FAO/WHO Expert Committee on Food Additives (JECFA) [Online]. [cited 2013]; Available from: URL: http://apps.who.int/food-additives-contaminants-jecfa-database/search.aspx?fc=47
10. Copat C, Vinceti M, D'Agati MG, Arena G, Mauceri V, Grasso A, et al. Mercury and selenium intake by seafood from the Ionian Sea: A risk evaluation. Ecotoxicol Environ Saf 2014; 100: 87-92.
11. Ministry of Health and Medical Education of Iran. Heavy Metals, Risk, Ducks, Food Additives, Humans [Online]. [cited 2015]; Available from: URL: http://behdasht.gov.ir/?siteid=1&pageid=1508&newsview=129600
12. United States Environmental Protection Agency. Risk based concentration table. Washington, DC: USEPA; 2009.
13. Chien LC, Hung TC, Choang KY, Yeh CY, Meng PJ, Shieh MJ, et al. Daily intake of TBT, Cu, Zn, Cd and As for fishermen in Taiwan. Sci Total Environ 2002; 285(1-3): 177-85.
14. Garcia-Leston J, Mendez J, Pasaro E, Laffon B. Genotoxic effects of lead: an updated review. Environ Int 2010; 36(6): 623-36.
15. Plaskett D, Potter IC. Heavy Metal Concentrations in the Muscle Tissue of 12 Species of Teleost from Cockburn Sound, Western Australia. Australian Journal of Marine and Freshwater Research 1979; 30(5): 607-16.
16. El-Sikaliy A, Khaled A, Nemr A. Heavy metals monitoring using bivalves from Mediterranean Sea and Red Sea. Environ Monit Assess 2004: 98(1-3): 41-58.
17. United Kingdom Lead in Food Regulations. Food and Drugs Act. London, UK: Her Majesty's Stationery Office; 1955.
18. The commission of the European communities. Commission regulation (EC) no 466: setting maximum levels for certain contaminants in foodstuffs [Online]. [cited 2001]; Available from: URL: http://ec.europa.eu/food/fs/sfp/fcr/fcr02_en.pdf
19. Dirican S, Cilek S, Ciftci H, Biyikoglu M, Karacinar S, Yokus A. Preliminary study on heavy metal concentrations of Anatolian Khramulya, Capoeta tinca (Heckel, 1843) from Çamlıgöze Dam Lake, Sivas, Turkey. J Environ Health Sci Eng 2013; 11(1): 1-7.
20. Binkowski LJ. Is the meat of wild waterfowl fit for human consumption? Preliminary results of cadmium and lead concentration in pectoral muscles of Mallards and Coots shot in 2006 in southern Poland. J Microbiol Biotechnol Food Sci 2012; 1: 1120-8.
21. Szymczyk K, Zalewski K. Copper, Zinc, Lead and Cadmium Content in Liver and Muscles of Mallards (Anas Platyrhychnos) and Other Hunting Fowl Species in Warmia and Mazury in 1999-2000. Pol J Environ Stud 2003; 12(3): 381-6.
22. Kalisinska E, Salicki W. Lead and Cadmium Levels in Muscle, Liver, and Kidney of Scaup Aythya marila from Szczecin Lagoon, Poland. Pol J Environ Stud 2010; 19(6): 1213-22.
23. Barbieri E, Passos EA, Filippini A, dos Santos IS, Garcia CA. Assessment of trace metal concentration

in feathers of seabird (Larus dominicanus) sampled in the Florianopolis, SC, Brazilian coast. Environ Monit Assess 2010; 169(1-4): 631-8.

24. Kim J, Oh JM. Metal levels in livers of waterfowl from Korea. Ecotoxicol Environ Saf 2012; 78: 162-9.

25. Gabriel UU, Ugwemorubong UG, Horsfall M. Trace Metals in the Tissues and Shells of Tympanotonus Fuscatus var. Radula from the Mangrove Swamps of the Bukuma Oil Field, Niger Delta). Eur J Sci Res 2008; 24(4): 468-76.

26. Bojar H, Bojar I. Monitoring of contamination of the Lublin region wetlands using Mallards [Anas platyrhynchos] as a vector of the contamination by various conditionally toxic elements. Annals of Animal Science 2009; 9(2): 195-204.

27. Kalisinska E, Salicki W, Myslek P, Kavetska KM, Jackowski A. Using the Mallard to biomonitor heavy metal contamination of wetlands in north-western Poland. Sci Total Environ 2004; 320(2-3): 145-61.

28. Wang SL, Xu XR, Sun YX, Liu JL, Li HB. Heavy metal pollution in coastal areas of South China: a review. Mar Pollut Bull 2013; 76(1-2): 7-15.

29. Qin CY, Fang ZQ, Tang YJ, An D, Yang XB. Contents and evaluation of heavy metals in common aquatic from Lingding Yang in Pearl River estuary, South China Sea. Journal of South China Normal University 2010; 1(3): 104-9.

30. Huang CJ, Zhao Z. Assessment on contents of heavy metals in seafoods from Zhanjiang Harbor. Journal of Shantou University 2007; 22(1): 30-6.

31. Qiu YW, Yu KF, Zhang G, Wang WX. Accumulation and partitioning of seven trace metals in mangroves and sediment cores from three estuarine wetlands of Hainan Island, China. J Hazard Mater 2011; 190(1-3): 631-8.

32. Ihedioha JN, Okoye CO. Dietary intake and health risk assessment of lead and cadmium via consumption of cow meat for an urban population in Enugu State, Nigeria. Ecotoxicol Environ Saf 2013; 93: 101-6.